SPring-8 Scientific Achievements

Challenging the Mysteries of Science with Dream Lights

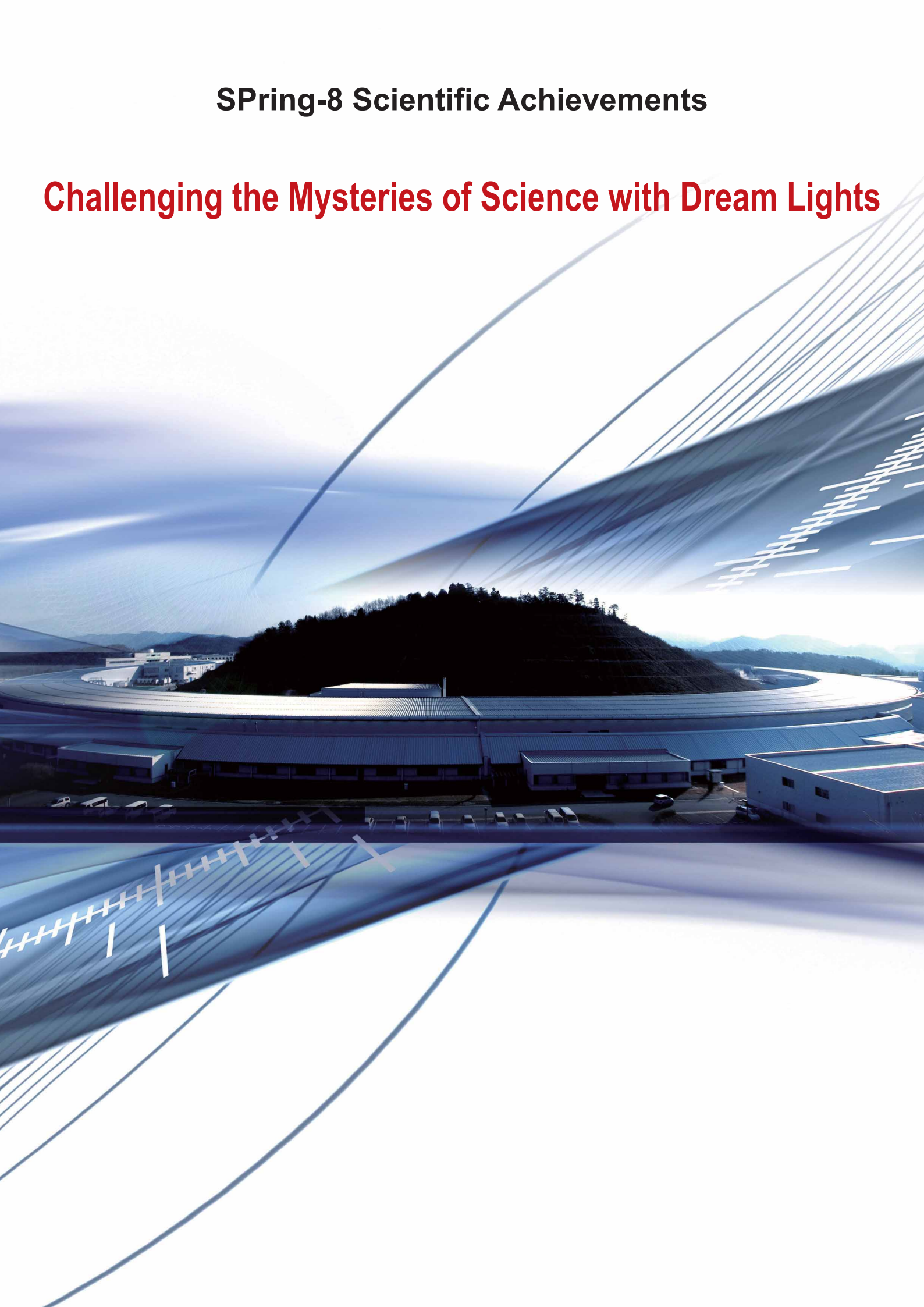

On the Publication of SPring-8 Scientific Achievements

In the more than 15 years since the SPring-8 was put into use in October of 1997, the large-scale radiation facility has matured into the world's highest-level advanced research foundation due to the installation and upgrading of a variety of equipment and devices, and has contributed to the advancement of science and industry in diverse fields. We currently have 26 shared Beamlines (BLs), 19 dedicated BLs, 9 BLs for RIKEN, and 2 BLs for accelerator diagnostics, for a grand total of 56 operational BLs, with an additional BL undergoing maintenance. With the use of these BLs, 8,043 research papers have been published in 15 years. Recently, close to 800 papers per year have been published, a figure that exceeds 1% of the total number of papers published in Japan per year (75,000 papers). The citations of papers from SPring-8 are high as well, averaging 16 times per paper. As can be seen, both the quantity and quality of the scientific research performed by the users of SPring-8 is high, and many excellent papers are being published.

This booklet is a collection of major achievements that we have selected from each of the following seven fields of research in the scientific application of SPring-8: Life Science, Soft Matter, Materials Science, Electronic Properties, High-Pressure Earth Science, Environment and Energy, and Nuclear Physics. In bringing this booklet together, various efforts have been made so that the achievements are presented in an easy-to-understand manner even to those who are not specialists in these fields, without compromising its scientific flavor.

Large-scale research facilities such as SPring-8 must win the understanding of the people on the significance and effectiveness of these research efforts, since the construction, operation, and management of the facility requires substantial national expenditure. Therefore, from the peoples' point of view, the Japan Synchrotron Radiation Research Institute (JASRI) needs to provide an adequate explanation of the achievements of SPring-8. We at JASRI hope that this booklet will be useful, even in the slightest way, far and wide for the people to comprehend the considerable contribution of SPring-8 to the sciences. We would be pleased if readers could gain an even deeper understanding of the significance and effectiveness of SPring-8 by taking a look at the "Successful Results of Industrial Applications at SPring-8" booklet, which has been published along with this work.

Finally, beginning with the members of the editorial board and the researchers - the users of SPring-8 - who have exerted themselves in bringing this booklet together, we would like to express our deepest thanks to all who cooperated in producing this collection.

Yoshiharu Doi, President
Japan Synchrotron Radiation Research Institute (JASRI)

Contents

What is SPring-8?

Many people believe the well-known proverb “seeing is believing”, indicating that humans obtain the majority of information through sight. You require light to see objects as your eyes perceive their images by the reflected light. Similarly, in science “seeing” is very important. Suppose you want to take a picture of a friend, lighting significantly impacts the photograph, and must be carefully selected based on the desired effect. Likewise in science, selecting the appropriate type of light to visualize an object is crucial. Thus, a facility that can produce many types of light is extremely beneficial.

SPring-8, one of the world’s largest synchrotron radiation facilities, is “a science eye” to microscopically see natural phenomena. Below is an overview of how the microscopic world and large science facilities are connected as well as an explanation of the benefits from this connection.

Temperature-controlled experimental hall of the storage ring at SPring-8. Numerous scientific and technological advances have been realized here.

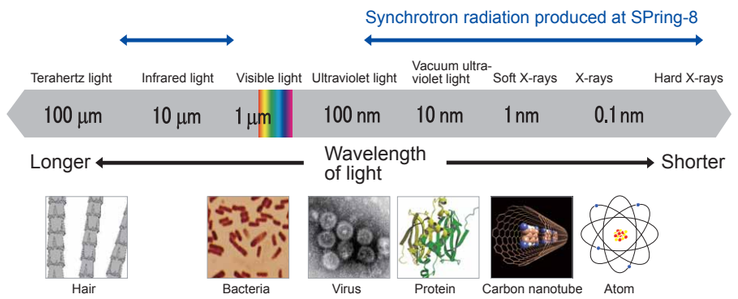

Fig. 1. Details of an object can clearly be seen by illuminating with bright light (visible light in this case).

Observing objects with X-rays

Scientists have already revealed many governing laws and principles using visible light such as sunlight. Hence, intellectual curiosity has shifted to exploring the microscopic world. At SPring-8, we target the atomic and molecular worlds by investigating the properties of materials’ electronic states. To reveal the vast world inside a material, including microscopic phenomena and structures, SPring-8 produces the world’s most powerful X-rays with a high penetrating power. Hence, SPring-8 is like a “giant microscope.”

When observing an object with a light microscope, the field of view darkens as the magnification is increased because the amount of light illuminating the object’s surface decreases as the observation area becomes smaller. Thus, to explore atomic and molecular worlds, well-collimated powerful X-rays, called synchrotron radiation, are necessary (Fig. 1). To realize highly directional powerful X-rays with a sufficient intensity to irradiate a small area, we constructed a large accelerator, called an electron storage ring at SPring-8.

Revealing the microscopic world through large facilities

SPring-8 is located in Harima Science Garden City, western Hyogo Prefecture, Japan. It is comprised of a storage ring built in a large torus-shape building with a 1,436 m circumference.

When bunches of electrons (electron beams) circulate at nearly the speed of light in the storage ring, each electron in the beam emits X-rays (synchrotron radiation). Electromagnets are placed along the orbit to bend the direction of the electron’s motion into a circular orbit, causing the electron beams to emit highly directional powerful X-rays called synchrotron radiation in the direction of the tangent to the circular orbit. At SPring-8, we utilize an accelerator (a storage ring) to produce synchrotron radiation by *intentionally* bending the direction of electron beams.

Synchrotron radiation has the following features:

- **Extremely bright**
- **Highly directional and well collimated**
- **Broad wavelength range spanning infrared light to X-rays**
- **Polarized**
- **Pulsed light blinking with short intervals**

Utilizing these features, we conduct diverse science experiments. Moreover, X-rays (synchrotron radiation) at SPring-8 have additional superior features; they possess extremely high energy and are bright. To obtain these high quality X-rays, we set the circumference of the storage ring to 1,436 m and accelerate electrons up to 8 GeV because higher energy electron beams produce higher energy X-rays. These higher energy X-rays, which are called hard X-rays, have very short wavelengths. The large circumference of the storage ring contributes to the better collimation of electron beams, resulting in highly collimated X-rays emitted from these electron beams. Such highly collimated X-rays can brightly irradiate a microscopically small area.

However, just being bright (possess a large number of photons) by itself is not enough. X-rays must also be well collimated without broadening, in other words, the X-rays must be highly “brilliant,” The large circumference of the storage ring enables undulators (insertion devices) to be placed along the electron beam’s orbit. Our undulators are used to produce powerful synchrotron radiation (Fig. 2), which allows many extraction lines of synchrotron radiation (beamlines). This configuration effectively utilizes this valuable facility. Currently, we can simultaneously conduct experiments at up to 62 locations at SPring-8.

Exploring with synchrotron radiation

What does synchrotron radiation reveal? Typically, when you observe an object sunlight hits it, and then the reflected light enters the lens of your eye to focus the object on the retina. However, X-rays are needed to reveal the microstructure of a material. X-rays emitted from a material irradiated with synchrotron radiation (X-rays) and the state of the material after irradiation provide information on the microstructure of the material.

Observations using X-rays can be divided into two major categories in terms of the underlying physical processes. The first category detects the resulting X-rays upon irradiating a material. X-rays have a high penetrating power and can enter deep into a material, which allows them to interact in various ways with the atoms and molecules and eventually exit with physical information about the material. For example, the resulting diffracted or scattered X-rays provide structural information specific to the material (Fig. 3a). The second category examines a material by physically stimulating it with X-rays. This method includes investigations of X-ray absorption of a material by varying the X-ray energy and analyzing secondary photons or electrons emitted from the material after X-ray irradiation (Fig. 3b). From a practical perspective, observations using X-ray can be divided into five methods.

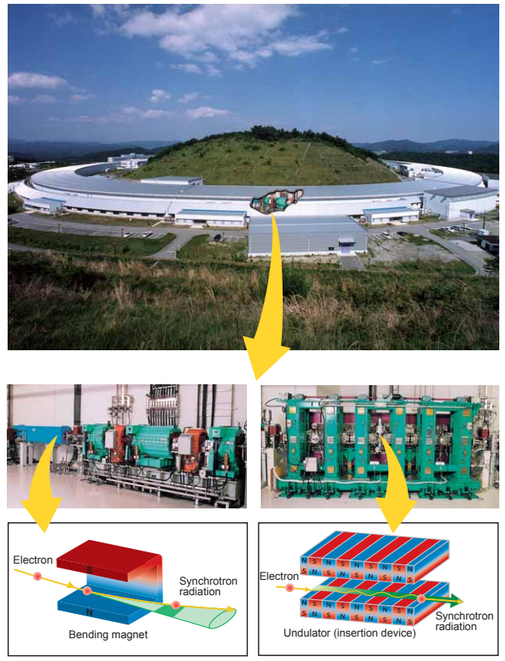

Fig. 2. Bending magnets and undulators (insertion devices), which can each produce synchrotron radiation, are situated in the storage ring.

(1) X-ray diffraction and scattering methods

Because X-rays are a type of light, they behave as a wave. Therefore, X-rays are diffracted (bent and broadened) if the formation of atoms/molecules and the wavelength of X-rays satisfy a particular condition (the Bragg condition) when X-rays are irradiated onto crystal-like materials. Examining the position and strength of diffracted X-rays provides information about the crystal structure. Employing small-angle X-ray scattering (SAXS), in which the scattering angles of the X-rays are extremely small, enables the crystal structure, the behavior of small particles (between 1 nm and 1 μm), and the nonuniform structure of a material to be elucidated.

(2) Imaging

Capturing X-ray transparent images and examining the differences in the material-dependent X-ray absorption rates can yield information about the internal structure of a material. Compared to conventional X-rays, synchrotron radiation, which is highly directional, provides images with a significantly higher resolution. Additionally, micro- or nano-beams, which are produced by further focusing highly directional X-rays, can yield X-ray computed tomography (CT) images of very small objects.

(3) X-ray absorption fine structure (XAFS) technique

Materials partially absorb irradiated X-rays. Varying the X-ray energy may significantly change the absorption rate at a specific energy. Because this change depends on the elements, the electronic states of a particular element and the alignment states of the surrounding atoms in a material can be determined by measuring the absorption rates at various energies.

(4) Photoelectron spectroscopy

Irradiating with vacuum ultraviolet light or soft X-rays causes a material to emit electrons (photoelectrons). Measuring the energy and angular distributions of the emitted photoelectrons via select X-ray energies can elucidate the electronic states on the surface or inside of materials as well as the chemical-bonding states.

(5) X-ray fluorescence analysis

Irradiating with X-rays causes the atoms within a material to emit fluorescent X-rays. Analyzing these fluorescent X-rays can reveal the species and elemental content because the energy of fluorescent X-rays depends on the element.

Giant yet precise SPring-8

SPring-8 produces the world's highest quality X-rays. We believe this is due to the superior performances of various apparatuses and devices, including the accelerators, and because SPring-8 itself is an exact integration of precision machineries in which cutting-edge technologies are incorporated. High quality electron beams are indispensable to produce extremely brilliant X-rays. In fact, electron beams in the storage ring at SPring-8 have excellent quality. Each bunch of electron beams circulating in the storage ring at nearly the speed of light has a flat shape that measures 6 μm and 300 μm in the vertical and horizontal directions, respectively (μm = 10^{-6} m; the thickness of hair is 100 μm) and 4 mm long along the direction of the beam (these values are based on the standard deviation). Additionally, each bunch contains about 10 billion (10^{10}) electrons with 8 GeV of uniform energy and is narrowly clumped to the utmost limit to fit in this tiny volume.

Electron beams circulate 200,000 times per second in the beam pipe, which is composed on an aluminum alloy and has an ellipse-shaped cross-section with a several cm bore. To prevent the electron beams from colliding with residual gases, air pressure in the beam pipe is maintained on the order of ten trillionth (10^{-13}) atmospheres, which is the vacuum level equivalent to satellite orbits in outer space. Additionally, four types of electromagnets are installed to stably circulate electron beams in the storage ring; they include bending magnets to shape and control the electron orbit, dipole magnets to correct the electron orbit, quadrupole magnets to focus the beams, and sextupole magnets to correct energy fluctuations. Together they account for over 1,500 magnets. Each electromagnet weighs on the order of 10 kg to 100 kg. The production error of the magnetic field performance is less then 0.01% and the installation error of the center of each magnet is less than 10 μm relative to the circle.

The electron beams orbit near the speed of light in the storage ring with a circumference of 1,436 m. Their orbits are continuously surveyed by 300 beam position monitors installed along the entire circumference with a measurement error less than 1 μm. By applying this measurement precision, the 1,436-m circumference varies by 10 μm with two cycles a day due to the deformation of the Earth's surface by the tidal force of the moon. This variation is equivalent to being 5 mm off when determining the distance between Tokyo and Osaka (about 500 km). However, our technology is sensitive enough to identify this minute variation.

Although very precise, SPring-8 is a massive world-class research facility. To ensure an extremely high level of stability, SPring-8 was constructed on the rock bed of Mihara-Kuriyama in Nishi-harima, Hyogo by grinding the rock hill to exposure the rock bed. However, even with these efforts, the building where the accelerator is housed expands and contracts due to various reasons, including the effects of sunshine. To avoid such variations, a chassis in which the body of the accelerator and its accompanying equipment are securely placed is physically decoupled from the building. Moreover, preventive measures are taken against temperature and vibrational fluctuations induced by air conditioners and cooling water as these variations can affect performance and cause beam instabilities.

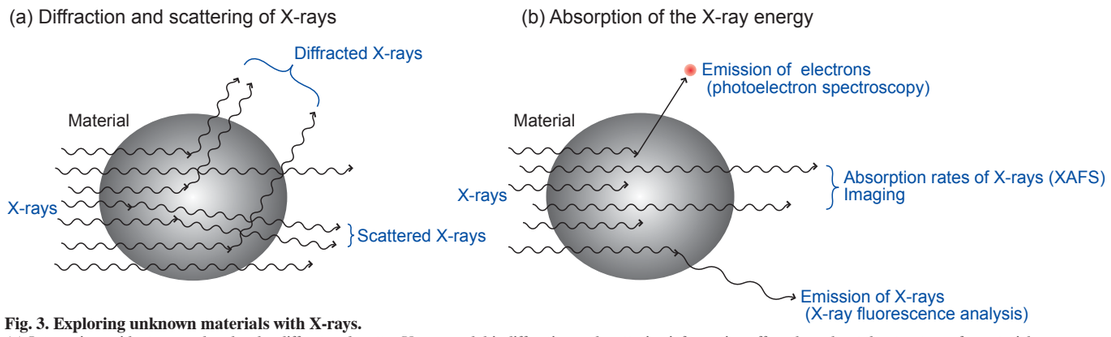

Fig. 3. Exploring unknown materials with X-rays.
(a) Interactions with atoms and molecules diffract and scatter X-rays, and this diffraction and scattering information offers clues about the structure of a material.
(b) Analyzing the X-ray absorption rates or the X-rays and electrons emitted from a material reveals information about the inside of a material.

Special features and contrivances

SPring-8 has two injection accelerators that in combination accelerate electron beams to 8 GeV. Prior to being injected into the storage ring, the electron beams are initially accelerated to 1 GeV by a linear accelerator measuring 140 m in length. The beams are then accelerated to 8 GeV by a booster synchrotron with a 400 m circumference. Even with the ultrahigh vacuum of the storage ring, electron beams are gradually lost and their intensities diminish over time due to disturbances such as the collision of electrons within each electron bunch. Hence, the beams have a finite lifetime, and consequently the brightness of the X-rays decreases. Thus, the loss of the electron beams is compensated to provide a stable X-ray intensity by injecting electron beams whose amounts are equal to the lost beams. (This is called a "top-up operation.") Both the booster synchrotron and that of the storage ring have energies of 8 GeV, which allows the full energy injection from the booster. If these two energies differed, we would have to first reduce the electron energy of the storage ring or dump all the beams in the storage ring before the injection and then accelerate the injected electron beams to 8 GeV in the storage ring, which would interrupt experiments during the injection period.

At SPring-8, extremely brilliant X-rays are produced over a vast wavelength range from soft (long wavelengths) to hard (short wavelengths). To achieve this, insertion devices (5 m in length) are installed on the electron beam orbit of the storage ring. Each insertion device is comprised of many permanent magnets (a few cm wide), which are placed above and below the electron orbit. As electrons pass through each insertion device, they undulate to produce powerful synchrotron radiation (Fig. 2). At SPring-8, we developed world-class technology to produce more powerful X-rays by placing arrays of permanent magnets in an ultrahigh vacuum and by narrowing the gap between the arrays to a few mm. This technology has significantly impacted the world. Additionally, SPring-8 is the only synchrotron radiation facility in the world to have a storage ring with four 25-m long straight sections where several insertion devices are serially installed to produce more powerful X-rays.

In conclusion, SPring-8 integrates numerous highly advanced technologies developed in Japan, such as high-precision processing technology, electronic control technology, civil engineering technology, measurement/monitoring technology, and ultrahigh vacuum technology. These technologies have led to many advances spanning basic science to industrial applications, clearly demonstrating that SPring-8 is a global leader in science and technology (Fig. 4).

This brochure highlights some of achievements realized at SPring-8.

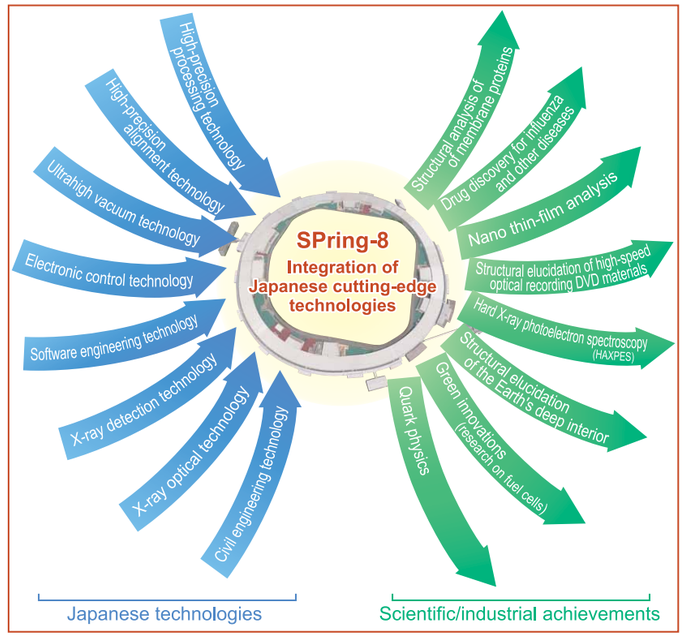

Fig. 4. Japanese technologies that support SPring-8 and various research achievements produced from the integration of these technologies.

Life Science

Exploration of the Mysteries of Life at the Molecular Level

Unparalleled Performance in the Analysis of Protein Structures

Life science research is an important component of basic science. In the life sciences, we explore the mechanisms of biological phenomena. Application of the knowledge obtained from life science research can lead to advancements in medicine, as well as help to solve food and environmental problems. All of these applications are expected to contribute to the improvement of people's lives and the development of the economy.

Biological bodies can be characterized as complex systems comprising numerous molecules, including proteins and DNA. At the same time, they contain multiple 3D layers of well-organized structures, and are capable of functioning in an orderly manner. To investigate such complex systems, we have to develop techniques that are optimized for making measurements at scales appropriate to various objects, ranging from atoms and molecules through intracellular organelles to cells and organs. It is also important to dynamically observe biological events in real time. In order to observe objects at such a broad scale, ranging from the whole body to the molecular level, the field of view for observation must also range from meters to sub-nanometers (Fig. 1). Synchrotron X-rays at SPring-8, which offer a wide field of view and high precision, are especially useful for visualizing biological systems through the interactions between X-rays and the electrons in the objects.

First of all, focusing attention on the molecular level, we find that proteins play a major role in biological phenomena. The unique 3D structure of each protein is responsible for the manifestation of its particular functions. Structural biology is the discipline that investigates the structures and functions of proteins. X-ray crystallography is the most promising technique for precisely determining these structures. The molecular structures of proteins can be determined by analyzing diffraction images obtained by subjecting crystallized proteins to X-rays (Fig. 2).

There are tens of million kinds of proteins, but their basic constituent structural components are believed to be less numerous, on the order of ten thousand. After the completion of the decoding of the human genome, the Protein 3000 Project was launched in 2002 as a national project in Japan. The aim of this project was to establish a research foundation to reveal the 3D structures and functions of proteins by strategically allocating resources. Structures of about 3,000 proteins, which account for one-third of the total, were targeted for investigation. This project promoted the establishment of appropriate intellectual property rights and technology transfer, with the goal of becoming the world leader in generating results and developing applications for these research findings. Since proteins are involved in the onset of many diseases, the exploration of their structures and functions is expected to accelerate the development of new drugs. This project is aimed at translating research outcomes into clinical advances that will benefit people's health and longevity over the long term. SPring-8 played a central role in this project, which was completed in 2006. More than 80% of protein structures registered to the international Protein Data Bank (PDB) are obtained from X-ray crystallography; and SPring-8 contributed to 65% of the structures submitted from Asia. The latter figure strongly emphasizes the importance of SPriong-8 in the analysis of protein structure.

The crystallization of proteins is indispensable in the analysis of the 3D structures of proteins. However, the crystallization itself remains challenging. It is even more difficult to obtain large protein crystals suitable for determining structures. It is especially hard to obtain good crystals for many membrane proteins and protein complexes, which play important roles in the understanding of biological phenomena and the development of new drug. Precise structural information can be obtained even from small protein crystals by using extremely brilliant synchrotron X-rays produced at SPring-8. These X-rays have been contributing to many breakthrough research projects by revealing the structures of proteins that are difficult to crystallize, such as rhodopsin, as well as the structures of calcium pumps, gap junction channels, and bacterial flagellar proteins (flagellins). Following on the successes of the Protein 3000 Project, a successor project was initiated: the Targeted Proteins Research Program, which aims to reveal the structures and functions of selected important proteins. To support this new project, we constructed the RIKEN Targeted Proteins beamline (BL32XU), which can produce narrow X-ray beams with a beam size of ~1 μm (10^{-6} m) in diameter (microbeams), to analyze even smaller crystals. BL32XU has been in full operation since May 2010. Hence, we expect further advancement in the structure analyses of proteins that have heretofore been difficult to analyze.

Visualizing Objects ranging from a Single Molecule to Organs

On the other hand, how can we investigate biological phenomena in real time? The crystal structures of proteins are static, but we can study their dynamic functions by applying the following technique: first, the movement of a protein is halted at several stages, in order to capture its structure at each stage; next, the captured structures are sequentially combined. Dynamic functions of calcium pumps have been described using this technique. Other features of proteins, which cannot be determined by crystal analysis alone, can also be elucidated by combining crystal analysis with other techniques, e.g., the combination of crystal analysis with electron diffraction; this technique has demonstrated its tremendous potential in the analyses of gap junction channels and flagella.

Direct observation of the behavior of proteins in solution is also an important way to examine their functions. X-ray solution scattering is a suitable technique for observing the dissociation and association of molecules as well as their macroscopic structural changes. Taking advantage of the features of this technique, we revealed the underlying mechanisms of the bacterial clock system by purifying several molecules out of the complex system and observing them in solution.

These techniques amplify the interactions of X-rays and electrons by treating multiple molecules collectively to produce a state that can easily be detected; thus, high-resolution images can be obtained. However, the description of the functions of each individual molecule is still difficult. To overcome this difficulty, new measurement techniques have been developed to directly observe the real-time functions of a single molecule by labeling it. The real-time movement of potassium channels has been observed by tracing the X-ray diffraction signals emitted from small gold crystals that are attached to proteins.

Additionally, the motion of molecules in the living bodies has been explored by using powerful X-rays at SPring-8. The functions of myosin, which is a protein responsible for myocardial contraction, were difficult to observe using existing techniques. At SPring-8, X-ray diffractions from myosin have been detected by transmitting X-rays through the hearts of live mice. This achievement can be applied to the diagnoses of cardiac dysfunction.

Transmission X-ray imaging is also indispensable beyond the cell level, in observations at the organ level. Refraction contrast imaging, synchrotron X-ray CT imaging, and micro CT imaging using X-ray microbeams can yield higher resolution images than those obtained from the conventional medical X-ray imaging commonly used in hospitals. Additionally, phase-contrast X-ray CT imaging, in which the wavefront distortion (phase contrast) is measured, can clearly reveal the structures of the rat brain. Furthermore, X-ray imaging of organs such as the hearts or lungs of live small animals, whose motions are rhythmic and extensive, can be enabled by synchronizing the timing of image capture with heartbeat or breathing. Real-time movement of the lungs of newborn rabbits has been observed using refraction contrast imaging. SPring-8 is the only facility in the world that enables such high-resolution measurement of the lungs.

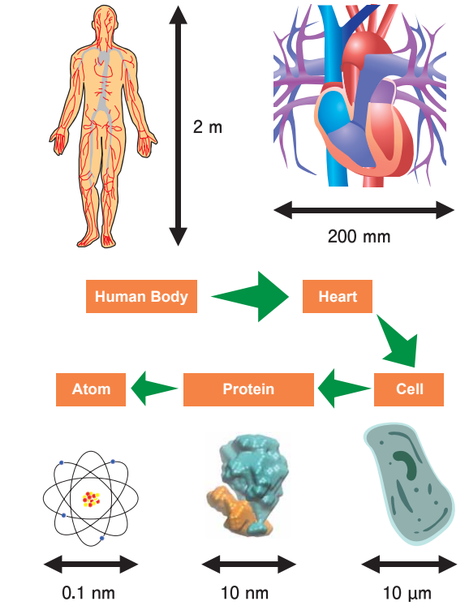

Fig. 1. Organisms and scales.

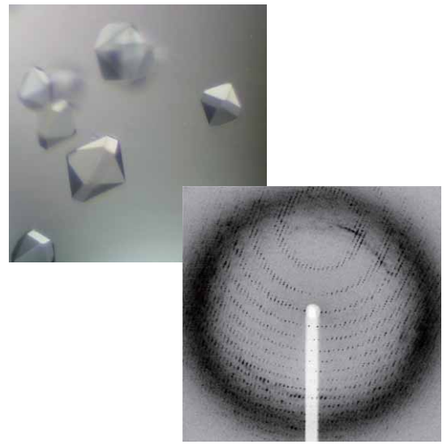

Fig. 2. Protein crystals (top) and diffraction image of proteins (bottom).

Exploration of the Behavior of Proteins in Biological Membranes

A cell, the basic unit of life, is encapsulated by a phospholipid bilayer called the cell membrane. Subcellular organelles such as nuclei and mitochondria are also enclosed by phospholipid membranes. These membranes contain various membrane proteins that account for one-third of all types of proteins, and which function in diverse ways. For example, membrane proteins expel sodium ions from cells, and bring potassium ions in, upon neural excitation. Investigation of the structures and functions of these membrane proteins, which are embedded in cell membranes and difficult to handle, is extremely challenging and regarded as a major target in biology. SPring-8 has visualized the structures of many membrane proteins, in order to lead the advancement of medicine and pharmacology.

Success in the Visualization of the Structure of Rhodopsin

Rhodopsins, vision sensor molecules contained in the retina, receive visual signals that contain a great deal of information. Rhodopsins are a member of the guanine nucleotide-binding protein-coupled receptor (GPCR) family. GPCRs function in many contexts as ultra-high sensitive sensor membrane proteins, and are responsible for the successive activation of numerous functions by sensitively responding to subtle signals such as visual/olfactory stimuli or immune signals.

Dr. Masashi Miyano (Chief Scientist, RIKEN Harima Institute, Japan)[1], Dr. Krzysztof Palczewski, (Professor, Washington University, the United States), and colleagues have been performing structural analyses of bovine rhodopsins. “About 80% of all GPCRs are similar in structure to rhodopsins, but structural analyses have not advanced far because crystallization of rhodopsins is difficult and the reproducibility of rhodopsin crystals is poor,” commented Dr. Miyano.

As expected, the crystallization of bovine rhodopsin was extremely difficult, but Dr. Tetsuji Okada (Washington University)[2] succeeded after 5 years of dedicated research at RIKEN and Nagoya University, Japan. In the spring of 2000, Dr. Masaki Yamamoto (RIKEN)[3] and colleagues conducted X-ray diffraction experiments to analyze a few tens of these crystals at the RIKEN Structural Biology I beamline (BL45XU), which is optimized for multi-wavelength anomalous diffraction (MAD). MAD is a wavelength-dependent measurement technique of X-rays scattered by atoms; the method allows us to analyze even a single crystal of protein by labeling it with mercury.

This research group determined the structures of rhodopsin and the vitamin A derivative retinal, which is complexed with rhodopsin (Fig. 1). Bovine rhodopsin has seven α-helices; an α-helix is a building block of protein consisting of amino acids in a spiral conformation. These seven α-helices penetrate the cell membrane; the last α-helix is shortened by a 90° bend. Many of the mutations that cause visual disorders have been identified as mutations of amino acids in the hydrogen bonding moieties that stabilize the gaps between these α-helices.

The results of these research findings were published in Science (August 2000) and received a highly commendable evaluation from the journal’s reviewers as the most important paper in this research field in the last 15 years. This paper has been cited for more than 2,700 times, making it one of the most cited papers in the world.

Surprisingly, half of the drugs currently being developed are targeting GPCRs. These findings relate to the structure of rhodopsin, which is a representative GPCR, and is therefore expected to be a basis for drug development.

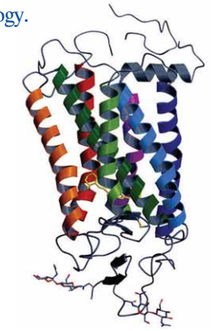

Fig. 1. Crystal structure of bovine rhodopsin.
Seven α-helices penetrate the cell membrane, and there is a short helix that is bent by 90°. Yellow molecules indicate retinal.

For this achievement, Dr. Miyano and Dr. Okada received the Prize for Science and Technology (Research Category) by the Minister of Education, Culture, Sports, Science and Technology of Japan in 2010.

Exploring the Structures of Calcium Pumps

Muscle cells contain bag-shaped sarcoplasmic reticula, which store calcium. Muscle fibers contract when calcium is released from the sarcoplasmic reticula, while they relax when calcium returns. Integration of these calcium transfer processes induces muscle motion. However, calcium concentration in the sarcoplasmic reticula is 10,000 times higher than the concentration outside, and thus it is easy for calcium to exit but difficult for it to return against the concentration gradient. The calcium pumps in the sarcoplasmic reticula are also membrane proteins. Calcium pumps are driven by the energy that is released when adenosine triphosphate (ATP) is hydrolyzed.

According to Dr. Chikashi Toyoshima (Professor, The University of Tokyo, Japan), he and his colleagues were conducting research on calcium pumps with the goal of clarifying the atomic structures of calcium pumps. In 1996, they succeeded in the crystallization of calcium pump proteins, for the first time in the world. They continued structural analyses of these crystals with high-performance electron microscopes. At the time, however, the resolution was limited to a level at which secondary structures, such as α-helices were barely observable; atomic resolution was not available.

SPring-8 started up around this time, and Dr. Toyoshima tried to analyze his crystals by applying X-ray diffraction techniques. In the autumn of 1998, he began his experiment on calcium pump crystals at the RIKEN Structural Biology I beamline (BL41XU). Although the thickness of the crystals was only several micrometers, not thick enough for X-ray analyses, he obtained potentially promising results from this first experiment. Therefore, he expected his goal would be achieved once thicker crystals became available. Since then, the quality of data had been improved as thicker crystals have been obtained.

In June 2000, they finally succeeded in collecting high-resolution diffraction data at 0.26 nm (1 nm = 10^{-9} m) to elucidate the 3D structures of pump proteins, both when they were coupled with calcium and when they were not. The detailed research results were reported in *Nature* (June 2000), and the world first 3D structure image of calcium pumps appeared on the cover of the journal.

Subsequently, in August 2002, this research group revealed the structures of calcium pumps after the transport of calcium. The calcium pump was found to consist of ten α-helices and three cytoplasmic domains (A, N, P). These α-helices are arranged in a configuration resembling the staves of a wooden barrel. One of the α-helices works like a piston to release the coupled calcium; the whole calcium pump moves extensively. No scientists had imagined that membrane pumps would work so similarly to a hand-pump.

Dr. Toyoshima and colleagues elucidated the four-stage mechanisms of calcium pumps (Fig. 2); the detailed results were published four times in *Nature* (June 2000, August 2002, June and November 2004). This achievement is comparable to the discovery of the sodium pumps with similar mechanisms, which were recognized with a Nobel Prize. Dr. Toyoshima received the Asahi Prize in 2009 for elucidating the mechanical operation of the calcium pump.

Gap Junction Channels that Interconnect Cells

Cells function by closely collaborating with each other. For example, heart muscle cells keep pace with each other in order to make the heart beat regularly. The key to this synchronization is the gap junction channel, which is also a membrane protein. The gap junction channel directly interconnects two cells like a bridge.

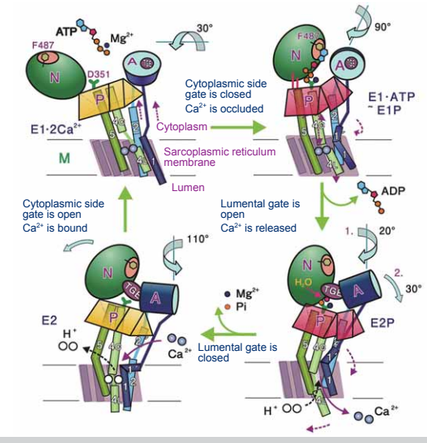

Fig. 2. Schematic images of the calcium pump mechanisms.
Bottom left: Three domains are standing in groups in the absence of calcium. Top left: Domains are open when calcium ions are bound with pump proteins. Top right: N-domain approaches the P-domain; ATP connects the N- and P-domains; and the A- and N-domains are also connected. The A-domain and M1-helix occlude the entrance to the pump. Bottom right: A-domain rotates; the M1-helix changes direction; the bottom half of the M4-helix changes direction; and the lumenal gate opens. Furthermore, the P-domain tilts, the M5-helix bends; and the M3- and M4-helices come down like a piston to eject calcium ions.

In 2007, a Kyoto University group found, by using electron microscopy, the structure of a closed gap junction channel. Subsequently, Dr. Tomitake Tsukihara[4] (Professor, The University of Hyogo, Japan) and colleagues discovered the structure of an open gap junction channel, through X-ray crystal structure analyses at SPring-8. “The gap junction channel has a shape similar to that of a Japanese hand drum, and has a 1.4-nm hole along the longer axis of the channel molecule. This hole allows small molecules and ions to go through the channel,” reported Dr. Tsukihara.

In the closed gap channel, there is a structure at the upper end that was speculated to block the channel. However, no such blocking structures were found on the channel in the open state; instead, six short α-helices formed the funnel-like structure (Fig. 3).

These research results were published in *Nature* (April 2009). More than 20 constituent proteins that construct gap junction channels have been discovered in humans. Variant proteins that have similar structures to these gap junction channel proteins are thought to cause many diseases; the exploration of their structures is expected to provide clues that will help us to develop effective therapies for these diseases.

[1] Currently Professor at Aoyama Gakuin University, Japan.
[2] Currently Professor at Gakushuin University, Japan.
[3] Currently a director of the Basic Research Division, RIKEN.
[4] Also Professor Emeritus at Osaka University, Japan.

References

1. K. Palczewski, T. Kumasaka, T. Hori, C. A. Behnke, H. Motoshima, B. A. Fox, I. Le Trong, D. C. Teller, T. Okada, R. E. Stenkamp, M. Yamamoto and M. Miyano; *Science*, **289**, 739 (2000)
2. C. Toyoshima, M. Nakasako, H. Nomura and H. Ogawa; *Nature*, **405**, 647 (2000)
3. C. Toyoshima and H. Nomura; *Nature*, **418**, 605 (2002)
4. C. Toyoshima and T. Mizutani; *Nature*, **430**, 529 (2004)
5. C. Toyoshima, H. Nomura and T. Tsuda; *Nature*, **432**, 361 (2004)
6. S. Maeda, S. Nakagawa, M. Suga, E. Yamashita, A. Oshima, Y. Fujiyoshi and T. Tsukihara; *Nature*, **458**, 597 (2009)

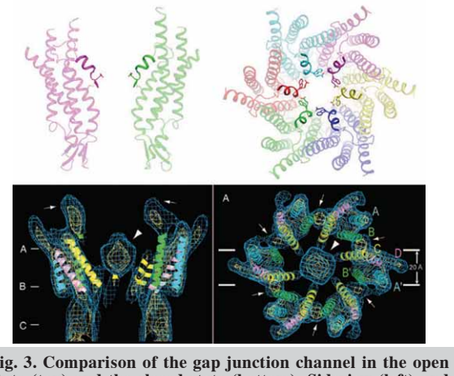

Fig. 3. Comparison of the gap junction channel in the open state (top) and the closed state (bottom). Sideview (left) and overhead view (right).
Six short α-helices that form a funnel-like structure have been identified at the upper part of the channel, but no structures block the channel path in the open state (top). In contrast, some structures can be seen in the center of the gap channel in the closed state; these structures are speculated to block the channel (Bottom: these figures are reproduced from A. Oshima et al., *Proc. Natl. Acad. Sci. USA* 2007 104(24)).

Elucidation of Ultimate Switching Mechanisms Hidden in Protein Molecules

Bacteria such as *Salmonella* and *Escherichia coli* move by rotating several flagella, which are similar to propellers. The flagellum comprises a rotary motor, bearing, and a rotating shaft at the base. The flagellar filaments rotate at 200–400 revolutions per second, like a propeller, allowing bacteria to move a distance 20 times larger than their body size each second. In humans, this would correspond to a speed of 100 km/hour. The flagellum is a powerful yet delicate nanomachine. The switching mechanisms of constituent protein molecules also enable bacteria to quickly change direction. At SPring-8, we have elucidated, for the first time, the switching mechanisms of the flagella, which are the ultimate energy-efficient ecological machine and can provide many clues to developing nanotechnology.

Crystal Structure Analyses of Proteins at the Atomic Level

A flagellar filament is comprised of a cylindrical bundle of eleven long, thin protofilaments, which are 20 nm (1 nm = 10^{-9} m) in diameter and 10^{-15} μm (1 μm = 10^{-6} m) in length (Fig. 1). Each protofilament is an assembly of a single protein, flagellin, with a molecular weight of about 50 kDa[1]. If all the flagellin molecules were to have equal size and shape, flagella filaments would only assume a linear conformation, and no propelling power would be produced even if the flagellar motor is rotating at high speed. However, bacteria can move freely and change direction quickly. This is achieved via the conformation of the left-handed helical structure of flagella, which are slightly twisted due to the existence of protofilaments with slightly different sizes (5.19 nm and 5.27 nm in the intersubunit distance).

When a flagellar motor rotating at high speed inside a cell membrane suddenly reverses its direction, flagella filaments are twisted, and the structures of several protofilaments are modified to change the helix from left-handed to right-handed. Then, flagella that are bundled together when moving straight are unraveled, and the propelling force becomes unbalanced; this results in a change in the direction of movement. This quick directional change is enabled by a very small, sub-nanoscale difference (0.08 nm) in the intersubunit distances of flagelin.

Many scientists around the world who aim to develop nanomachines have been intensely studying flagella. The secondary structure distributions and alignment patterns of flagellar filaments had been elucidated, but the high-precision switching mechanisms remained to be identified. To clarify the mechanisms, detailed structure determination was required.

In August 1996, Dr. Kei-ichi Namba[2] (the research director of the Advance Technology Research Laboratories, Matsushita Electric Industrial Co., Ltd., Japan.) led the Namba Protonic Nanomachine Project[3] to explore the frontiers of flagellar research. "We tried to elucidate the 3D structures of flagellin molecules but the size of the flagellin crystal samples was at most a few micrometers, with which we had no hope of obtaining reliable data using conventional X-ray sources at that time," recalled Dr. Namba, looking back on that time.

Then, they decided to use highly brilliant X-rays at SPring-8, which offered the world best analyzing power, for their experiments.

However, they faced another difficulty. Determination of the 3D structures of flagellin molecules requires crystal molecules to be perfectly aligned. Crystallization of flagellin molecules was difficult, since they tend to be polymerized in a long fibrous form. To overcome this difficulty, they removed the domains important for fiber formation and structure stabilization from flagellin molecules of *Salmonella* flagella. Removal of these domains yielded a 41-kDa fragment (F41) that lacked fiber formation capability. Using this fragment, they succeeded in preparing high-quality crystal samples.

In February 1998, the researchers started experiments on these samples, applying the multi-wavelength anomalous diffraction (MAD) technique at the RIKEN Structural Biology I beamline (BL45XU). MAD is a method of analyzing crystal structures, based on the fact that the strength of X-rays scattered off of a specific type of atoms in protein crystal samples depends on the wavelength of irradiated X-rays. "We faced crushing difficulties in obtaining good data from these crystal samples, since they were in thin plate-shape and only a few micrometers in thickness. After undertaking tireless efforts to keep the samples flat after freezing, we finally determined the structure of flagellin molecules with 0.2-nm resolution," recalled Dr. Namba.

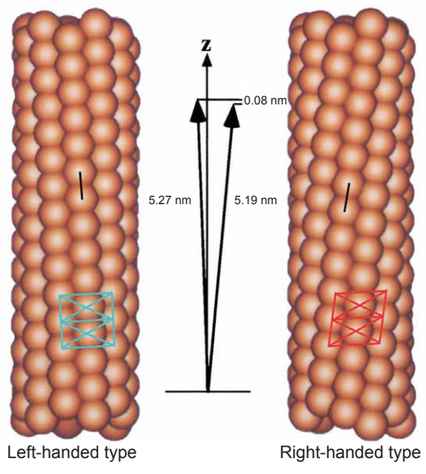

Fig. 1. Two states of flagellar filaments, each of which comprises eleven protofilaments Flagellin molecules are depicted in particle-shape.
The intersubunit distance of protofilaments is ~5.2 nm. However, that of the right-handed form and that of the left-handed form differ by 0.08 nm. This difference enables the conformation of a curved and twisted helical propeller.

Reproduction of Switching Actions using Computer Simulation

F41 consists of three domains: D1, D2, and D3. Domain D1 comprises three long α-helices and a β-hairpin. An α-helix has a structure in which the polypeptide backbone (the basic building block of proteins) are folded in right-handed helical form, whereas a β-hairpin has a structure in which the polypeptide backbone is sharply bent, like a hairpin. Domains D2 and D3 mostly comprise β-sheets and β-hairpins. Surprisingly, the conformation of flagellar protofilaments could be observed in the crystal, which had not been expected because the monomers are crystallized. The protofilament forms a sheet structure by alternatively overlapping to conform with the shape of the crystal.

Additionally, this research group performed computer simulation studies on the behavior of flagellin molecules, in order to examine the switching structures of protofilaments in further detail. A computer model of protofilaments consisting of three flagellin molecules was constructed. The bottom molecule was pulled down step-by-step in 0.01-nm increments, with the top molecule staying fixed, in order to observe structural deformations of the middle molecule under tension. In the beginning, the middle flagellin molecule was only stretched gradually. However, at a certain point, β-hairpins in the areas where two molecules contact each other changed their structure slightly but suddenly (Fig. 2). "This finding indicates that there is a switch that is responsible for changing the intersubunit distance by 0.08 nm in the structure near the hairpins," said Dr. Namba. This is exactly the moment when the "0.08 nm shift" of flagellin molecules was revealed at SPring-8. Thus, Dr. Namba and colleagues had finally discovered the sophisticated mechanical switch hidden in flagellin molecules.

"Flagellin molecules are not special proteins. In our study, we demonstrated one example of a sophisticated action mechanism by which many proteins function," said Dr. Namba.

Nanotechnology researchers are investigating the structures and functions of proteins, since proteins behave as nanomachines and share many design principles. Therefore, the amazing mechanisms of proteins serve as a model for artificial nanomachines. By elucidating the 3D structures of proteins that function as nanomachines, we will better understand the design principles of highly flexible and sophisticated nanomachines. Analysis technologies offered by SPring-8 are driving extensive exploration of the nanoscale world.

This achievement of the ERATO Namba Protonic Nanomachine Project that elucidated the high-precision switching mechanisms of protein molecules was published in *Nature* (March 2001). The 3D structure of rotating flagellar filaments appeared on the journal's cover.

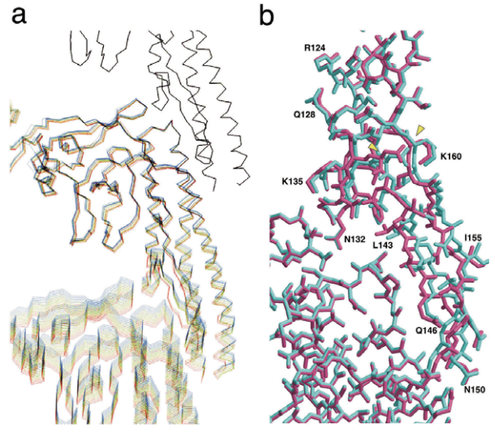

Fig. 2. Computer simulation of switching actions.
a. Computer simulation of a protofilament consisting of three flagellin molecules. Structure changes of flagellin molecules, which contribute the high precision switching that changes the intersubunit distance of protofilaments, are depicted. The bottom molecule is gradually pulled down at 0.01-nm intervals, while the top molecule remains fixed. This process is intended to stretch the protofilament and add mechanical stress to the middle molecule. Simulated images of twelve steps are overlaid every 0.05 nm by color-coding these steps with rainbow colors ranging from blue to red. Entire molecules are gradually stretched in the first nine steps (total stretch of 0.45 nm) but clear structural changes around β-hairpins can be observed between steps 9 and 10 (total stretch of 0.5 nm).
b. Magnified views of β-hairpins and surrounding areas where structural changes are observed. Two images before (cyan) and after (dark pink) the switching are overlaid. Only the β-hairpins (a structure stretching from middle right toward bottom right; from N132 to K160 via L143, Q146, N150, and I155) of the upper flagellin molecule show sudden structure changes, suggesting the existence of switching actions in this area.

[1] 10^3 Da (molecular mass unit)
[2] Currently Professor at Osaka University, Japan.
[3] The Exploratory Research for Advanced Technology (ERATO), Japan Science and Technology Agency.

Reference
1. F. A. Samatey, K. Imada, S. Nagashima, F. Vonderviszt, T. Kumasaka, M. Yamamoto and K. Namba; *Nature*, **410**, 331 (2001)

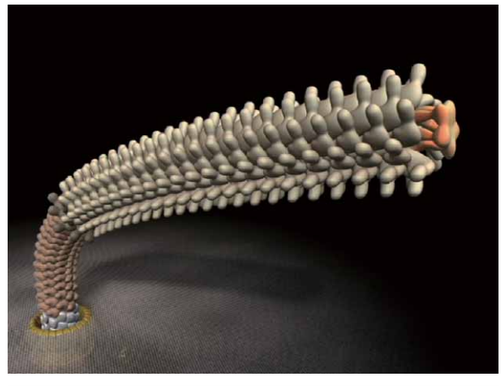

Fig. 3. Computer graphic image of a flagellum.
A flagellum consists of ring and helix structures in which ~30 kinds of constituent protein molecules self-assemble to form a cluster. The number of molecules in each cluster ranges from several for the smallest to tens of thousands for the largest. The well-organized self-assembly process of these structures also provides clues that will be invaluable in the development of nanomachines.

Clarification of Mechanisms How the "Biological Clock" of Cyanobacteria Ticks

Many organisms on Earth have precise biological clocks; humans also possess an intrinsic chronometer, which acts like a metronome for our biological functions. Organisms conduct essential biological functions, such as metabolism and photosynthesis, according to a circadian rhythm with a 24-hour cycle. A group of proteins called "clock proteins" control these biological clocks. Numerous species of organisms are used to research these clock proteins. Highly brilliant X-rays at SPring-8 can visualize real-time changes in clock proteins of cyanobacteria (the simplest form of organisms with biological clocks), which had never been expected to be possible. This achievement will open up a new dimension for the basic research on biological clocks, including the relationship between biological clocks and diseases.

The Principle of "Clocks" is the Assembly and Disassembly of Three Types of Proteins

Clock functions of cyanobacteria are governed by proteins called "Kai." There are three types of Kai proteins: KaiA, KaiB, and KaiC. KaiC plays a role of the "clock pendulum," and its state varies according to its interactions with the other two Kai proteins.

Adenosine triphosphate (ATP) plays an important role in these interactions. ATP is an essential component that organisms use to store and utilize energy; it is often referred to as the "energy currency" of the cell. Energy is stored when adenosine diphosphate (ADP) is converted into ATP, and released when ATP is converted into ADP. In a process called phosphorylation, ATP-derived phosphates are transferred to specific proteins, modifying their structures and functions.

In cyanobacteria, KaiA induces phosphorylation of KaiC, and KaiB suppresses the functions of KaiA, which induces dephosphorylation of KaiC. KaiC is "oscillating" through phosphorylation and dephosphorylation by using ATP as an energy source. It is an amazing biological phenomenon that only three types of proteins govern the stable ticking of this cellular clock.

To elucidate this astonishing mechanism, the structures of the Kai proteins need to be revealed. The 3D structure of each Kai protein has been individually determined, but the structure of their composite form has yet to be explored. The difficulty lies in the fact that the complex is constantly changing its size and shape, instead of maintaining a stable binding state. Since such assembly and disassembly phenomena cannot be observed by static measurements, the existing techniques of structural biology is of only limited use for this purpose.

Sophisticated Collaborative Work between KaiA and KaiB

In October 2005, Dr. Shuji Akiyama[1] (a researcher in the Precursory Research for Embryonic Science and Technology funded by the Japan Science and Technology Agency) and Dr. Yuichiro Maeda[2] (Chief Scientist at RIKEN, Japan) led a research group to address the challenge of studying the Kai complex using the RIKEN Structural Biology I beamline (BL45XU).

First of all, KaiA, KaiB, and KaiC were incubated with ATP to initiate the phosphorylation cycle. A constant quantity of samples was extracted from this incubation solution every three hours. The fraction of KaiC that was phosphorylated by ATP was quantitated using a portion of this extracted sample solution.

The remainder of each extracted sample solution was irradiated with X-rays at BL45XU for 72 hours, and small-angle X-ray scattering (SAXS) data were taken. SAXS is an experimental technique in which scattered X-rays are detected at very low angles to obtain information about the structures of samples at the level of a few nanometers (1 nm = 10^{-9} m). Scattered X-rays were captured with X-ray cameras, and the intensity and angular distribution of scattered X-rays were obtained from the recorded X-ray images in order to determine the composition of the structures of the Kai proteins.

These measurements revealed that the intensity of the scattered X-rays in the forward direction (scattering intensity at the origin) was robustly oscillating with a 24-hour cycle. This indicates that the Kai proteins are continually assembling and disassembling in solution. Additionally, it was revealed that the phosphorylation state of KaiC was oscillating with a 24-hour cycle (Fig. 1). "Interestingly, the phosphorylation process preceded the timing of the increase and decrease of the weighted-average molecular weight (Mw) of the sample by a quarter cycle. We conducted similar experiments on the system lacking KaiA and KaiB to investigate the cause of this phase difference," said Dr. Akiyama.

The timing of the interactions between KaiC and KaiA significantly differs from that of between KaiC and KaiB, which proceeds in the following manner. When the three types of Kai proteins are mixed, KaiA first quickly binds KaiC and phosphorylates it. After the phosphorylation of KaiC is completed,

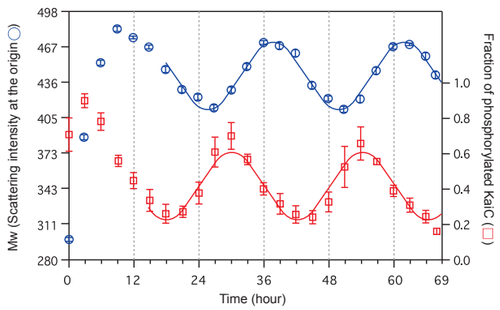

Fig. 1. Time courses of the assembly and disassembly processes of the Kai proteins measured with SAXS.
The left axis represents the weighted-average molecular weight (Mw) of samples, estimated from the intensity of the scatted X-rays (scattering intensity at the origin); the right axis represents the fraction of phosphorylated KaiC (phosphorylated state) measured at the same time. The phosphorylated state precedes Mw by a quarter cycle.

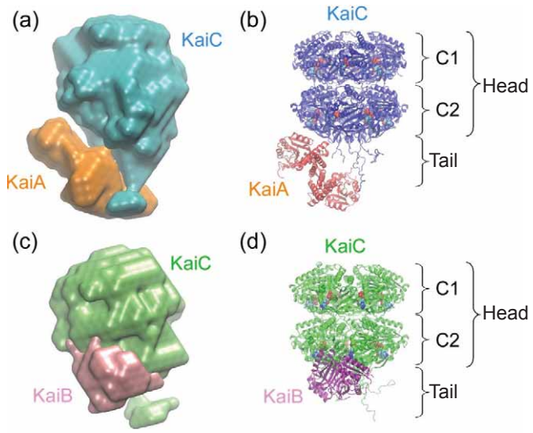

Fig. 2. Model structures of Kai protein complexes.
KaiA and KaiB interact with the C2 domain and tail region of KaiC.

KaiB slowly binds KaiC to dephosphorylate it, and then dissociates from KaiC. The combination of the quick process involving KaiA and the slow process involving KaiB induces the phase difference.

Furthermore, this research group elucidated the structures of the KaiA–KaiC and KaiB–KaiC complexes, which are produced during assembly and disassembly processes, by examining the molecular shape of these two complexes based on the information obtained from the SAXS measurement (Fig. 2).

The size of the KaiA–KaiC complex is 15 × 15 × 11 nm. KaiC occupies 80% of the total volume and consists of a spherical head region, which has a cavity in the center, and a short tail region. The head region of KaiC is divided into two domains: C1 and C2. The remaining 20% of the complex, which corresponds to KaiA, is clustered near the tail.

The size of the KaiB–KaiC complex measures 14 × 13 × 10 nm, slightly smaller than the KaiA–KaiC complex. Similar to the KaiA–KaiC complex, the structure characteristic to KaiC can be observed in the KaiB–KaiC complex. KaiB, which occupies 13% of the entire volume, is acting on the C2 domain.

These molecular structures discovered through SAXS are consistent with the structures of individual Kai proteins that were determined by other research groups; therefore, it can be concluded that the determination of the complex structures proceeded smoothly. Finally, Dr. Akiyama and colleagues have used visualization methods to elucidate, for the first time, the real-time assembly/disassembly dynamics of the Kai proteins. The results of their studies on the crystal structures of the biological clocks of cyanobacteria was published in *Molecular Cell* (March 2008).

True Identity of the "Clock Pacemaker"

"We identified gears that play the role of pacemakers to control the ticking of the biological clock. We believe this is a more important achievement than the visualization," said Dr. Akiyama. The next question then, is "Where is the pacemaker?"

This research group paid attention to the fact that amino acids that are to be phosphorylated are localized in the C2 domain of KaiC; the interactions with KaiA and KaiB are induced in the C2 domain and tail region of KaiC as well. These facts indicate that KaiC alters the structures of the C2 domain and tail region, according to its own phosphorylation state, to pull or repel KaiA and KaiB and then to control the timing of the reactions (Fig. 3). KaiC, which seems to be driven by KaiA and KaiB, is actually the pacemaker.

How can KaiC keep such a precise timing? To answer this question, it is necessary to elucidate the mechanisms of the structure changes of KaiC in solutions. This research group, now armed with SAXS, will investigate the mechanisms by which KaiC exerts its functions as a pacemaker. The mechanisms of the biological clocks of humans will also be elucidated eventually. When that is achieved, the development of breakthrough therapies for sleep disorders caused by biological rhythm dysfunction will no longer be a dream.

[1] Currently Associate Professor at Nagoya University, Japan.
[2] Currently Professor at Nagoya University, Japan.

Reference
1. S. Akiyama, A. Nohara, K. Ito and Y. Maéda; *Molecular Cell*, **29**, 703 (2008)

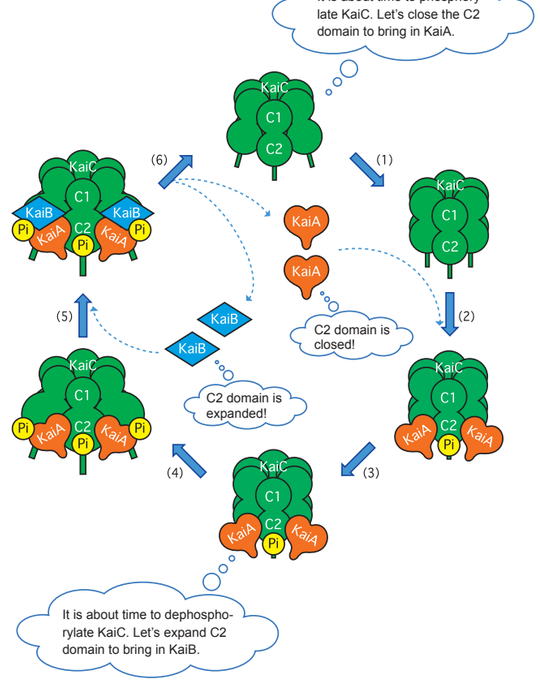

Fig. 3. Assembly and disassembly model of the Kai proteins.
KaiA, orange heart; KaiB, blue diamond; KaiC, green barrel; phosphate, "Pi." (1) KaiC alters the C2 domain structure to bring in KaiA. (2) KaiA binds KaiC. (3) KaiC is phosphorylated. (4) KaiC further alters the C2 domain structure to bring in KaiB. (5) KaiB binds the KaiA–KaiC complex. (6) KaiC is dephosphorylated; KaiA and KaiB dissociate from KaiC.

Detection of the Precise and Dynamic Conformational Changes of Channel Molecules

Cells contain various kinds of pore-forming proteins, termed channel molecules, that penetrate the cell membrane. These channels regulate the flow of ions across the membrane by receiving various stimuli. The total number of channel molecules on the cell membrane of a single cell may reach a maximum of 200,000–300,000. Potassium channels are representative channel molecules through which only potassium ions can selectively flow. These proteins are found in cells of a wide variety of organisms, ranging from bacteria to humans. Various diseases, including sudden infant death syndrome, are caused by dysfunctions of ion channels. To contribute to the development of therapies for such diseases, many researchers around the world are studying the mechanisms of channel molecules around-the-clock. In particular, experiments conducted at SPring-8 have succeeded for the first time in visualizing the detailed real-time motion of the opening and closing of channel molecules. These findings have captured the world's attention.

"Video Images," not Still Images, are Required

Potassium channel molecules quickly take in or block only potassium ions upon receiving stimuli. By what mechanisms do potassium channel molecules regulate the flow of potassium ions?

Dr. Erwin Neher, a German biophysicist, and Dr. Bert Sakmann, a German physiologist, established a technique for isolating a single ion channel molecule and measuring its electronic properties. For their achievements, they received the Nobel Prize in Physiology or Medicine in 1991.

Dr. Roderick MacKinnon, an American neurophysiologist, revealed the three-dimensional structures of potassium channel molecules, and received the Nobel Prize in Chemistry in 2003. However, only a few studies have been conducted to reveal the three-dimensional structures of protein molecules in biomembranes (membrane protein).

In October 2001, a project called "Research on *in vivo* dynamic structures and functions of proteins using diffracted X-ray tracking (DXT)" was initiated as part of the Core Research for Evolutional Science and Technology (CREST) project, funded by the Japan Science and Technology Agency (JST). Dr. Yuji Sasaki[1] (Senior Scientist, JASRI) led a group to conduct this project. Also participating were Dr. Shigetoshi Oiki (Professor, Fukui University School of Medicine) and Dr. Hirofumi Shimizu (Assistant Professor, Fukui University School of Medicine). An important target of this group was to explore the dynamic structures of potassium channel molecules by detecting the real-time motion of potassium channel molecules.

In 1997, Dr. Sasaki invented the "DXT method," for which he received the IBM Japan Science Prize in 2007. In this method, a gold nanocrystal is first bound to a single potassium channel molecule. This gold nanocrystal that he developed is a layered crystal 20 nm (1 nm = 10^{-9} m) in thickness. Unlike conventional crystals, from which many diffraction spots are produced by the diffraction of X-rays, this crystal provides only one or two diffraction spots from each crystal. The crystal is exposed to X-rays, and the movement of the target molecule is determined from the movements of diffraction spots emitted from the gold crystal. Dr. Sasaki, an expert on measurement, sought applications of this method and found potassium channels. "The static structures of potassium channels had been determined, but their dynamic mechanisms had not been known at all. Therefore, I believed that the elucidation of their dynamic mechanisms would be highly impactful," said Dr. Sasaki to explain the background of his research.

X-ray diffraction utilized in this experiment is a phenomenon through which rotary motions of diffraction spots can be monitored with an angular resolution of less than 1 milliradian. A 1-milliradian angle is equivalent to a 1-mm displacement of a diffraction spot when the distance from the sample increases by 1 m. This level of precision cannot be achieved in other diffraction experiments that use visible light. Moreover, a special X-ray source is required to measure the continuous motions of spots. Highly brilliant white X-rays produced at the RIKEN Structural Biology II beamline (BL44B2: currently renamed to the RIKEN Materials Science beamline and only monochromatic X-rays are available) were indispensable to this measurement. Unlike monochromatic X-rays, white X-rays contain various wavelengths of X-rays, from which a broad range of information about molecular motions can be obtained.

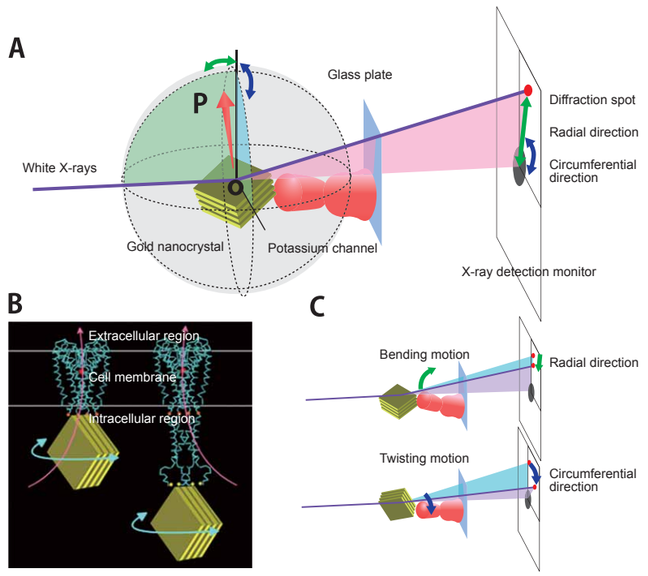

Fig. 1. Schematic view of the measurements. A: A gold nanocrystal is attached to a channel molecule that is fixed on a glass plate. Upon irradiation with X-rays, diffraction spots emitted from the gold nanocrystal are observed on an X-ray monitor. An arrow (OP) indicates the direction of the X-ray diffraction plane of the gold nanocrystal. B: Observation of potassium channel motions under two conditions. By using two types of molecules (whole molecules and those without intracellular regions), the opening/closing regions of the channel were directly examined in order to identify the locations where the motions were initiated. The gold nanocrystals were attached on the intracellular side of the channels. Motions were examined just below the cell membranes (left) and at the end of the channel on the intracellular side (right). Red circles indicate the locations where channel inhibitors bind. Orange and yellow circles represent the binding locations with the gold nanocrystals. C: Correlation between conformational changes of the channels and the diffraction spots. Diffraction spots move in the radial direction when the channels bend, and in the circumferential direction when the channels twist.

Opening and Closing of the Potassium Channels are "Twisting Motions"

This experiment was conducted according to the procedure explained in Fig. 1. Two kinds of samples, whole molecules and molecules without intracellular regions, were provided from Dr. Oiki for the purpose of observing the opening/closing positions of channels. First, potassium channel molecules were attached to a glass plate outside the cell, and a gold nanocrystal was bound to the inside of the cell. Highly brilliant white X-rays were shined on the potassium channel molecules, and diffraction spots emitted from the gold nanocrystals were detected with high precision using an X-ray detection monitor. As gold nanocrystals moved, bright spots corresponding to diffraction spots moved on the monitor. Since the gold nanocrystals are bound to the channel molecule, the conformational changes of the channel can be observed as motions of bright spots on the monitor. Deformation of the channel can be observed as motion in the radial direction, and twisting motion can be observed as movement in the circumferential direction.

A passageway for ions is located at the center of the potassium channel molecule (Figs. 1B and 2C). Which functions of potassium channel molecules are responsible for opening/closing of this ion passage? Answering this question is the aim of this experiment.

The data revealed that the answer is "twisting motion" (Fig. 2). When the channel molecule was being closed, only radial motions were observed, indicating that the channel molecule is slightly bent. However, notable twisting motions of the channel molecules were observed when opening and closing were repeated. Moreover, conformational changes in the opposite direction were observed when the channel was closing. These findings indicate that the intracellular aperture of the channel is closed and opened according to the twisting motions of the channel molecule. Thus, the secret of the opening and closing of channel molecules has been revealed for the first time.

This potassium channel molecule has a structure that extends into the cytoplasm (Fig. 1B right). Similar twisting motions were observed in the measurement of the opening and closing of the channel molecule by binding a gold nanocrystal to the end of this extended domain. This finding indicates that the twisting motions are extended all the way to the end of the molecule, within the cytoplasm.

More interestingly, the mechanisms of action have been determined for therapeutic agents, "channel inhibitors," used to treat diseases in which channel protein molecules are involved. The molecules of these agents reach deep into the pores of the channel molecules, where ions are passing, and block ions by occluding the pore. Indeed, the study of conformational changes revealed that the twisting motions were halted. This finding reveals that the channel inhibitors not only block the flow of ions but also fix the conformations of the channel molecules. Furthermore, it reflects the fact that the conformational changes of the channel molecules take place near the pore.

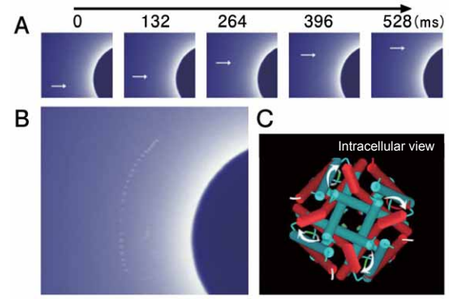

Fig. 2. Twisting conformational changes of the potassium channel. A: Sequential images of the movements of diffraction spots. Actual images were taken every 33 ms, but only selected images are shown. B: Trajectory of diffraction spots. Images taken every 759 ms are overlaid. A blue circle found on the right-hand side corresponds to a black circle located in the center of the X-ray monitor in Fig. 1A. The circular motion of the diffraction spots indicates the twisting motion of the channel. C: The conformational changes of the channel upon opening and closing, viewed from the intracellular side. The ion aperture is open as the state changes from blue (closed state) to red (open state).

These research achievements were published in Cell (January 2008) and highly commended. One writer commented, "This observation of single-molecule conformational changes has made a significant mark on the history of channel research."

Capturing the Changes in Channel Molecules at Microsecond Timescales

Channel molecules exist ubiquitously in all cells of all organisms. Dysfunctions of ion channels cause various "channel diseases" such as sudden infant death syndrome, heart attack during exercise in the young, and sudden death from an unknown cause during sleeping. Epilepsy is also believed to be caused by dysfunctions of ion channels. Thus, this research can offer highly promising clues regarding the dynamic mechanisms of dysfunctions of ion channel molecules in these patients. Once new concepts of drug development are established based on the dynamics of molecules, it will be possible to obtain revolutionary therapeutic drugs that exert dramatic effects.

"Our next target is to simultaneously observe the conformational changes of ion channels at the single-molecule level. At SPring-8, real-time measurement techniques at the microsecond level have been already established, so that simultaneous observations will become possible in the not-so-distant future," mentioned Dr. Sasaki to explain future prospects. This project has been appointed as one of the SPring-8 Core Research Projects, and experiments will continue until 2011. A related new CREST research project is also ongoing.

[1] Currently Professor at the University of Tokyo, Japan.

Reference
1. H. Shimizu, M. Iwamoto, T. Konno, A. Nihei, Y. C. Sasaki and S. Oiki; *Cell*, **132**, 67 (2008)

Observation of the Changes in Myocardial Tissues of Live Animals

In advanced countries, including Japan, heart failure accounts for an increasing proportion of the cause of death. Treatment of heart failure has advanced over time; however, the prognosis of heart failure is far from satisfactory, and it continues to be a significant disease that affects the quality of life for middle-aged and senior adults, as well as the medical economy. Recent advances in diagnosis of cardiovascular diseases have been extensive, but the pathologies of many diseases, including dilated cardiomyopathy, have yet to be clarified. Under these circumstances, in 2006 researchers at SPring-8 developed new techniques to examine the mechanisms of myocardial contraction. These new methods are based on dynamic analyses of myocardial structural proteins of live animals. Such new progress is expected to help us develop new diagnostic methods for cardiovascular diseases.

Analyses of the Movement of Cardiac Muscle at the Nano Level

Reductions in cardiac contractile and relaxing/diastolic capacities are among the problematic pathological conditions of myocardial dysfunctions. Actin and myosin, which are abundant proteins in cardiac muscle, are responsible for muscle contraction, which is essential for the pumping of blood. Therefore, these proteins are intimately involved with the pathological conditions of cardiac diseases.

Cardiac muscle and skeletal muscle have a three-layer structure: muscle, muscle fiber, and myofibril. Myofibril has a systematic periodic structure that exhibits stripes in the direction of the long axis; it is also called "striated muscle." The unit of this periodic structure is the sarcomere, which consists of the myosin filament and the actin filament (Fig. 1). The area where myosin filaments exist is called the A-band, and the area where only actin filaments exist is called I-band. When cross-bridges are formed between these filaments, the myosin and actin filaments slide past each other to shorten the length of sarcomeres, causing the cardiac muscle to contract. This process provides the force for the heartbeat. The contractile force is determined by the binding force between the filaments.

A double-hexagonal lattice, which is comprised of myosin and actin filaments, is found in the cross-section of the A-bands of the sarcomeres in cardiac cells (Figs. 1 and 2a). A plane that is formed by myosin filaments is defined as a (1,0) lattice plane; a plane formed by myosin and actin filaments is defined as a (1,1) lattice plane. Both myosin and actin are protein molecules, with sizes ranging from a few nm to a few tens of nm (1 nm $= 10^{-9}$ m); the size of the muscle filaments and the lattice structures are also on the order of nanometers.

Myofibril Functions that Regulate the Expansion and Contraction of Myocardial Cells

Dr. Ryuji Toh (Assistant Professor, Kobe University School of Medicine, Japan), and Dr. Masakazu Shinohara (Researcher, *ditto*), Dr. Mitsuhiro Yokoyama (Director, Hyogo Prefectural Awaji Hospital, Japan), Dr. Naoto Yagi (Chief Scientist, JASRI), and colleagues have been studying these fine structures and functions in order to elucidate the pathological conditions of myocardial dysfunctions.

Traditionally, conformational analyses at the nano scale have used electron microscopes. In electron microscopy, myocardial tissues are extracted and chemically fixed in order to make measurements. As a result of exposure to fixative agents, these specimens adopt different conformations than they do *in vivo*. In order to overcome this problem, X-ray diffraction method is applied. Diffraction is the apparent bending of electromagnetic waves (such as X-rays) by obstacles. In the case that obstacles have a periodic structure, such as crystals or muscle fibers, diffracted X-rays produce specific patterns (diffraction patterns), depending on their structures. However, in order to apply the existing observation techniques using X-ray diffraction to visualize cardiac muscle, either extraction of the heart or open-chest surgery is required. In either case, the environment in which the heart is exposed is radically different from real *in vivo* conditions.

To overcome this challenge, this research group attempted an analysis of myofibril functions using the High Flux Beamline BL40XU at SPring-8. X-rays available at BL40XU have high directionality (parallelism) and a hundred times higher intensity than is available at other monochromatic beamlines with which the movements of protein molecules in cardiac cells can be observed.

By irradiating the lattice structures of the sarcomeres of cardiac cells with X-rays, the hexagonal structures can be identified by diffraction. Diffraction from the (1,0) and (1,1) lattice planes are called the "(1,0) reflection" and "(1,1) reflection," respectively (Fig. 2). Reflection comes out at a right angle to the long-axis of the muscle, which can be compared to the meridian of the Earth; this reflection is then called the "equatorial reflection." This equatorial reflection indicates that myosin and actin filaments are systematically aligned in the sarcomeres.

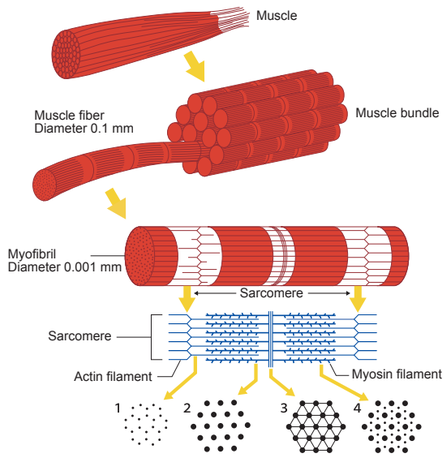

Fig. 1. Muscle structure.
Each muscle cell contains many myofibrils and sarcomeres, which are the minimum units of muscular contraction, aligned in tandem. Filaments (microfibers), which are comprised of many actin and myosin molecules, form systematic hexagonal lattices in the sarcomeres.

Myosin and actin filaments overlap with each other along their lengths. The two types of filaments slide past each other, which induces the expansion and contraction of cardiac cells and ultimately makes the heart contract as a whole.

We can compare the filaments to a bundle of elastic cords. In this model, the gaps between elastic cords narrow when they become expanded, and gaps widen when they contract. The distance between the center of the diffraction pattern and the equatorial reflection spot represents the distance between elastic cords. That is, the expansion and contraction of cells negatively correlate with the distance between filaments. On the other hand, the ratio of the intensity of the (1,0) reflection to that of the (1,1) reflection varies with contraction. This is because the part of the mass of the myosin filament moves closer to the actin filament when the head portion of myosin molecules binds to the actin filament upon contraction. The larger the variation in the distance, the stronger the binding, indicating that a stronger muscle contraction force is produced.

"We can obtain information about the amounts of binding force produced between filaments, as well as those of dynamic expansion and contraction of cells, by using X-ray diffraction," said Dr. Toh.

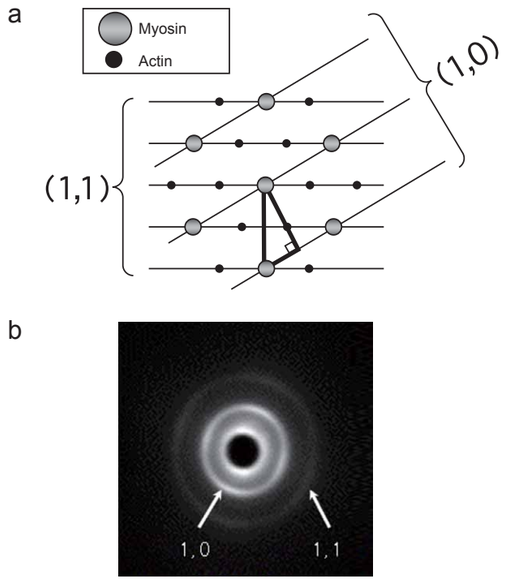

Fig. 2. (a) A cross-sectional view of sarcomeres of myocardial cells in the A band. (b) An X-ray diffraction pattern obtained from the heart.
Actin and myosin filaments form the hexagonal lattice structure. Diffraction occurs when X-rays are exposed to objects that have systematic molecular configurations. The equatorial reflections images, produced from (1,0) and (1,1) lattice planes shown in (a), can be observed in the diffraction pattern of the cardiac muscle shown in (b).

Behavior of Live Muscle Tissues Unraveled

X-ray diffraction patterns are observed as expected when the mouse heart is irradiated with X-rays under anesthesia (Fig. 2b). Measurements of the (1,0) lattice spacing and the intensity ratio (1,0)/(1,1) as a function of time revealed that the (1,0) lattice spacing increased in inverse proportion to the shortening of sarcomeres during contraction. Additionally, as the head portion of myosin forms a crossbridge with actin filaments upon contraction, the mass moves to the actin filament side, resulting in increased intensity of the (1,1) reflection. This indicates that the ratio (1,0)/(1,1) decreases. On the other hand, the reverse is true for contractions, in which the (1,0) reflection surpasses the (1,1) reflection upon relaxing.

A study was conducted on the affected myocardial fibers of mice that develop symptoms similar to dilated cardiomyopathy, in which the contractile function of cardiac muscle was impaired. In this analysis, the X-ray diffraction patterns were blurred. This finding indicates that the alignment of these muscle filaments is irregular, unlike normal muscle filaments (Fig. 3). This study yielded the first ever demonstration of abnormality in muscle filaments in myocardial diseases.

"We have demonstrated that X-ray diffraction patterns obtained by using extremely brilliant and parallel X-rays can offer a highly promising diagnostic technique at the molecular level to identify abnormalities in the myocardial filaments, which could not be detected with the existing techniques," said Dr. Toh, expressing enthusiasm for the use of X-ray diffraction at SPring-8. "We often encounter cases of heart failures, even with the normal contraction capacity of the heart. Several studies have recently suggested that the reduction in the relaxation capacity of the heart is related to the mechanisms of such heart failures, but its detailed pathophysiological conditions have yet to be elucidated. The techniques developed in our research are expected to contribute to the elucidation of the pathophysiological conditions of unexplained diseases, including dilated cardiomyopathy. Ultimately, we hope to quickly identify abnormalities that cannot be detected with the existing diagnostic techniques."

The research achievements of this project were published in *Biophysical Journal* (March 2006), the journal of the Biophysics Society, and received international attention.

Reference
1. R. Toh, M. Shinohara, T. Takaya, T. Yamashita, S. Masuda, S. Kawashima, M. Yokoyama and N. Yagi; *Biophysical Journal*, **90**, 1723 (2006)

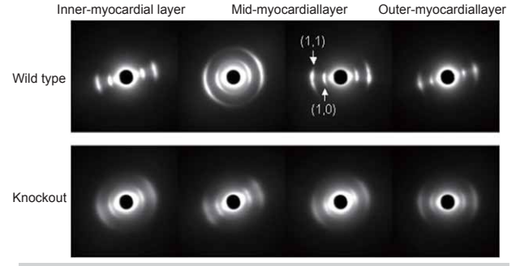

Fig. 3. X-ray diffraction patterns of the heart of normal mice and that of a mouse model of myocardial disease.
Compared with the X-ray pattern of the heart of normal mice (top), that of a myocardial disease mouse (bottom) is blurred, indicating that the alignment of muscle filaments in the latter heart is irregular.

Elucidation of "How Newborns Start Breathing?"

A fetus does not require oxygen exchange via the pulmonary system; consequently, the lungs are filled with "lung water" until birth. Immediately after birth, however, the lung water must be removed so that air can enter the lungs, thereby the newborn can begin breathing in a normal way. If this process does not go well, a newborn cannot breathe, and it will die. To avoid such an event, we need to understand the mechanisms by which a newborn's lungs begin breathing. However, because there have heretofore been no practical methods for observing the process of lung water being replaced with air, the details have remained unclear — but that is where SPring-8 comes in. The process of the initiation of breathing has now been observed, yielding many new discoveries about the lungs.

Image Analysis Techniques using X-ray Refraction

While in the womb, a fetus gets oxygen from the mother's blood through the placenta. The placenta acts as a filter, providing oxygen to a fetus through the umbilical cord. Upon birth, the lungs are filled with air and breathing begins. Most newborns manage this without difficulty, but in fact it is not an easy task at all. Neonatal asphyxia, in which a newborn cannot begin breathing on its own and therefore requires resuscitation, occurs in ~10% of deliveries.

How does a newborn inhale air into the lungs to begin breathing? The amount of lung water that a newborn expels from the mouth is small compared to the volume of the lungs. Thus, it is unclear how lung water is eliminated. It has been speculated that lung water gradually decreases over time, and is replaced with air by some unknown mechanism. One hypothesis was that osmotic gradient created by epithelial Na channel gradually moves water across the wall of alveolus. In 2003, a collaborative research group consisting of researchers from JASRI and Monash University in Melbourne, Australia initiated research with the aim of unraveling this mystery.

At SPring-8, researchers from JASRI have been playing a central role in developing the novel technique of refraction contrast imaging. This is a method for obtaining density distribution images with enhanced edge contrast by exploiting the characteristics of X-rays. In refraction contrast imaging, X-rays are superimposed at the edge of an object according to the slight differences in the refractive index of the object's materials (Fig. 1). The diffraction angle is extremely small (0.1 mm displacement at a distance of 10 m from the object) but the high-resolution image detector developed at JASRI can distinguish such a small angle. Using this technique, we can obtain higher-resolution images than those obtained with existing radiographic visualization techniques (absorption contrast imaging) such as medical X-ray imaging, which exploits the differences between an object's absorption and penetration by X-rays.

Collimated (i.e., perfectly parallel) X-rays are essential for detecting images based on the extremely small differences in the refractive index. Generation of collimated X-rays is among the special technologies that are available at SPring-8.

The energy of X-ray employed also differs between refraction contrast imaging and absorption contrast imaging. The higher the X-ray energy, the higher the penetration and the lower the absorption. When high-energy X-rays are used, satisfactory data will not be obtained unless there are sufficient differences in absorption in soft tissues. However, even in such a situation, differences in the refractive index will be useful.

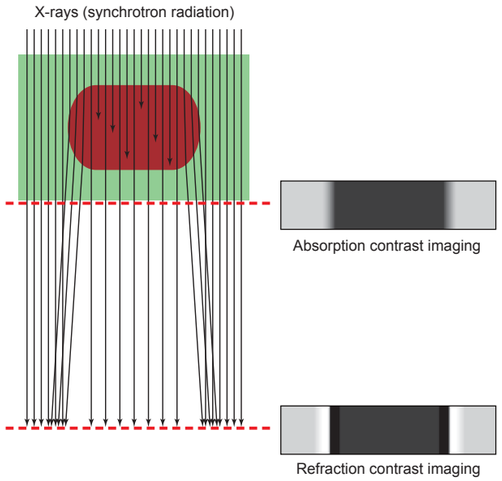

Fig. 1. Refraction contrast imaging and absorption contrast imaging.
When X-rays (arrow) enter an object (brown), X-rays are partially absorbed by the object and refracted at the surface as well. Refraction changes the direction of the X-rays. X-rays recorded immediately behind the object yield images with contrast caused primarily by absorption, but with only small effects from refraction (absorption contrast imaging). On the other hand, when X-rays are recorded at a distant location, both refracted and transmitted X-rays overlap to generate bright regions. This overlap enhances the edge of the object, allowing high-contrast images to be obtained (refraction contrast imaging).

On the other hand, when low-energy X-rays are used, information about tissues in front of and behind a hard tissue cannot be obtained. By using refracted waves of high-energy X-rays, the structures of multi-layered hard and soft tissues can be observed.

Air Compresses Lung Water —Unexpected Phenomenon

The Monash University research team wrestled with the observation of the lungs of newborn rabbits by applying the refraction contrast imaging that SPring-8 has developed over the last 10 years.

At the 220-m-long Medical and Imaging I Beamline (BL20B2), samples were placed at 210 m from the deflection electromagnets that produce X-rays, and a detector was installed 2 m behind the samples. Since it was difficult to control the delivery timing, fetuses were taken out by cesarean section.

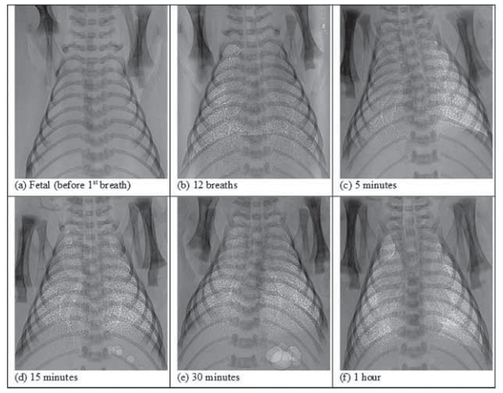

Fig. 2. Chest images of newborn rabbits.
(a) Prior to initial breathing. The lungs are filled with lung water and airways are not observed. (b–f) After initiation of breathing (numbers indicate elapsed time after the initiation of breathing), the tracheae and bronchi are visible. Additionally, increasing number of white spots show the delivery of oxygen into the peripheral parts of the lungs. At 30 and 60 min, the edges of the lungs and the existence of the diaphragm can be clearly identified.

However, some special manipulation is required to observe temporal changes, since newborns begin breathing almost immediately after birth. Newborns begin breathing after the amnion, which is a thin membrane covering the fetus, is removed. To control the timing of breath initiation, rabbit fetuses were taken out from the womb and placed in warm water containers (37°C) without removing the amnion. They were immobilized in the containers, and X-rays were controlled so that they ran parallel to the fetal chest. Next, the amnion was removed, and irradiation was initiated in order to start the observation.

Irradiated X-rays entered the detector after experiencing a slight refraction. X-rays that penetrated the newborn's body also entered the detector. Data were continuously recorded every 0.8 sec and processed by computer. Realistic lung images were displayed on a display monitor (Fig. 2). How is lung water replaced with air? These images of newborn rabbits revealed an unexpected phenomenon. When newborns begin breathing, air simply enters and fills the lungs upon each breath.

"It looks like air enters the lungs upon breathing and compresses the water inside the lungs. This unexpected phenomenon suggests that inspiration plays an important role in removing lung water," explained Dr. Naoto Yagi (Chief Scientist, JASRI). Dr. Yagi is an expert in X-ray image analysis who has been participating in the development of refraction contrast imaging. He has played a central role in the collaboration with Monash University.

The respiratory organs cooperatively work to push lung water deep into the lungs; therefore, backflow upon exhalation was much smaller than the advance associated with inhalation. It is speculated that upon breathing thorax expands and lung water is sucked into tissues through the walls of peripheral organs such as the alveoli, and is gradually processed via the lymphatic and blood vessels.

This research group has succeeded for the first time in elucidating the mechanisms of breath initiation at birth, by visualizing the process of air entering into the lungs of newborn mammals. This research achievement was published in FASEB Journal (2007), a major journal for biomedical researches in the US.

Mechanical Ventilation that Compresses Lung Water is Effective

If lung water remains in the lungs after birth, the newborn will go into respiratory distress. To avoid this, mechanical ventilation is required for premature infants or newborns with respiratory disorder. The same mechanical ventilation used for adults has been applied in both premature infants and newborns.

However, now that the research conducted by Dr. Yagi and colleagues including researchers of Monash University revealed that newborns push lung water deep into the lungs by breathing in, we must reconsider how to use ventilation in underdeveloped lungs of premature infants without causing injury. Therefore, procedures for mechanical ventilation of newborns must be significantly revised. Lung water should be pushed by air using mechanical ventilation. A limited number of hospitals have applied such mechanical ventilation, but this treatment has not been widespread. After this treatment demonstrated the efficacy, however, increasing numbers of hospitals in Australia and the Netherlands have been adopting this treatment method.

References
1. S. B. Hooper, M. J. Kitchen, M. J. Wallace, N. Yagi, K. Uesugi, M. J. Morgan, C. Hall, K. K. W. Siu, I. M. Williams, M. Siew, S. C. Irvine, K. Pavlov and R. A. Lewis; *FASEB J.*, **21**, 3329 (2007)
2. A. B. te Pas, M. Siew, M. J. Wallace, M. J. Kitchen, A. Fouras, R. A. Lewis, N. Yagi, K. Uesugi, S. Donath, P. G. Davis, C. J. Morley and S. B. Hooper; *Pediatric Research*, **65**, 537 (2009)

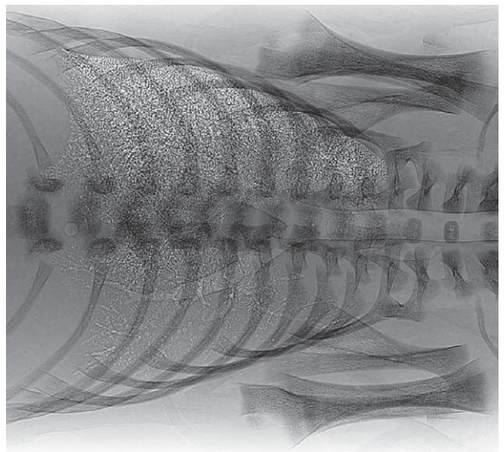

Fig. 3. A chest refraction contrast X-ray image of a rabbit newborn during air feeding.
Lying sideways, as shown in this figure, often causes the non-uniform entry of air across the upper and lower parts of the lungs. A larger amount of air, indicated by white spots, enters the upper part; however, air enters only the major bronchi in the lower part.

Soft Matter

Exploring Nano- and Meso-Structures of Polymers and Organic Surfaces

Possibility of Polymers as Functional Materials

Soft matter is organic compounds composed of molecules in which numerous atoms (mainly carbon, hydrogen, oxygen, and nitrogen) are linked by covalent bonds. Soft matter includes polymers, plastics, liquid crystals, micelles, etc. Polymers include proteins, DNA, polysaccharides, as well as natural rubbers and fibers (e.g., natural silk and wool). Soft matter is utilized in diverse materials such as automotive parts, household goods, electronics (e.g., LCD televisions and mobile phones), and biomedical products, as well as used as films in various fields such as printing, adhesive bonding, and coatings.

The first synthetic polymer, a phenolic resin, was made in the early 20th century. In 1926, Hermann Staudinger, who later won the Novel Prize in Chemistry in 1953, proposed the concept of a polymer, which he defined as a macromolecule of which hundreds to tens of thousands of atoms are linked in a corded form. This concept was accepted by the academic community in 1930, and in 1935, Wallace H. Carothers (DuPont, USA) synthesized nylon,[1] the world's first synthetic polymer that is stronger than silk. Then Ichiro Sakurada (Kyoto University, Japan) and colleagues synthesized Japan's first synthetic polymer, vinylon (polyvinyl alcohol), in 1939.

Polymers are chain-like macromolecules that soften when heated, but maintain their original form at room temperature. This characteristic is called *plasticity*, which is the word origin of *plastic*. Hence, polymers have vast potential in practical applications. Paul J. Flory, who received the Nobel Prize in Chemistry in 1974, revealed the relationship between molecular structure and polymeric properties. This discovery advanced the research of polymer physics and chemistry. In the synthetic chemistry of polymers, Michael Szwarc developed living polymerization, which is the basis of Topic 10 (Three-Component Copolymers), to produce polymers with a uniform molecular weight, as well as radical polymerization and polycondensation. Karl Ziegler and Giulio Natta (they shared the Novel Prize in Chemistry, 1963) established the stereoregular polymerization of polyethylene and polypropylene. Figure 1 lists the Nobel Prizes relating to synthetic polymers.

Hence, in the 1970–80s, it was believed that all the necessary techniques for polymerization were known, and research focused on the synthesis (polymerization), structures, and physical properties of polymers. However, around 1980 polymer scientists began examining the possibilities of polymers as functional materials. Hideki Shirakawa (Nobel Prize in Chemistry, 2000) was the first to reveal that polymers, which are primarily insulators, will become conductors if they contain successive conjugated double bonds in their molecular structures, and he discovered a synthetic method to fabricate conductive films using such polymers. His pioneering work has led to the development of conductive films used in mobile phones, and has resulted in the development of organic thin film transistors (TFTs) [see Topic 9 (Analysis of Nanosurfaces)]. Additionally, studies on functional polymers such as photofunctional polymers and organic EL (which have transparency, fluorescence, photodiscoloration, nonlinear optical effect, and optical responsivity), biopolymers, biomedical polymers, and micelles have advanced.

Accordingly, new polymers with various structures can now be synthesized based on molecular design by modifying nanoscale molecular linkages. Thus, the development of innovative analysis techniques to determine the molecular or higher-order structures of these polymers is highly anticipated.

Synchrotron X-rays —Powerful Weapons for Manufacturing

Two approaches are available to determine the structures of materials: microscopy and diffraction/scattering measurements.[2] In the 1950–60s, the primary method to determine polymer conformations was X-ray structure analysis of crystalline polymers. However, advances in microscopy technologies in the 1980–90s produced atomic force microscopes, optical near field microscopes, and confocal microscopes, as well as transmission and scanning electron microscopes, which significantly developed surface observation techniques on the micron- to nano-scales. Although powerful, these microscopes can only explore a small region, but not the entire object. Moreover, these techniques are mainly used for surface observations, and the internal atomic or higher-order structures of materials or the rapid movements of materials cannot be visualized. This is where the advantages of X-ray and light diffraction and scattering measurements for structural analyses shine through.

Visible light has a wavelength greater than 400 nm (1 nm = 10^{-9} m). In contrast, X-rays have a wavelength on the order of 0.1 nm, which allows the crystal structures of atoms and molecules to be observed on the nanoscale level. Furthermore, small angle X-ray scattering (SAXS) can reveal the structures of various non-crystalline materials as well as non-uniform structures of materials. Topic 7 (Nano-Oriented Crystal Polymers) covers the first direct observation of the nucleation processes in polyethylene nanocrystals using highly brilliant synchrotron X-rays, while Topic 10 (Three-Component Copolymers) reports the discovery of quasicrystals on the order of 100 nm in size by SAXS measurements. Realization of a drug delivery system by identifying nanoparticles is covered in Topic 8 (Supramolecular Assembly). Topic 9 (Analyses of Nanosurfaces) would not be possible without third-generation synchrotron radiation available at SPring-8, which is highly brilliant and directional. In addition to enabling structures within a few nanometers from the surface of a crystal to be detected using grazing incidence X-ray diffraction (GIXD) within the critical angle of total reflection, third-generation synchrotron radiation can also reveal the local structures of materials in a small region (~10 μm) using microbeams (MBs). These are two reasons why synchrotron radiation at SPring-8 is crucial for soft matter research (Fig. 2).

Figure 3 shows an X-ray crystallographic image of vinylon using cutting-edge technology in the 1950s. The image was recorded by combining several fiber bundles of vinylon and exposing them to X-rays for several hours. Figure 4 is an image of a single ultra-thin fiber (diameter ~15 μm) from the same vinylon sample, which was stored at the Institute for Chemical Research, Kyoto University. The sharp wide-angle [wide-angle X-ray diffraction (WAXD)] and small-angle [small-angle X-ray scattering (SAXS)] diffraction-scattering patterns were acquired at the Advance Softmaterial Beamline (BL03XU: in operation since February 2010) in just 20 sec. It is amazing that SPring-8 can now reveal a detailed structural model of what was only a theoretical model 50 years ago.[3]

In summary, synchrotron radiation X-rays are powerful weapons for investigating the secrets of soft matter. SPring-8's X-rays can reveal the structures of materials at the nano- and meso-scales. SPring-8 is awaiting new challenges from researchers in soft matter science and manufacturing science.

[1] Minoru Imoto. 1971. *Nylon no hakken* [Discovery of Nylon], Tokyo, Japan: Kagaku Dojin.
[2] Takuhei Nose , Kazuyuki Horie, and Toshiji Kanaya, eds. 2006. *Wakate kenyusha no tameno yuki-koubunshi sokutei labo guide* [Laboratory guide for the measurements of organic molecules and polymers for young researchers], Tokyo, Japan: Kodan-sha.
[3] SPring-8's homepage > Press Release > February 4, 2010 http://www.spring8.or.jp/ja/news_publications/press_release/2010/100202 (in Japanese)

1926 - 30 Staudinger	Establishment of the polymer concept (1953)
1940 - 50 Flory	Systematization of polymer physical chemistry (1974)
1953 - 55 Ziegler-Natta	Polymerization by array catalysts (1963)
1970 - 80 de Gennes	Phase transition theory of polymers and liquid crystals (1991)
1964 - 70 Merrifield	Solid-phase peptide synthesis (1984)
1976 - 80 Shirakawa, MacDiarmid, and Heeger	Conducting plastics (2000)

Fig. 1. Nobel Prizes in the field of synthetic polymers (year).
First four are universal research on polymers while the latter two are related to functional polymers.

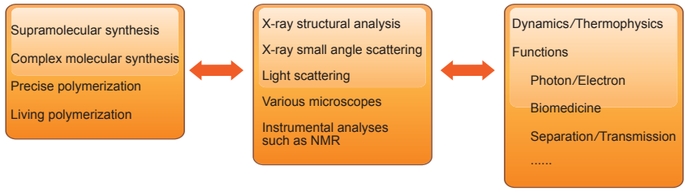

Fig. 2. Relationship between syntheses, structures, and physical properties in soft matter research.
In manufacturing science, which strives to realize innovative physical properties and functions, SPring-8 can determine the nano- and meso-structures of newly synthesized materials.

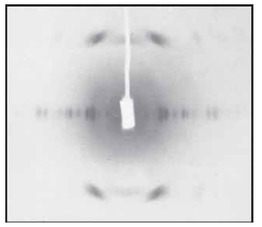

Fig. 3. X-ray image of vinylon fibers reported in the 1950s.
(reproduced with permission from Nitta, Isamu ed. 1959. X-sen kesshou-gaku [X-ray crystallography] Tokyo, Japan: Maruzen Company)

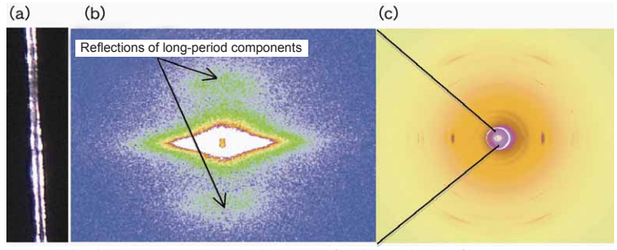

Fig. 4. X-ray crystallographic image of a single vinylon fiber.
a: Single vinylon fiber (diameter ~15 μm).
b: Small-angle X-ray scattering (SAXS) image.
c: Wide-angle X-ray diffraction (WAXD) image.

Supercritical Elongation-Induced Crystallization Creates Plastic Stronger than Steel

"Why is plastic weaker than steel?" Although common knowledge prevents most people from posing this question, Dr. Masamichi Hikosaka (Professor, Hiroshima University, Japan) and colleagues set out to answer this question. They employed the highly brilliant and precise X-rays at SPring-8, which can closely analyze processes of polymer crystallization and the internal structures of polymers at the nanometer level (10^{-9} m), along with quiet dedication to successfully develop a plastic that is much stronger than steel in terms of unit weight. They termed this plastic "nano-oriented crystals (NOCs)." Amazingly, the production cost of NOCs is equivalent to that of commodity plastic. Hence, their efforts may cause a new paradigm in the basic materials industry.

Unraveling the Mystery of Polymer Crystallization—A Reckless Attempt

Since the 1930s, the theory that when a material crystallizes, a nanometer-sized nucleus (nano-nucleus) is initially created, which then grows into a larger crystal, has been commonly accepted. Moreover, when a liquid is cooled below its freezing point (supercooling state), it solidifies, specifically by crystallization. However, the mechanisms of nucleation remained a mystery. A nano-nucleus, or "a baby crystal," is extremely small and rare, and exceedingly difficult to demonstrate.

Most researchers have long given up demonstrating the existence of a nano-nucleus. However, Dr. Hikosaka has continued his quest. In 1987, he hypothesized the sliding diffusion theory of polymer crystallization; entangled long string-like molecules untangle themselves, slide along a crystal lattice like a snake, and arrange themselves to form a crystalline polymer. In general, crystalline polymers such as polyethylene and polypropylene, which are composed of long string-like molecules, are finely folded in equal intervals to form a plate structure (Fig. 1). Dr. Andrew Keller (University of Bristol, UK), a leading authority in polymers, discovered a folded chain-polymer crystal in 1957, and an "extended chain-polymer crystal" was identified in 1964. Dr. Hikosaka's sliding diffusion theory of polymer crystallization attempts to explain both types of crystals in an integrated manner. Originally his theory was a global controversy, but today is widely accepted with the support of Dr. Keller.

Dr. Hikosaka was 43 years old when he proposed the sliding diffusion theory of polymer crystallization. However, he himself could not confirm the initial state of polymer crystallization. "It was 1992 when I decided to try to confirm the entire process; from nucleation to crystallization. However, everybody said I was crazy," recalls Dr. Hikosaka. Major properties of solid materials are determined in the early stage of crystallization. However, if the crystallization process can be controlled at the nano-nucleus level, then the development of previously unknown materials would be possible. Hence, revealing of the mechanisms of nucleation is industrially significant.

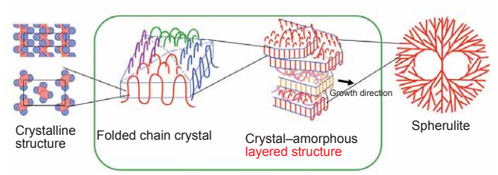

Fig. 1. Folded structures of existing polymer crystals and spherulite.
In polymers, polymer chains are often folded to form a 10-nm thick folded chain crystal. This crystal further forms an amorphous layered structure where the layers grow to construct a 100-μm sized golf ball-like giant crystal, called a spherulite. Herein, the crystallinity of a spherulite is less than 50%, which results in a weak solid.

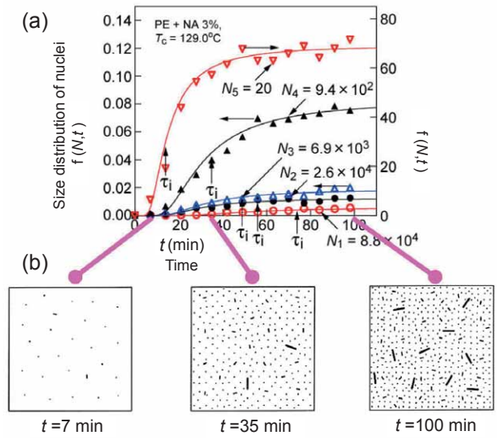

Fig. 2. Size distribution of nuclei with time.
(a) Size distribution of nuclei with time where the longitudinal axis represents the size distribution of nuclei f (N, t) and the horizontal axis represents time t. Nuclei sizes (N) are represented as repeating molecular units. Initially the number of small nuclei (N = 20) rapidly increases but slowly increases with large nuclei, revealing nucleation processes for the first time.
(b) Schematic views of nucleation in a melt. Numerous small nuclei are initially created, but as large nuclei form the rate decreases.

Revealing the Behavior of a Nano-Nucleus for the First Time

Small-angle X-ray scattering (SAXS) is the only promising observation technique to detect nano-nuclei. However, the X-ray intensity available at the existing synchrotron X-rays was too low to distinguish valid data from noise. Thus, Dr. Hikosaka put his hope on the highly brilliant synchrotron X-rays at SPring-8. In 2002, he examined nano-nucleation of a supercooled polyethylene melt by irradiating X-rays in the Structure Biology II Beamline (BL40B2) at SPring-8. The melt is liquid where only pure material is being melted. As expected, SPring-8 yielded much clearer data than ever before. However, the number density of the produced nano-nuclei was so low that the data statistics were poor.

Thus, innovation was needed to produce sufficiently high-density nano-nuclei. Dr. Hikosaka thought of utilizing nucleating agents (NAs), which are crystals to promote nucleation. If nuclei are created on NA particles, they can easily start growing. This is the same mechanism where dust promotes cloud formation. However, it is very difficult to uniformly distribute NAs because a polymer melt is highly viscous, and a non-uniform production of nano-nuclei would result in unreliable data. However, Dr. Kiyoka Okada (Hiroshima University), a former fourth-year undergraduate student in Dr. Hirosaka's lab, volunteered to research producing a uniform distribution of NAs. Eventually, she developed a technique to mix solvent, polymers, and NAs using ultrasound. "I dedicated myself to this research for more than a year beginning in 2003, and finally succeeded in increasing the production of nuclei more than 10,000 times," recalls Dr. Okada. Ultimately, highly brilliant X-rays were irradiated on the polyethylene melt in which NAs were uniformly distributed.

The increased scattering intensity confirmed in real time that various sized nuclei (> 1 nm) are produced, and this is the first observation of nano-nucleation. This analysis revealed that nano-nuclei are being continuously produced, but most disappear instantaneously. Only one in one million nuclei survives. Additionally, nucleus size measurements indicate that initially the number of nano-nuclei rapidly increases, but as the larger nuclei are produced the rate decreases (Fig. 2). This research became Dr. Okada's doctoral dissertation, and was published in *Polymer* (2007), drawing international attention.

Brilliant Idea—Crushing Polymer Melt

Because a crystalline polymer is a long string-like molecule, the molecules tend to become entangled in the melt. Thin plates with folded chain-structures form a layered conformation, which becomes a golf ball-like crystalline body called a "spherulite" (Fig. 1). More than half of the content inside a spherulite cannot crystallize, and it becomes a solidified amorphous instead (Fig. 1). This high amorphous fraction is thought to cause the low strength and low heat resistance of plastic. Hence if the amorphous fraction can be reduced to nearly zero, the properties of the polymer should significantly improve. However, reducing the amorphous fraction proved to be extremely difficult.

Then Dr. Hikosaka conceived the idea to "stretch" the polymer, which causes randomly directed crystals or molecules to point in the same direction (or "orientation") because an entangled string can assume a linear form by pulling it left and right. Stretched and oriented string-like molecules are easily crystallized, significantly reducing the amorphous fraction. However, it is impossible to pull liquid. "So we tried crushing the melt," recall Drs. Hikosaka and Okada. They instantaneously applied high pressure to a melt that was poured into a long and narrow channel spanning to the left and right. This produced a rapid current in the melt, which expanded to the left and right, stretching the string-like molecules (analogous to clothes stretching when exposed to a rapid stream), and realizing a high orientation. In their experiments, high pressure, which corresponded to a stretching force with 1,000-fold stretch per second, was applied to the melt poured in a channel. The flow rate of the melt, which was induced by this stretching force, was termed "elongational strain rate."

This experiment revealed an interesting phenomenon; above a critical elongational strain rate, the crystallization speed increases one million-fold, even at the same temperature. It is hard to imagine such a drastic change occurring within the same material. To unravel the mechanisms of this phenomenon, Dr. Hikosaka and colleagues stretched a polypropylene melt at rates above the critical elongational strain rate to create a crystalline solid, which they examined at SPring-8 in BL40B2. They found that polymer chains in the melt arranged in parallel to form an almost perfectly oriented melt, and infinite number of nuclei were created, which grew to form nanocrystals on the millisecond order. The final product was a solid of which 90% were crystallized. This is the birth of NOCs.

Although NOCs are paper thin, their stretching fracture strength is 2–5 times higher than that of steel with the same weight. In addition to a higher transparency, its heatproof temperature is 176 °C, which is more than 50 °C higher than that of common polypropylene. Furthermore, its production costs are comparable to existing plastics, and more than 90% of the body may be recyclable. Hence, NOCs are an economical, ultra-high performance polymeric material.

Nanocrystals are stronger than steel because they are rigidly bound by a "string" (Fig. 3). Dr. Hikosaka has attributed some of his success to SPring-8, "X-ray diffractometry at SPring-8 has revealed that more than 100 crystals measuring 20–30 nm are bound by a single 2-μm long string-like molecule chain, which is formed with a strong force (covalent bond)." Details of this NOC production were reported in *Polymer Journal* (June 2010), and patent applications were filed in Japan and internationally. NOCs can replace steel and ceramics in various products, including automotive steel sheets, and have the potential to realize energy and resource conservation. Thus, researchers are working toward practical applications of NOCs in a wide range of areas with the support of the Japan Science and Technology Agency(JST). The 40 years of effort that Dr. Hikosaka and his colleagues have dedicated to polymer crystallization is beginning to produce revolutionary results.

References
1. K. Okada, K, Watanabe, I. Watanabe, A. Toda, S. Sasaki, K. Inoue, M. Hikosaka; *Polymer*, **48**, 382 (2007)
2. K. Okada, J. Washiyama, K, Watanabe, S. Sasaki, H. Massunaga, M. Hikosaka; *Polymer J.*, **42**, 464 (2010)

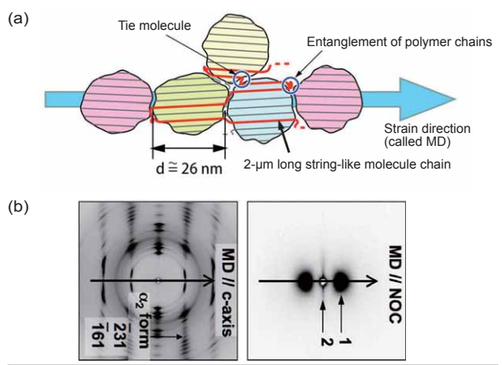

Fig. 3. Structures of nano-oriented crystals (NOCs).
(a) NOC has a structure where a 2-μm long string-like molecule chain, which has the equivalent strength of diamond, binds about 100 nanocrystals. This structure is called an "armor model." NOCs exhibit almost 100% crystallinity.
(b) X-ray diffraction images reveal NOC creation (left: WAXD, right: SAXS). Nanocrystal has a diameter of 26 nm.

Revealing the Properties of Nanoparticles to Realize Drug Delivery Systems

The technology to precisely administer the desired quantity of a pharmaceutical, to the desired part of a living body at the desired time is called a drug delivery system (DDS). DDSs can increase the efficacy of pharmaceuticals, while reducing their side effects. Hence, DDSs are innovative in establishing safe drug therapy systems. Nanotechnology plays a central role in DDSs because nanoparticles as ultrafine capsules that can pass through small holes in blood capillaries and cell membranes need to be fully controlled. To this end, SPring-8's capability has been utilized to reveal the structures of nanoparticles.

Precisely Analyzing the Behaviors of Nanoparticles

To realize highly functional DDSs, nanoscale capsules on the order to 10–100 nm (1 nm = 10^{-9} m) need to be able to encapsulate and deliver drugs to desired sites through small holes in blood capillaries and cell membranes. The most promising candidates for next generation DDSs are polymeric micelles and micelles composed of lipids.

What are micelles? For example, surfactants such as soap have a configuration similar to marking pins used in sewing where the needle tip corresponds to a lipophilic or hydrophobic group that becomes attached to oil, and the needle head corresponds to a hydrophilic group that becomes attached to water. Materials with such a configuration, when dissolved in water and the concentration exceeds some specific value, will associate with each other with the hydrophilic groups facing outward and the hydrophobic groups facing inward. Association is a phenomenon where two or more identical types of molecules bond with each other and behave as if they are a single molecule. A micellar structure is a structure where several of such molecules containing hydrophobic and hydrophilic groups gather to form a specific structure with the hydrophilic groups facing outward and the hydrophobic groups facing inward. A micellar structure, which is composed of polymers containing numerous hydrophobic and hydrophilic groups, forms a double-structure where the shell is comprised of hydrophilic chains and the core contains hydrophobic chains.

Micelles autonomously construct a particle when the concentration and other conditions are appropriately controlled, enabling drugs to be encapsulated in the core. The radii of the constructed particles range between 10–100 nm and can pass through the blood capillary walls, which is a required feature of DDSs. However, to realize DDSs using nanoparticles such as polymeric micelles, various technological hurdles must be overcome. In particular, it is extremely difficult to have the target deliver drugs to only desired sites and to precisely control the release of drugs at the desired site. A complete understanding of the structures of nanoparticles in solution as well as the correlation of nanoparticles and pharmacological effects are necessary to resolve these issues.

Dr. Kazuo Sakurai (Professor, The University of Kitakyushu, Japan) and colleagues, who strive to establish molecular design techniques, have focused on nanointerfaces. "The structures and functions of nanoparticles such as polymeric micelles are controlled by the interactions between the shell and core on nanointerfaces. The development of DDS particles requires the internal structures of particles, the behavior and formation of drugs on hydrophilic and hydrophobic interfaces in DDS particles, and the fusion of biomembranes and DDS particles to be thoroughly examined," explains Dr. Sakurai. Thus, investigating the interface between the shell and core is essential to their research.

Investigating the Behavior of Drugs Encapsulated in Polymeric Micelles

Dr. Sakurai's research group began experiments to reveal the structures of micelles by examining nanointerfaces at the Structural Biology Beamline II (BL40B2) at SPring-8. In October 2008, this project was approved as part of the Core Research for Evolutional Science and Technology (CREST) program by the Japan Science and Technology Agency (JST).

Small-angle X-ray scattering (SAXS) is the only technique to examine nanosized biomolecules and their aggregates. X-rays with small scattering angles can reveal the structures of samples at the 1-nm to 1-μm level. Although SAXS allows the configuration of these particles to be visualized on such small scales, the sample concentration of these particles needs to be more than 100 times higher than that in the body because the data signals are very small. Hence, the observed structures would substantially differ from those in the living body condition.

The principal reason why such a high concentration is required is parasitic scattering, which is the optical noise produced from the air around a sample upon irradiation of X-rays. "To conduct experiments using ultra-diluted solutions with the lowest possible particle concentration, which is close to the living body condition as possible, parasitic scattering had to be eliminated," mentions Dr. Sakurai when explaining the progress of his experiments. To this end, his group developed an innovative device to measure sealed cell encapsulating sample solutions in a vacuum chamber. This system drastically improved valid data (signal: S) to noise such as the parasitic scattering (noise: N) ratio (S/N ratio) (Fig. 1). Regardless of the experimental difficulties, the highly brilliant X-rays at BL40B2 and the RIKEN Structural Biology Beamline I (BL45XU) have been indispensable in their research.

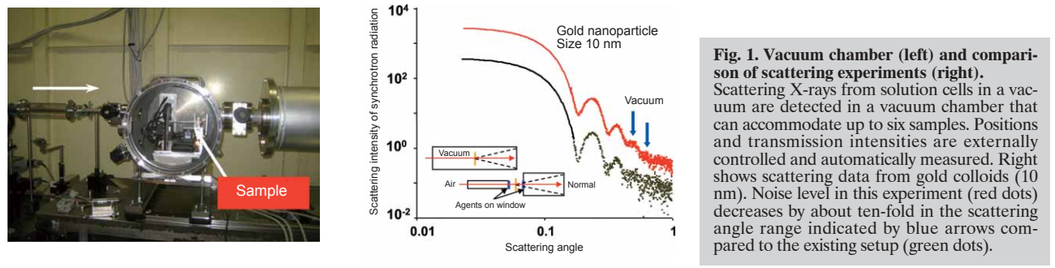

Fig. 1. Vacuum chamber (left) and comparison of scattering experiments (right).
Scattering X-rays from solution cells in a vacuum are detected in a vacuum chamber that can accommodate up to six samples. Positions and transmission intensities are externally controlled and automatically measured. Right shows scattering data from gold colloids (10 nm). Noise level in this experiment (red dots) decreases by about ten-fold in the scattering angle range indicated by blue arrows compared to the existing setup (green dots).

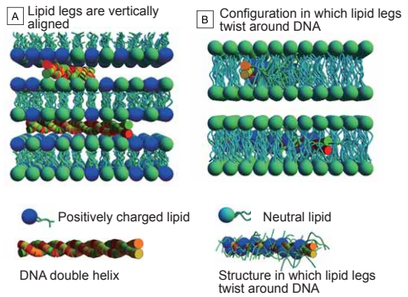

Fig. 2. DNA transfer structural model of gene transfer agents comprised of lipid micelles.
A: DNA in the hydrophilic phase caught between the head parts of two-molecule membranes comprised of cationic lipids. Dr. Cyrus R. Safinya and colleagues proposed this model. B: Lipid alkyl chains twisting around DNA hydrophobizes DNA, which is then captured in the hydrophobic phase. Dr. Victor A. Bloomfield and colleagues proposed this model.

As an example, this research group initially used the block copolymers of polyethylene glycol/polyaspartic acid (PEG/PAA) in which a synthesized retinoid LE540 was encapsulated. Retinoid has received attention as a compound with various bioactivities, including anticancer effects, and many studies on synthesized retinoids have been conducted. In Dr. Sakurai's sample, synthesized retinoids were encapsulated in polymeric micelles composed of PEG as a shell and PAA as a core. "Several clinical studies are being conducted on polymeric micelles as DDSs of anticancer drugs. However, a detailed examination of the condition of encapsulated drugs has yet to be conducted," explains Dr. Sakurai. Ultra-diluted samples encapsulated in sealed cells were placed in a vacuum chamber and SAXS measurements were conducted. LE540 addition caused the crystal structures of aspartic acids in the cores to become amorphous. This change, which is not induced by LE540 addition under normal conditions, suggests that the transformation phenomenon occurs in a tiny area inside a 6-nm radius. This result was published in *Langmuir* (2010).

Factors Affecting the Expression Efficiency of Gene Transfer Agents

Additionally, gene transfer agents comprised of lipid micelles were analyzed. Gene transfer agents are utilized in gene therapy to incorporate DNA and deliver it to genes in desired cells. This gene therapy, which is an application of DDSs, is expected to provide therapeutic effects for constitutional symptoms such as allergies.

Dr. Sakurai and colleagues used SAXS at SPring-8 to study the relationship between the composition of gene transfer agents and gene transfer efficiency. In particular, the effects of the composition of gene transfer agents on the probability of DNA being transferred into target cells were examined. The gene transfer efficiencies were measured at various solubilities and biocompatibilities by mixing various proportions of neutral lipids, specifically dioleoyl phosphatidylcholine (DOPC) and dilinoleoyl phosphatidylcholine (DLPC), with cationic lipids, benzylamine derivatives (BAs). Gene transfer agents with a high transduction efficiency (Fig. 3A) had hexagonal cylindrical structures prior to adding DNA. However, the addition of DNA increased the regularity of the structures. In contrast, agents without a transduction efficiency (Fig. 3B) had spherical micelle structures prior to adding DNA, but after adding DNA, the agents were converted into hexagonal cylindrical structures and were eventually transferred to lamellar structures composed of alternating layers of hydrophilic and hydrophobic phases. "DNA was transferred into the hydrophilic phase in cases with a high transduction efficiency (Fig. 2A), but was transferred into the hydrophobic phase in cases with a low transduction efficiency (Fig. 2B). We speculated that this difference is responsible for the expression efficiency of gene transfer agents," explains Dr. Sakurai. Thus, the transduction efficiency of gene transfer agents strongly depends on the state of the neutral lipids, which is related to the micellar structures. "Visualization of nanoparticles, which was once impossible, can extensively promote the realization of nano-DDSs," describes Dr. Sakurai.

Dr. Sakurai received the Society of Polymer Science of Japan (SPSJ) Mitsubishi Chemical Award in 2008 for his contributions, including those explained here as well as his research on DDSs using polysaccharides. SPSJ honored him by recognizing that his research on nano-DDS particles is a basic technology in polymer science that will contribute to industry.

References
1. K. Koiwai, K. Tokuhisa, Y. Kudo, S. Kusuki, Y. Takeda and K. Sakurai; *Bioconjugate Chem.*, **16**, 1349 (2005)
2. I. Akiba, N. Terada, S. Hashida, K. Sakurai; *Langmuir*, **26**, 7544 (2010)
3. M. Sakuragi, S. Kusuki, E. Hamada, H. Masunaga, H. Ogawa, I. Akiba and K. Sakurai; *J. Phys: Conference Ser.*, **184**, 012008 (2009)

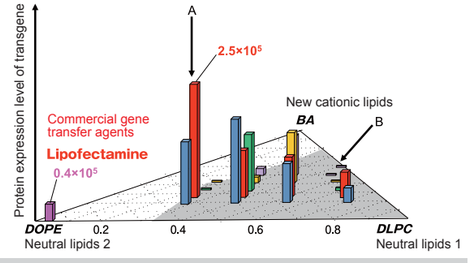

Fig. 3. Relationship between the composition of lipids and gene expression efficiencies.
Composition of lipids and gene expression efficiencies (vertical axis) are depicted on a triangular correlation plot. Plane coordinates plot the composition ratio among BAs, dilinoleoyl phosphatidylcholine (DLPC), and dioleoyl phosphatidylcholine (DOPE) of neutral lipids. Composition ratio of BA:DOPE:DLPC is 1:2:1 for the case with the highest expression efficiency (indicated by A), whereas the composition ratio of BA:DLPC is 1:1 for the case with nearly zero expression (indicated by B), which we speculate correspond to A and B in Fig. 2, respectively.

Exploring Surfaces of Organic Thin Films at the Nanolevel

The surfaces of organic thin films and polymeric films have received increasing amounts of attention in the fields of organic molecules and polymers because the recent trend is that fields involving materials whose functions largely depend on the surface structure such as fields relating to organic thin film transistors (TFTs) are expanding. Moreover, in its ten year history, the research on surface structures of organic molecules and polymers has received varying degrees of attention, depending on their utilities at different scales from on the order of 1 nm to 10 nm (1 nm = 10^{-9} m). The structural evaluation of these nanosurfaces has been made possible due to the grazing incidence X-ray diffraction (GIXD) technique, which uses highly brilliant and directional X-rays available at SPring-8. In this topic, the following two studies are reported: (1) achievements in the explorative studies on the formation mechanisms of the crystal structures of organic semiconductor thin films and (2) achievements in surface structures of polymer films using GIXD.

GIXD—Evaluation Technique of Crystal Structures of Nanosurfaces

Because most materials have refractive indexes of X-rays slightly less than one, grazing incidence X-rays on a flat surface of a material results in total reflection. GIXD is a technique to measure the reflection, refraction, and diffraction of X-rays by slightly varying the incidence angle of X-rays around the total reflection angle. This technique can reveal the structures of materials within 10 nm from the surface as well as deeper structures distinctly at the atomic and molecular levels. Grazing incidence is also called small-angle incidence.

X-ray diffraction measurements are suitable to structurally evaluate thin films such as organic molecules and polymers because the samples do not have to be pretreated and X-ray radiation causes minimal damage. However, crystals of organic molecules and polymers have low X-ray scattering intensities. Thus, the detection of the intensity and peak width of faint scattered X-rays is impossible for X-rays with conventional intensities. Furthermore, highly directional X-rays are required to precisely control the incident angle. Hence, the highly brilliant and directional X-rays at SPring-8 are required for these measurements.

Changing the Mechanisms of Membrane Formation by Terminal Functional Groups

Devices comprised of organic semiconductors, e.g., TFTs, have many advantages such as being cost-efficient, lightweight, and flexible, but certain defects are common, including the creation of polycrystals whose molecular arrangements easily crack. Additionally, their crystal structures show variations and often exhibit a non-uniform electrical conductivity. Besides questioning the reproducibility, such defects make it difficult to increase the mobility of electrons or holes, which is a measure of the processing capacity of a device.

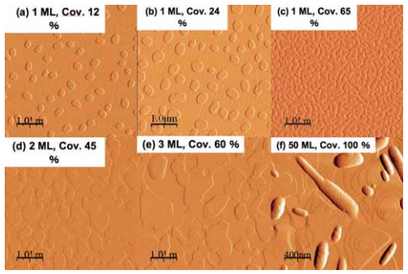

Fig. 1. AFM images of DS-2T evaporated films with hexyl groups on their terminals in the early stage of crystallization.
a–c Islands with a single molecule thickness expand in-plane to cover the entire plate. **d–f** Structures become 3D upon the formation of a second layer.

To overcome these issues, the molecular arrangements of crystal layers and the structures of thin films as well as the crystal growth mechanisms must be understood. Dr. Noriyuki Yoshimoto (Professor, Iwate University, Japan), Dr. Christine Videlot–Ackermann (Centre Interdisciplinaire de Nanoscience de Marseille (CINaM), France), Mr. Yoshiyuki Asabe (Alps Electric Co., Ltd., Japan), and colleagues at the Japan Science and Technology Agency (JST) Iwate have attempted to reveal the structures of organic thin films at the single molecule level. CINaM has synthesized derivatives of 30 types of organic molecules, and out of which they selected distyryl-oligothiophene (DS-nT) and its derivatives as target molecules because DS-nT has a relatively high mobility and long-term stability. In November 2006, GIXD measurements began at the Surface and Interface Structures Beamline (BL13XU), but were later moved to the Engineering Science Research III Beamline (BL46XU) because the thin film diffractometer was transferred there in 2007.

When DS-nT does not have a substituent, the second and third layers simultaneously form with the first layer of the molecular assembly ("island"). In contrast, when the substituents are hexyl groups (C_6H_{13}-), the second layer does not form until the first layer completely covers the plate, and the formation of the 3D crystalline structure is initiated as the second layer is formed. Figure 1 depicts these processes using atomic force microscope (AFM) images. The first layer grows in a 2D plane, but a 3D structure quickly appears as the second layer is formed. As shown in Fig. 2, the GIXD measurements of these processes reveal that the intermolecular distances decrease upon the formation of the second and subsequent layers, which can be observed from the position of the (020) peak. While forming the second layer, the island shows a remarkable dynamism. However, the formation processes of the first and second layers in samples without hexyl groups are the same. Their research has provided the first molecular level example of how the interaction between thin films and plates differs according to the terminal functional group, and consequently demonstrated that the formation mechanisms of membranes change. These experiments would not be possible without GIXD at SPring-8 to precisely observe the changes, including variations in intermolecular distances and the crystal structures from the first to second molecular layers (MLs).

As their research has progressed, it has been found that the crystal orientation anisotropy, or the variation in crystal structures, which is a disadvantage of organic crystals, can be converted to an advantage. "The existence of the island, which has various electromagnetic properties, indicates the possibility of the numerous different combinations," explains Dr. Yoshimoto. Moreover, their research group has revealed the 3D crystal

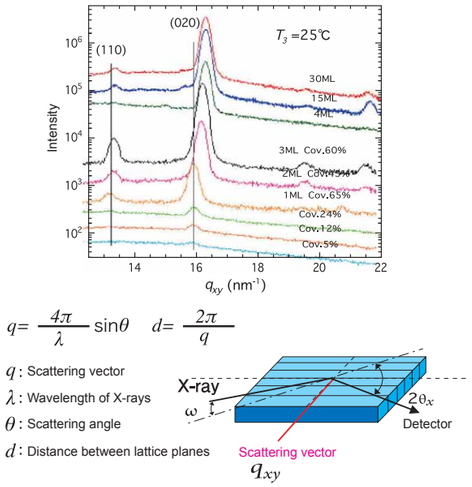

Fig. 2. GIXD data in the early developmental process of DS-2T evaporated films with hexyl groups on their terminals.
Data shows that the intermolecular distances and structures of the first molecular layer (ML) differ from those of second or higher ML. Horizontal axis, q, represents the amplitude of the scattering vector, which is related to the lattice spacing (distance between lattice planes), d, by equations shown in the figure. As q increases, the intermolecular distance decreases. For example, the lattice spacing in the (020) lattice is 0.39 nm in the first layer and 0.38 nm in the second and subsequent layers, indicating that the intermolecular distance decreases in the second and subsequent layers.

structures of organic semiconductor ultra-thin films in the early stage of crystallization as well as the molecular structures of thin films exhibiting desirable electric properties. Currently, their group is conducting real-time temporal observations of organic semiconductor molecules to unravel the mechanisms of aggregation and crystallization using GIXD.

Exploring Problems in Polymer Thin Film Surfaces

In the fields of electronics and photonics, manufacturing technologies of thin films using organic molecules and polymers are advancing. It is not an exaggeration to say that thin films are mostly occupied by surfaces. Thus, the structures and physical properties of material surfaces greatly influence the functional properties of materials. Although several studies on the structural observation of a polymer surfaces have been reported for polyimide and polyethylene terephthalate (PET), similar studies using the most common polymer, polyethylene, were considered nearly impossible due to difficulties in sample preparation. However in 2002, Dr. Chisato Kajiyama[1] (Professor, Kyushu University, Japan), Dr. Atsushi Takahara (Professor, *ditto*), Dr. Sono Sasaki[2] (Assistant Professor, *ditto*), Dr. Osamu Sakata (Senior Scientist, Japan Synchrotron Radiation Research Institute (JASRI)), and colleagues challenged the impossible using the highly brilliant and direct X-rays at SPring-8 for GIXD.

Their research has revealed aggregation structures of polymer chains on polyethylene film surfaces. They prepared polyethylene thin films (about 400-nm thick) on silicon substrates by minimizing the film's surface asperity. After melting on the substrates, these films were annealed at arbitrary temperatures between 72 and 122 °C to control crystallization. At BL13XU, the diffraction intensity data were recorded with the grazing incidence at 0.11° for the surface regions (Fig. 3**a**) and at 0.20° for the inside (bulk) regions (Fig. 3**b**) to analyze crystal structures. Numerous sharp diffraction peaks were observed, and the GIXD measurements at SPring-8 definitely met their research group's expectations.

Examining the crystal lattice, which represents the molecular configuration in a crystal, has revealed that the lattice size in the surface region is smaller than that in the bulk regions, indicating that the intermolecular distances of the surface regions are smaller and the crystals are more densely-packed compared to the bulk regions. An organic polymer solid consists of a mixture of crystal and amorphous components; its low crystallinity is the cause of its poor strength. Their study has demonstrated that the crystallinity of the surface region is 12% smaller than that of the bulk regions.

Furthermore, investigating the orderliness of a crystal lattice in the in-plane direction of the surface region has revealed that the lattice arrangement contains considerable variation without a long-range order. It is presumed that the large heat dissipation and large degree of freedom of molecular motion in the surface region may induce an unstable environment for crystallization. Dr. Sasaki, who witnessed the significant analyzing power of synchrotron radiation and realized SPring-8 provides indispensible light to study the surfaces of polymeric thin films, has stated, "The aggregation states of polymer chains in the surface region sometimes determine their own physical properties and functions of thin film materials."

Their research group is the first to reveal that the surfaces of polyethylene thin films have unique molecular aggregation structures on the nanolevel, and unlike the bulk regions, the surface regions have large deformations and displacements. These results were published in *Macromolecules* in 2003. Dr. Sasaki and colleagues are currently working on real-time high-speed time resolving measurements of structural changes using synchrotron radiation to reveal how polymer chains in the surface regions alter their structures according to various external stimuli such as temperature, humidity, light, and stress.

[1] Currently the President at the Japan Student Services Organization.
[2] Currently Associate Professor, Kyoto Institute of Technology.

References
1. N. Yoshimoto, K. Aosawa, T. Tanisawa, K. Omote, J. Ackermann, C. Videlot-Ackermann, H. Brisset and F. Fages; *Cryst. Res. Technol.*, **42**, 1228 (2007)
2. H. Yakabe, S. Sasaki, O. Sakata, A. Takahara and T. Kajiyama; *Macromolecules*, **36**, 5905 (2003)
3. H. Yakabe, K. Tanaka, T. Nagamura, S. Sasaki, O. Sakata, A. Takahara and T. Kajiyama; *Polym. Bull.*, **53**, 213 (2005)

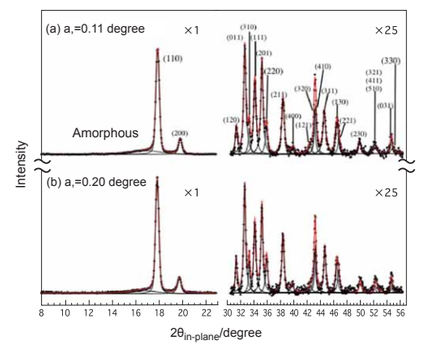

Fig. 3. In-plane GIXD patterns of polyethylene thin films formed on silicon substrates.
Peak positions and widths of Bragg reflections reveal that the atomic arrangement in a crystal is more random near the surface **a** than inside **b**. Approximately 400-nm thick films are used in the measurements.

"Quasicrystals"—A Mysterious Material Discovered in Polymers

Quasicrystals, which have similar structures but different properties than crystals, have drastically changed the framework of crystallography. Until a Japanese research team discovered quasicrystals in polymers, quasicrystals had only been observed in alloys. Polymeric quasicrystals are 50–100 nm (1 nm = 10^{-9} m), which are enormous (more than 100 times larger) than those found in alloys. Compared to common materials, quasicrystals refract light in the opposite direction (negative refraction index). Due to this property, quasicrystals should contribute to the development of a "superlens," which will focus on images of objects smaller than the light wavelength. Moreover, because polymeric materials are easily designed, quasicrystals have great potential in practical applications. Although polymeric quasicrystals are relatively large, the domain size of quasicrystals is about 5 μm (1 μm = 10^{-6} m). Therefore, SPring-8 is indispensable for structural analyses.

Discovering Quasicrystals in Polymers

In 1982, materials scientist Dr. Dan Shechtman (Professor, the National Institute of Standards and Technology[1] , USA) discovered an unfamiliar state that differed from common crystals in aluminum–manganese alloys where primitive unit cells (basic building blocks of a crystal) were regularly aligned to comprise crystals. Diffraction spots are observed due to the interference of X-rays according to the conformation of the primitive unit cells upon X-ray irradiation of a crystal. However, the state that Dr. Shechtman discovered did not contain primitive unit cells, but some level of regularity provided the diffraction spots. Moreover, its structure was a regular icosahedron (polyhedron with 20 identical equilateral triangular faces), which is impossible for a crystal. Although it had some level of regularity (or quasi-periodicity), this material lacked the same level of regularity as the crystal. It could not be crystallographically defined but had some level of regularity (or quasi-periodicity), which was later named "quasicrystals."

Following this original discovery, it was revealed that quasicrystals have peculiar properties, and new types of quasicrystals were found. Eventually 10-nm quasicrystals, which are much larger than the 0.5-nm size (atomic level) that Dr. Shechtman discovered, were observed. Then in April 2007 Dr. Yushu Matsushita (Professor, Nagoya University, Japan), Dr. Atsushi Takano (Associate Professor, *ditto*), Ken-ichi Hayashida[2] (graduate student, *ditto*), Dr. Tomonari Dotera[3] (Associate Professor, Kyoto University, Japan), and colleagues discovered for the first example of quasicrystals in complex polymers. The precise polymer-synthesizing technologies that their research group developed contributed to this achievement.

Exploring the Potential of Quasicrystals using Highly Brilliant X-rays

A macromolecule is a large molecule, which is composed of mainly carbon and hydrogen and is connected by sharing electrons via covalent chemical bonds. A monomer is the basic building block of a macromolecule, e.g., the monomer of polyethylene is ethylene. The process of connecting monomers is called polymerization, and thus a macromolecule is often called a polymer. When multiple types of monomers are polymerized, the resulting polymers are called copolymers. Copolymers have several variations. A block copolymer is a common copolymer composed of chains of multiple types of monomers; each monomer chain consists of a single type of monomer consecutively connected. For example, two types of monomers A and B form a combination of monomer chains like "-A-A-A-A-A-A-B-B-B-B-B-B-."

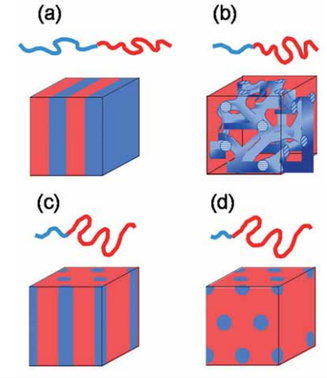

Fig. 1. Transition pattern diagrams of microdomain structures according to the component changes in AB two-component block copolymers.
(a) Lamella structure. **(b)** Double gyroid (bicontinuous) structure. **(c)** Cylindrical dispersion structure. **(d)** Spherical dispersion structure.

Block copolymers are the targets of Dr. Matsushita and colleagues. When two types of monomers (A and B) comprise a block copolymer, it is called a two-component block copolymer, which consists of an A-phase (chains of monomer A) and a B-phase (chains of monomer B). As shown in Fig. 1, the phase structure can be divided into four groups according to the length ratios of A and B. These phases range in size from a few nanometers to several tens of nanometers. Thus, this separation is called nanoscale phase separation.

On the other hand, increasing the number of monomer types to three opens a new horizon. The different components are phase-separated from each other and spatial binding forces increase to easily form a cylinder structure (Fig. 2**c**). Moreover, the cross-section of each cylinder forms a regularly aligned regular polygon (Fig. 2**d**). There are only 12 ways to fill a plane using regular polygons that are the same size, including triangles, squares, hexagons, and dodecagons (polygon with 12 sides and 12 angles). This was originally studied by a mathematician Archimedes in the 3rd century BC and was later completed by astronomer Johannes Kepler in the 17th century. For example, when the only component is a regular hexagon, (6.6.6) tiling where three regular hexagons align to their vertices is the solution. If conditions permit, polymers will spontaneously conform such a regular structure, which is called self-assembly.

Prior to starting this research, Dr. Matsushita and colleagues had already experimentally observed a block copolymer undergoing a molecular construction where three polymer components were connected via single point. This copolymer easily conformed to a cylindrical phase-separation structure. "We decided to utilize SPring-8 to examine the tiling formation of three-component block copolymers," explains Dr. Matsushita. Their research group utilized a microbeam small-angle X-ray scattering instrument installed at the High Flux Beamline BL40XU. When irradiated, the electrons in a material scatter the X-rays. Hence, scattering with a small scattering angle can provide information about nanosized structures. Herein, X-rays at SPring-8 with an ultra-high brilliance and extremely small beam size are indispensable to explore such a tiny region.

The ratios of the three components were varied in the experiments. The polymers altered their conformations according to the components, and exhibited a series of tiling structures. Dr. Matsushita and colleagues focused on (3.3.4.3.4) tiling composed of regular triangles and squares. According to Dr. Matsushita, "We observed 12 distinctive diffraction spots of X-rays, which have not been observed in other polymers. Prior studies with other materials have revealed that such diffraction spots suggest the emergence of quasicrystals nearby." Upon observing these unique diffraction spots, they realized that this could be the first example of a quasicrystal in a polymer.

Although they continued varying the composition of (3.3.4.3.4), quasicrystals had yet to materialize. "There was logically no question about our experimental strategy. However, we could not find them. We repeated our experiments through trial and error by encouraging staff members," recalls Dr. Matsushita, and six month later, they finally identified quasicrystal structures (Fig. 3).

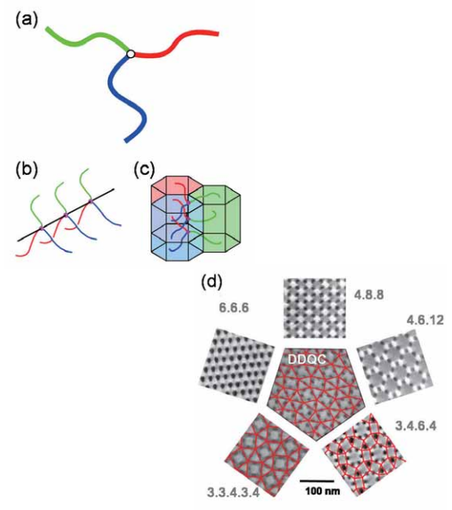

Fig. 2. Molecular structure and self-assembly processes of star-shaped copolymers.
(a) Any combination between two green, red, or blue block chains is repulsive when they are packed in a small area due to their negative relationships. **(b)** Consequently, such repulsion in a, the points of union form a line (the black line is to guide the eye and does not exist). **(c)** Self-assembly into cylindrical aggregation structures. Points of union exist only on a line formed by gathering three hexagonal cylinders. **(d)** Cross-sections of tiling structures. Outer five structures represent Archimedean tilings, while the center represents 12-fold symmetrical quasicrystal tilings.

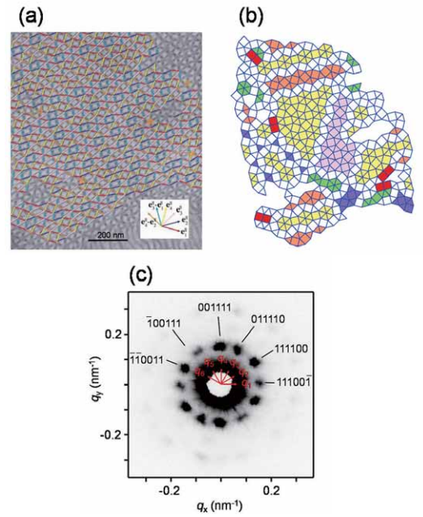

Fig. 3. Quasicrystal structures of star-shaped copolymers.
Relative fractions of three block chains comprising the sample are 1:2.7:2.5. **(a)** Wide-field transmission electron microscopic image. Virtual quasicrystal tilings are distinguished by six colors with differentiating directions. **(b)** Transition pattern diagram that is transferred from **a** by a regular triangle and square. **(c)** 12 diffraction spots of the 12-fold symmetrical quasicrystals obtained at SPring-8.

Possibility of Freely Designing Metamaterials

The most significant achievement of Dr. Matsushita and colleagues is that they demonstrated the universality of quasicrystals, which are commonly observed across materials with various spatial scales. Additionally, quasicrystals have potential as metamaterials. Metamaterials refract light in the opposite direction (negative refraction index) compared to common materials. When light passes through a metamaterial, a phenomenon, which can be described as the apparent bending of light around obstacles, will make previously visible materials invisible. The tile sizes of metamaterials range between 50–100 nm, and are about ten-fold larger than those in conventional materials. "If a tile size compatible with visible light is achieved by contriving molecular design methods, then it may be possible to develop a superlens with which images of objects smaller than light wavelength can be obtained. Then the development of synthetic fibers, or "transparent mantles" that could make a person wearing them invisible would not be a dream," mentions Dr. Matsushita.

Although very few studies have investigated 100-nm (mesoscale) size tilings, the possibility of discovering various quasicrystals has been suggested. Therefore, this discovery is significant and has received both national and international attention. In particular, it has been referenced in various publications, including *Nature*: Research Highlights (May 2007), *Physical Review Focus* (May 2007), and *Science*: Editor's Choice (June 2007).

[1] Formnerly the National Bureau of Standards.
[2] Currently a researcher at Toyota Central R&D Labs., Inc., Japan.
[3] Currently a professor at Kinki University, Japan.

Reference
1. K. Hayashida, T. Dotera, A. Takano and Y. Matsushita; *Phys. Rev. Lett.*, **98**, 195502 (2007)

Materials Structure Science

Extracting Functions from the Arrangement of Atoms and Molecules

Fundamental Understanding of the Functional Properties of Materials due to Precise Structural Analyses

Modern society is prosperous due to the support of various materials and basic substances with diverse functions. However, society is currently facing serious energy and environmental issues. In order to continue sustainable development, it is imperative that society creates innovative materials and utilizes their functions more effectively. To meet these demands, materials structure science strives to understand the structures and functions as well as design innovative materials. Materials structure science research conducted at SPring-8 employs the most precise and powerful technologies currently available. SPring-8 is one of three operational third-generation large synchrotron facilities in the world, and continues to be a leader in international materials structure science research by expanding the research frontier and further advancing technologies for materials science.

SPring-8 Has Opened the Door to Precise Structural Analyses

Diverse devices and instruments are constructed and protected by mechanically strong and chemically stable materials. Moreover, in today's information society, metals and semiconductors with superior electron transport properties are indispensable for electronic components in devices and instruments, and materials with high chemical activities such as catalysts are necessary to address energy and environmental issues. Regardless of the organic or inorganic composition, all materials are composed of elements found in the periodic table. Thus, in principle, the physical properties of all materials can be revealed by identifying the species and arrangements of the constituent elements. Research that investigates the relationship between structure and the physical properties of materials is called "materials structure science research", which is a major academic field to promote materials design with advanced functions.

Materials structure science research has been advancing rapidly since the discovery of diffraction phenomena of X-rays and electron beams, and is now indispensable in understanding the physical properties of materials and designing functional materials. However, in cases where the physical properties are controlled by structural changes on scales smaller than the precision of techniques currently available, materials structure science research must be based on empirical factors and information obtained from other measurement techniques. In other words, much of the history of materials structure science research involves improving the precision of structural analysis. In the beginning, materials structure science research contributed significantly to a few research fields such as research on ferroelectrics in which dielectric polarization is induced by relatively large position displacements of atoms on the 0.01 nm scale (nm = 10^{-9} m). However, because modern cutting-edge experiments require extremely precise measurements, techniques developed in the early era of materials structure science research are fast becoming obsolete. On the other hand, SPring-8 can contribute to modern materials structure science research.

Synchrotron radiation at SPring-8 has superior properties, including high brilliance, low emittance (small beam size, low dispersion, high directionality), and a wide range of available energies (wavelengths). Precise experiments using such superior synchrotron radiation have made it possible to obtain sufficiently strong signals (information) even from minuscule sample amounts, and have yielded highly accurate diffraction images. Two examples to demonstrate the capabilities of synchrotron radiation at SPring-8 are the research projects involving $BaTiO_3$ and $Fe(phen)_2(NCS)_2$. $BaTiO_3$ is a ferroelectric material, and diffraction images were measured on a ~100 nm sample, which has 1/1,000,000,000 of the volume of samples commonly used in conventional experiments (~100 μm (μm = 10^{-6} m)). Additionally, the anisotropy of Fe–N binding in a spin crossover complex, $Fe(phen)_2(NCS)_2$, was determined with a precision less than 0.001 nm, and revealed the diversity of electron spin states induced by photoirradiation.

Advances in high-precision structural analysis are not limited to reduced sample size or improved precision. Because diffraction data is best suited to determine the position of atoms, conventional analyses are limited to examining periodic atomic arrangements. However, the high precision diffraction data obtained from new analysis techniques can visualize the spatial distributions of electrons in atoms as well as provide information about the electronic properties, which determine the chemical bonds between atoms and the electric conductivity of materials. Moreover, the spatial distribution density gradient of electrons enables the spatial distributions of electric fields (distributions of electric physical quantities) to be visualized. For example, the spatial distributions of electric fields of nanoporous materials, which exhibit molecular storage and transport functionalities, as well as those of $PbTiO_3$, which is a potential next generation piezoelectric material, have been visualized (Fig. 2). At SPring-8, materials structure science research has reached the point where the mutual relationship between structures and material properties can be directly investigated.

Conducting Materials Structure Science Research at SPring-8

Given the fact that even resource-rich countries like the United States have fully supported materials research by constructing a third-generation synchrotron radiation facility, for Japan, a resource-less country, to thrive in the international community, the highly effective utilization of natural resources and the development of man-made resources are fundamentally important. To sustain an information society, it is especially urgent to develop substances and hardware essential for high-speed operations of electronic devices as well as to elucidate the reaction processes of catalytic reactions and chemical reactions.

Besides conducing conventional static science research under normal conditions, the dynamic structures of materials and their electron states under special environments such as high temperature, high pressures, and strong magnetic fields must be elucidated to fully understand and utilize the advanced functions of materials. By taking advantage of the superiority of synchrotron radiation sources at SPring-8, researchers can study material structures under locally reproduced extreme environmental conditions. SPring-8 has already contributed to the elucidation of the dynamic changes in material structures through its stable pulse performance of synchrotron radiation and control technologies. For example, the high-speed time resolved analysis techniques available at SPring-8 have helped reveal the dynamic changes that occur during the writing process, which is on a 0.3-μs time scale, of a high-speed high-density readable/writable DVD. Additionally, SPring-8 is the only facility that can conduct diffraction experiments under conditions exceeding 350 GPa (GPa = 10^9 Pa = ~10,000 atm) and 5,000 K, which encompass all environmental conditions found inside the Earth (Fig. 3). These unique experimental environments will not only aid in understanding the Earth's interior, but will also assist in the discovery of new material phases and the development of innovative functional materials.

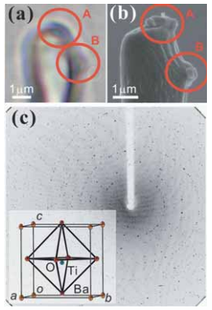

Fig. 1. Diffraction images of X-rays scattering from $BaTiO_3$ crystals, which are smaller than 500 nm.
Images of nanocrystal particles (A, B) attached on a glass rod: (a) optical image and (b) scanning electron microscope image. (c) Measured diffraction image and structure model reconstructed from the analysis results. (Reprinted with the permission from Yasuda, Murayama, Fukuyama, Kim, Kimura, Toriumi, Tanaka, Moritomo, Kuroiwa, Kato, Tanaka and Takata (2009), *J. Synchrotron Rad.* Vol. 16. pp.352-357.)

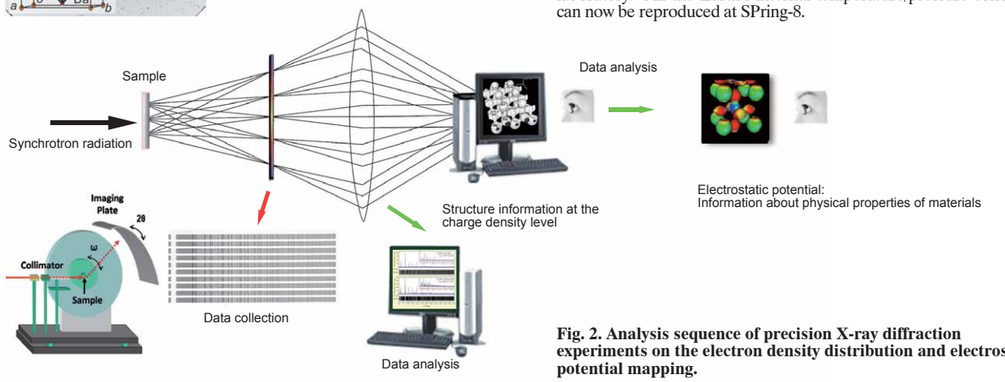

Fig. 2. Analysis sequence of precision X-ray diffraction experiments on the electron density distribution and electrostatic potential mapping.

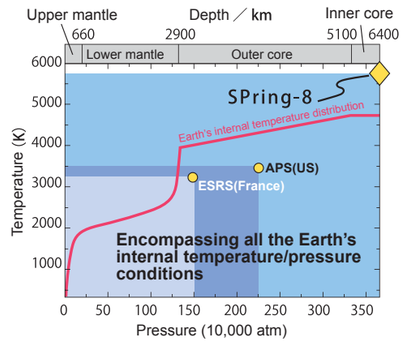

Fig. 3. Extreme environments that have been reproduced at SPring-8.
For the first time, an extremely high pressure/temperature environment (364 GPa (GPa = 10^9 Pa = ~10,000 atm), 5,500 K) equivalent to the center of the Earth has been reproduced in a laboratory. All the Earth's internal temperature/pressure conditions can now be reproduced at SPring-8.

Mysterious Polyhedral Groups in the Nanoworld—Unraveling their True Characters

Fullerenes and carbon nanotubes have attracted much attention as promising raw materials for next generation nanotechnologies. At the same time, basic research aiming to explore their characteristics and establish application technologies of these new raw materials has been advancing. However, the true characters of fullerenes and nanotubes have been elusive. A fullerene is a soccer ball shaped molecule composed of 60 or more carbon atoms, while a carbon nanotube is a long and thin tubular material composed of a rolled hexagonal net-like graphene sheet. Hence, highly brilliant X-rays with extremely short wavelengths, which can brightly light the nanoworld on the order of 1/1,000,000 mm, are indispensable to reveal their characters.

Fullerenes and Nanotubes —Promising Raw Materials

A fullerene (C_{60}), which was discovered by Richard E. Smalley, Harold W. Kroto, Robert F. Curl, (who shared the Nobel Prize in Chemistry in 1996) and two others in 1985, is unique due to its soccer ball shape. This molecule, which is composed of pentagonal and hexagonal molecular chains, was named fullerene after a famous architect, Buckminster Fuller, who designed geodesic domes consisting of pentagonal and hexagonal panels. Since its discovery, many have claimed to identify variations of fullerenes such as spheroid-shaped C_{70} and those containing metal atoms inside (Fig. 1A). However, even ten years after the discovery of fullerenes, the fundamental question about the existence of endohedral metallofullerenes remained, "Do they actually contain metal atoms inside?"

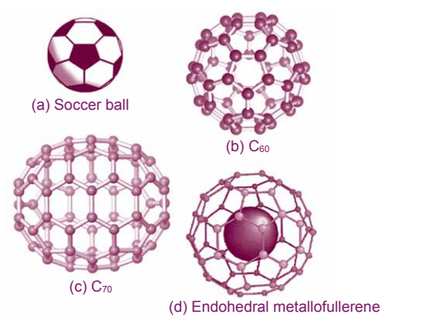

Fig. 1A. Molecular models of C_{60} and C_{70} molecules and endohedral metallofullerene.
(a) Soccer ball. **(b)** Pentagon surrounded by five hexagons. **(c)** Spheroid-shaped fullerene. **(d)** Endohedral metallofullerene enclosing a single metal atom.

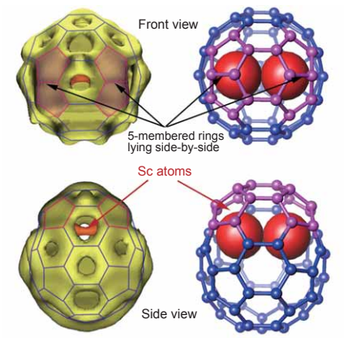

Fig. 1B. Electron density and structure model of $Sc_2@C_{66}$.
Unconventional structure of a fullerene is revealed.

In 1991, Dr. Sumio Iijima[1] (Researcher, NEC Tsukuba Research Laboratories, Japan) discovered a carbon nanotube (Fig. 2). A carbon nanotube, which is composed solely of carbon, is a tubular shape with a radius about 1/10,000 of that for a strand of hair (Fig. 2). Due to their electrically and physically superior properties nanotubes have attracted attention as fundamental materials in nanotechnology. Carbon nanotubes are expected to replace silicon devices, which are rapidly approaching their size reduction limit, as next generation electronic raw materials. However, the development of highly precise conductivity control technologies is indispensable to realize these next generation devices.

Revealing the True Characteristics of Endohedral Metallofullerenes

Using synchrotron radiation at SPring-8, Dr. Makoto Sakata[2] (Professor, Nagoya University, Japan), Dr. Masaki Takata[3] (Associate Professor, *ditto*), and colleagues directly observed that a fullerene consisting of 82 carbon atoms (C_{82}) actually contains a metal atom, yttrium (Y). They published their crucial data in 1995. This fullerene is termed $Y@C_{82}$, where "@" indicates "endohedral." Subsequently, their team has revealed the structures of fullerenes containing other metals such as scandium (Sc) and lanthanum (La), which are denoted as $Sc@C_{82}$, $Sc_2@C_{84}$, $Sc_3@C_{82}$, $La@C_{82}$, $La_2@C_{80}$, and $Sc_2@C_{66}$.

The powder X-ray diffractometer installed at the Powder Diffraction Beamline (BL02B2) at SPring-8 and the MEM/Rietveld method that Dr. Takata and colleagues developed have contributed significantly to their research. Even atoms and molecules beyond the scope of visible light can be observed using X-rays because the wavelength of an X-ray is equivalent to the size of an atom. Hence, analyzing the data obtained from the diffraction measurements of irradiated X-rays can visualize images of atoms and molecules.

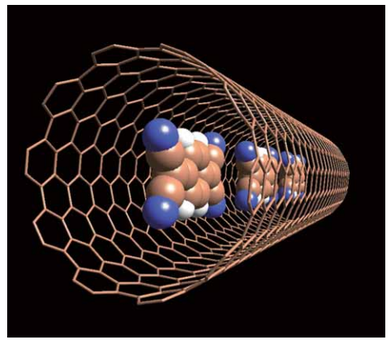

Fig. 2. Structural image of a carbon nanotube containing several organic molecules.
Electrons, which are supplied from the inside organic molecules including various fullerenes, carry electricity to the outer tube, creating a tubular conductor. Carbon nanotubes in which fullerenes are doped are called "pea pods" due to their shape.

In 2000, Dr. Hisanori Shinohara (Professor, Nagoya University) and colleagues created a new endohedral metallofullerene, $Sc_2@C_{66}$ (containing 2 Sc atoms) (Fig. 1B) in their effort to refute a traditional theory about the conformation of stable fullerene molecules, the isolated pentagon rule (IPR). IPR[5,6] postulates that, "In fullerenes composed of multiple combinations of pentagonal and hexagonal carbon atom coupled rings (5- and 6-membered rings), none of the pentagons are in contact with each other. In such a conformation of the pentagons, some electrons are left over and do not hold the atoms together, causing the structure to become unstable. Thus, a single pentagon must be surrounded by five hexagons." Through a stringent structure determination of $Sc_2@C_{66}$, Dr. Takata and colleagues successfully refuted IPR. They found that in this fullerene, the spherical structure containing two metal atoms (Sc) is significantly deformed, allowing two 5-membered rings to come into contact at two locations (Fig. 1B). This major breakthrough has removed limitations in designing the structures of fullerenes for semiconductors and superconductors as well as expanded the possibilities in the development of various raw materials in nanotechnology. Their research was published in *Nature* (November 2000) and received headline media coverage.

Leading the Way toward Nanointegrated Circuits (Nano-ICs)

"We were very excited about what kinds of unknown phenomena would occur if organic molecules were to be doped (inserted) into nanotubes," explains Dr. Yoshihiro Iwasa[7] (Professor, The University of Tokyo, Japan), who along with his colleagues in 2003 were the first to successfully control the electric conductivity of carbon nanotubes by doping organic molecules into them. Their research group doped various organic molecules into nanotubes and analyzed the functions and structures of the doped nanotubes using the powder X-ray diffractometer at BL02B2. Their analysis revealed that electrons move from inserted organic molecules to the carbon nanotubes. They also found that changing the type or number of molecules to be doped can precisely control the properties and electric conductivity of nanotubes without restrictions. Their achievement, which has boosted the development of next generation IC elements, was published in *Nature Materials* (October 2003), and a 3D structural view of a carbon nanotube appeared on its cover (Fig. 2). A new type of nanostructures, termed "pea pods," has been recently created by doping endohedral metallofullerenes into nanotubes, which look like frog eggs. Hence by varying the type of endohedral metallofullerene to be doped, the dream of designing nanocircuits with various electric properties is now reality.

Furthermore, Dr. Iwasa, Dr. Takata, Dr. Yasuhiro Takabayashi (chief researcher, Ideal Star, Inc., Japan), and colleagues have conducted collaborative research on endohedral metallofullerenes. Their research has revealed that a new fullerene ($Cs_3@C_{60}$), which is created by doping three cesium (Cs) atoms, is an insulator under ordinary pressures, but upon pressurization becomes a superconductor at 38 K (the highest superconducting transition temperature (T_c) achieved in a molecular superconductor). Their finding was published in *Nature Materials* (July 2008). However, the underlying mechanisms of how $Cs_3@C_{60}$ becomes a superconductor only under high pressures were unknown.

Hence, their research group then focused on elucidating the insulator to superconductor mechanism. They conducted experiments using the High Pressure Research Beamline (BL10XU) at SPring-8 to unravel the mystery. They demonstrated that $Cs_3@C_{60}$ is in a Mott insulator state (a singular state in which electrons are bound by the fullerene itself and cannot move) under normal pressures, but the electrons are released from this restriction to metalize $Cs_3@C_{60}$, which develops superconductivity at high T_c when pressurized (Fig. 3). Their accomplishment was published in the online edition of *Science* (March 2009). Dr. Iwasa has expressed his aspiration, "Now that the superconductivity mechanisms of fullerenes have been elucidated, we would like to promote the syntheses of high performance electronic elements based on this advancement."

[1] Currently Professor at Meijo University, Japan.
[2] Currently Professor Emeritus at Nagoya University, Japan.
[3] Currently Chief Scientist at RIKEN, Japan.
[4] A revolutionary structural analysis technique that can determine the detailed atomic configurations of a material with an unknown structure based on the rough structure model of the material.
[5] Kroto, H. *Nature* **329**, 519-531 (1987).
[6] Schmalz, T. G., Seitz, W. A., Klein, D. J. & Hite, G. E. *J. Am. Chem. Soc.* **110**, 1113-1127 (1988).
[7] Previously Professor at Tohoku University, Japan.

References

1. C.-R. Wang, T. Kai, T. Tomiyama, T. Yoshida, Y. Kobayashi, E. Nishibori, M. Takata, M. Sakata and H. Shinohara; *Nature*, **408**, 426 (2000)
2. T. Takenobu, T. Takano, M. Shiraishi, Y. Murakami, M. Ata, H. Kataura, Y. Achiba and Y. Iwasa; *Nature Materials*, **2**, 683 (2003)
3. A. Y. Ganin1,1, Y. Takabayashi, Y. Z. Khimyak, S. Margadonna, A. Tamai, M. J. Rosseinsky and K. Prassides; *Nature Materials*, **7**, 367 (2008)
4. Y. Takabayashi, A. Y. Ganin, P. Jeglic, D. Arcon, T. Takano, Y. Iwasa, Y. Ohishi, M. Takata, N. Takeshita, K. Prassides and M. J. Rosseinsky; *Science*, **323**, 1585 (2009)

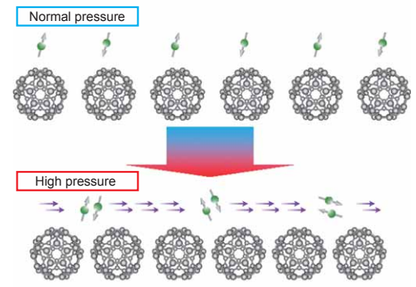

Fig. 3. Experimentally revealed pressure dependent electron states of $Cs_3@C_{60}$.
Under normal pressures, intermolecular distances between neighboring C_{60} molecules are relatively large, and electrons cannot move across the gap and remain on each molecule. This state is called the Mott insulator state. When high pressure is applied, neighboring C_{60} molecules come closer, allowing electrons to leap to neighbors. Simultaneously a strong attractive force is produced between electrons to create electrons pairs, resulting in superconductivity.

Changing Cement Raw Materials into a Metal-like Conductor

All materials can be categorized broadly as a conductor and an insulator in terms of their electric properties, but the boundary between these two categories is not definite due to the existence of a semiconductor, which exhibits properties of both. Materials such as cement raw materials are categorized as insulators. However, Dr. Hideo Hosono (Professor, Tokyo Institute of Technology, Japan), Dr. Yoshiki Kubota (Associate Professor, Osaka Prefecture University, Japan), Dr. Masaki Takata (Chief Scientist, RIKEN, Japan), and colleagues successfully converted cement raw materials into conductors. Additionally, they revealed the conversion mechanisms using synchrotron radiation at SPring-8, and were the first to develop new conductors using common materials as raw materials.

Can Cement Raw Materials, which Are Insulators, Really Be Converted into Conductors?

About 99% of the Earth's crust is composed of the following eight elements: oxygen, silicon, aluminum, iron, calcium, sodium, potassium, and magnesium. All the aforementioned elements, except oxygen, exist as an oxide. Most oxides are in the form of light metal oxides and are common raw materials in glass, cement, and ceramics. It is a common knowledge that they are not electrically conductive.

Dr. Hosono and colleagues have been unraveling the crystal structures of various light metal oxides, which are known as insulators, on the nanometer level (nm = 10^{-9} m). By skillfully utilizing their knowledge of these nanostructures, their research group has been investigating the conversion of light metal oxides, which are originally insulators, into semiconductors or conductors (metals). "I have been keeping my eye on light metal oxides for a long time. Long-term studies on glasses and ceramics have taught me that there must be something hidden behind them. Then I came up with a research idea about combining light metal oxides and electrons," explains Dr. Hosono.

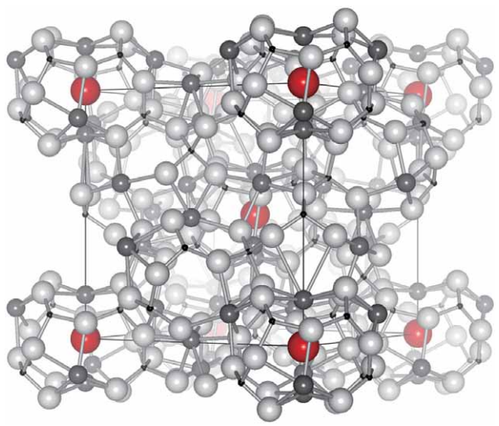

Fig. 1. Crystal structure of C12A7, which is comprised of nanocages (with or without trapped O^{2-}).
Each cube represents the unit cell where each cell is comprised of 12 cages, and only two of which contain oxygen ions (red).

Lime (CaO), a compound composed of calcium and oxygen, and aluminum oxide (Al_2O_3), a compound comprised of aluminum and oxygen, are representative insulators that commonly appear in textbooks. In 2003, Dr. Hosono and colleagues successfully converted one of the constituent materials of cement, 12CaO•7Al$_2$O$_3$ (C12A7), which is composed of CaO and Al_2O_3, into a semiconductor. However, C12A7 remained semiconductive, and could not be converted into the metallic state, which defied common knowledge. It is known that if a semiconductor such as silicon is doped (injected) with more electrons, the conductivity continually increases until the doped electron density exceeds some specific value until it is eventually converted to the metallic state. Thus, Dr. Hosono and coworkers continued to make small strides toward converting C12A7 into the metallic state, but definite conclusions remained unclear.

Drastic Conversion of C12A7, an Insulator, into the Metallic State

C12A7 is a crystal composed of interconnected nanosized cages that contain oxygen ions (O^{2-}) (Fig. 1). Dr. Hosono and his research group focused on the fact that although the oxygen ions remain in the cages, the ions move across the interconnected cages of C12A7 when the temperature exceeds 700 °C. In their experiments, C12A7 was enclosed in a glass tube with titanium metal, which can produce stable compounds by capturing the moving oxygen ions but does not react with the C12A7 cages themselves. The tube was subsequently heated to 1,100 °C. Titanium was selected because a reaction with C12A7 destroys the cages, enabling almost 100% of the oxygen ions in the cages to be replaced by electrons from titanium. This replacement can be controlled so that C12A7 is converted from an insulator to a semiconductor, and eventually into the metallic state (Fig. 2).

The following two observations confirmed metallization of C12A7. First, the electric resistance decreases as the temperature decreases. (The electric resistance of semiconductors should increase as temperature decreases). Second, upon adding a small amount of impurities with magnetism, the electric resistance does not vary monotonically with temperature, but instead has a minimum at a specific temperature. This latter phenomenon is called the Kondo effect, which is induced by the interactions between magnetic impurities and conduction electrons.

This metallized C12A7 has a high conductivity; the conductivity is at the same level as manganese metal and is twice that of graphite. When a normal semiconductor such as silicon is converted into a metal, the number of conduction electrons

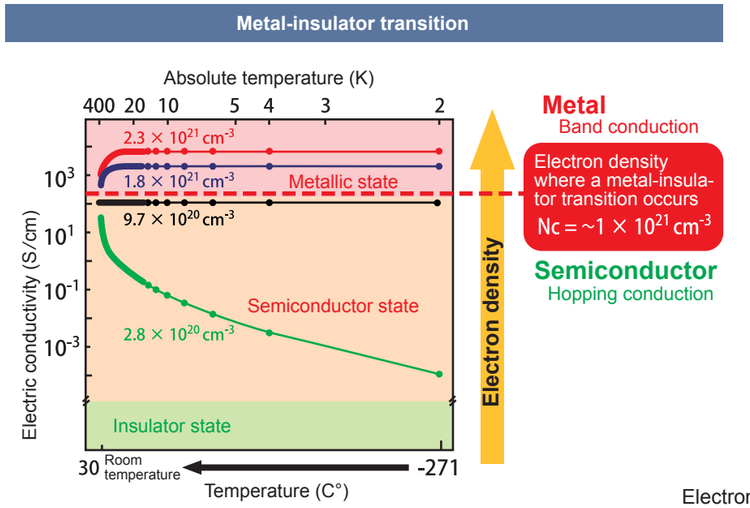

Fig. 2. Metal-insulator transition.
Electron doping induces metallization of C12A7 (insulator).

increases, but the average electron mobility per electron decreases. However, their research revealed that the average electron mobility of metallized C12A7 is more than ten times higher than that of semiconductive C12A7 (Fig. 3, top).

To investigate the reason for this phenomenon, they conducted structural analyses of C12A7 using a powder X-ray diffractometer at the Powder Diffraction Beamline (BL02B2) at SPring-8 and the MEM/Rietveld method. The MEM/Rietveld method, which was developed by Dr. Takata and colleagues, is an innovative structural analysis technique to determine the detailed atomic structures of materials based on a rough structure model of a material with an unknown structure. The MEM/Rietveld method was developed by combining electron density imaging and powder diffraction pattern fitting.

According to Dr. Hosono, "The shapes of cages are deformed in the insulator state when oxygen ions are trapped inside these nanosized cages. However, as we decrease the number of oxygen ions by replacing them with electrons, this deformation is gradually released, and a perfect shape is recovered for all the cages when the electron density exceeds a specific value. Then the electrons suddenly are free to move, and the semiconductor becomes a metal (Fig. 3, bottom right). The high precision diffraction data obtained by utilizing highly brilliant X-rays at SPring-8 revealed the detailed mechanisms for the structural conversion from the insulator state into the metallic state. The unique property of C12A7 is that it is chemically stable but similar to potassium metal, easily releases electrons. I presume that electronic devices based on this property will be realized in the not-so-distant future."

Transparent metals such as indium (a rare metal) are indispensable to manufacture LCDs. If this research advances, commonly available elements (Dr. Hosono calls them "ubiquitous elements") could replace rare metals. In particular, 70% of visible light can penetrate a 100-nm thick C12A7 film. Their research achievements were published in *Nano Letters* (April, 2007). Furthermore, three months after successful metallization of C12A7, Dr. Hosono and colleagues converted C12A7 into a superconductor, and have since discovered another new iron-based high-temperature superconductor.

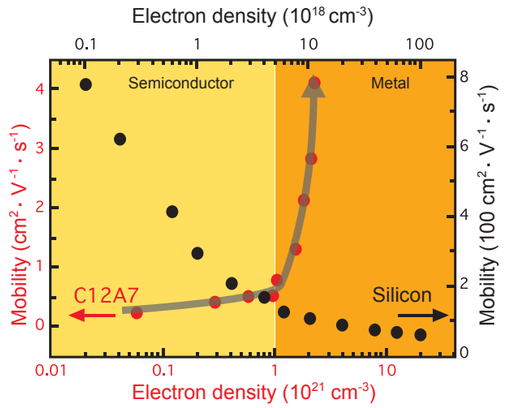

Fig. 3. Singularity of C12A7 metallization and its mechanism.
Top: Contrary to conventional semiconductors, electrons can move easily when C12A7 becomes a metal. The grey sphere represents an oxygen ion.
Bottom: State changes in C12A7 when an oxygen ion in the cage is replaced by electrons. Red arrows represent the movement of conduction electrons.

Reference
1. S. W. Kim, S. Matsuishi, T. Nomura, Y. Kubota, M. Takata, K. Hayashi, T. Kamiya, M. Hirano and H. Hosono; *Nano Lett.*, **7**, 1138 (2007)

Ultrafast Transition in a Crystal Structure —Secret of Nanosecond Optical Recording

DVD-RAM, a rewritable optical disc, is a common recording media for video, music, and computer data. Surprisingly, the mechanisms enabling high-speed writing, reading, deleting, and rewriting were unknown. Although it is known that the atomic bonding state of materials comprising thin-film memory layers on disc surfaces is repeatedly altered between transition and recovery according to the intensity of the irradiated light, the process of such changes could not be determined because a technique did not exist to observe ultrafast changes in atomic bonding on the nanosecond (1 nanosecond = 10^{-9} sec) level. Fortunately, the synchrotron radiation at SPring-8 overcame this difficulty, and research has revealed the underlying mechanisms.

Principle of DVDs and the Mystery of their Mechanisms

Thin-film memory layers on the surfaces of unused DVD-RAM are composed of regularly arranged composite crystals such as $Ge_2Sb_2Te_5$ (germanium antimony telluride), which are comprised of multiple metal atoms. Instantaneously irradiating such crystals with intense laser light liquefies the irradiated parts for a split second, but these parts are quickly cooled by room temperature, yielding an amorphous phase where atomic bonding is distorted and hardened. Re-irradiating the thin-film layers in such a state with weak laser light causes the light reflectance of the crystal phase to differ from that of the amorphous phase. Herein, "write" and "read" of digital data become possible by creating a crystal phase for "0" and an amorphous phase for "1." To delete old data and rewrite new data, the intensity of irradiated light must be stronger than that for reading and must be adjusted so as not to melt the amorphous phase but allows the phase to recrystallize.

Although this is the principle of DVD-RAM, (1) the structures of the crystal or the amorphous phase were not elucidated. Furthermore, (2) the processes of inducing the phase transition and reverse-phase transition between the crystal and amorphous phases upon irradiating with laser light were unknown and (3) the mechanisms of such ultrafast phase transitions, which occur on the order of nanoseconds, remained mysteries. "You might not believe it, but these facts were true. Thus, I was totally engrossed in unraveling this mystery by any means," mentions Dr. Masaki Takata (Chief Scientist, RIKEN, Japan) to explain the motivation behind his studies.

Restoring the Original State of DVD is Similar to an Umbrella

Dr. Junji Tominaga (Director, The Center for Applied Near-Field Optic Research, National Institute of Advance Industrial Science and Technology, Japan), Dr. Alexander Kolobov (Chief Researcher, *ditto*), Dr. Paul Fons (Staff Researcher, *ditto*), and colleagues are the ones who initiated research to unravel the mysteries of DVDs. In 2004, their research group answered a longstanding question when they revealed the underlying mechanisms for the ultrafast writing/deleting processes of DVDs by thoroughly examining the crystal and amorphous structures of $Ge_2Sb_2Te_5$ using a combination of synchrotron radiation at SPring-8 and an X-ray absorption fine structure (XAFS) technique. When an object is irradiated with X-rays, the atoms in the object absorb X-rays and emit photoelectrons. Because the wave of this photoelectron is reflected from neighboring atoms and the waves interfere with each other, characteristic oscillations appear in the X-ray absorption spectrum. The XAFS technique analyzes these oscillations to determine the distance between a specific atom and its neighboring atoms as well as to examine the interactions between these atoms.

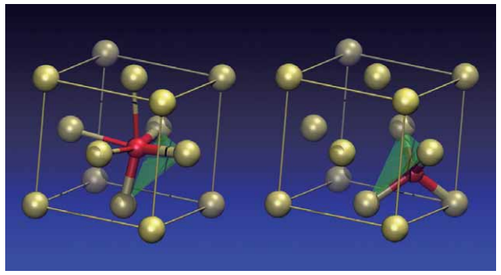

Fig. 1. Crystal–amorphous transition model of germanium antimony telluride.
Movement of a germanium atom (red) through a plane (green) induces a phase transition.

Dr. Tominaga and colleague's analysis revealed that the transition of $Ge_2Sb_2Te_5$ from the crystal phase to the amorphous phase maintains the reversible basic bonding relationship between atoms. This phenomenon is analogous to an umbrella that is turned inside out due to a strong wind, but instantaneously recovers its original shape. Herein, pivotal germanium atoms shift to a different bonding state at a high speed, which induces an instantaneous and reversible phase transition (Fig. 1). Hence, the amorphous phase of $Ge_2Sb_2Te_5$ differs from the normal amorphous phase where atoms are randomly situated and this shift does not occur. Thus, energy and time required in this phase transition are small. This breakthrough discovery was published in *Nature Materials* (October 2004).

Directly Observing Ultrafast Phase Transition Processes for the First Time

As mentioned above, the mechanisms enabling a phase transition of $Ge_2Sb_2Te_5$, which occurs at a speed on the 20 nanosecond level, were revealed. However, a detailed study on the state changes of the atomic bonding in an ultrafast phase transition had not been performed. Dr. Takata, Dr. Noboru Yamada (Researcher, Panasonic Corp., Japan), Dr. Shinji Kohara (Associate Senior Scientist, the Japan Synchrotron Radiation Research Institute (JASRI)), and colleagues undertook the "X-ray pinpoint structural measurement of reaction phenomena" project to investigate the effects of the structural differences on the phase transition speed. Their research group conducted experiments at the High Energy X-ray Diffraction Beamline (BL04B2) and at the Powder Diffraction Beamline (BL02B2) at SPring-8 to compare the atomic structure of $Ge_2Sb_2Te_5$ and that of germanium telluride (GeTe), which has a slower phase transition speed on the 100-nanosecond level, in the crystal, liquid, and amorphous phases. Their analysis of the diffraction data yielded a breakthrough.

The basic structural component in the crystal phase is a 4-membered ring (four atoms are connected in square shape) in both $Ge_2Sb_2Te_5$ and GeTe. Upon irradiating with laser light, these two materials are converted into the amorphous phase via transient liquefaction. $Ge_2Sb_2Te_5$ is converted into aggregates composed of rings with an even number of atoms (4, 6, 8, and 10 atoms), whereas GeTe is converted into rings with an odd or even number of atoms (3, 4, 5, 6, and 7 atoms). When they return to the crystal phase, $Ge_2Sb_2Te_5$, which consists solely of even-numbered rings, easily regains the original structure containing only 4-membered rings with minimal recombinations, whereas GeTe, which is comprised of mainly odd-numbered rings, requires a complicated recombination to recover only the 4-membered ring structure (Fig. 2). Hence, their study revealed the origin of the differences in the phase transition speeds between these two materials (especially those from the amorphous phase to the crystal phase), and their results were reported at the International Symposium on Optical Memory (October, 2006).

In 2008, Dr. Shigeru Kimura (Associate Chief Scientist, JASRI), Dr. Yoshihito Tanaka (Senior Scientist, RIKEN), and colleagues, who are affiliated with above project group, observed the first real-time ultrafast transition processes from the amorphous phase to the crystal phase (data deletion processes) of $Ge_2Sb_2Te_5$ and $Ag_{3.5}In_{3.8}Sb_{75.0}Te_{17.7}$ (silver–indium–antimony–tellurium quaternary compound), which are representative raw materials of optical discs. Using synchrotron radiation at SPring-8, which is pulsed X-rays with a 40-picosecond duration (1 picosecond = 10^{-12} sec), a phase transition can be observed using time-resolved X-ray diffraction by synchronizing an irradiated laser light pulse onto an amorphous solid with an X-ray pulse at the picosecond level. To this end, an X-ray pinpoint structural measurement system, which is capable of recording X-ray diffraction data and optical reflectance variation data at a time resolution of 40-picoseconds, was installed in the High Flux Beamline BL40XU at SPring-8.

This system revealed that in $Ge_2Sb_2Te_5$ comparatively large crystal grains are initially created. These grains then multiply until the entire body is filled with them. This process differs from that for $Ag_{3.5}In_{3.8}Sb_{75.0}Te_{17.7}$ in which many tiny crystal grains are initially created. These small grains combine to form larger crystal grains, and eventually yield the final crystal structure (Fig. 3). Moreover, the data deletion processes and phase transitions in both materials occur at the same nanosecond level. These results were published in the online edition of *Applied Physics Express* (March 2008). "I would like to apply the outcomes obtained from these studies toward realizing the 'dream of directly measuring electrons' using pulsed X-rays on the order of a femtosecond (femto = 10^{-15}) duration," Dr. Takata explains about his future research plans.

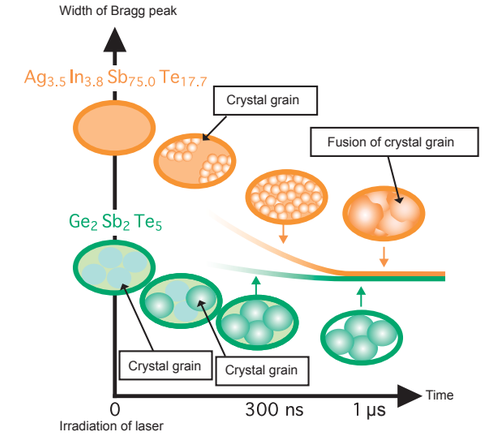

Fig. 3. Phase transition model of the raw materials of $Ge_2Sb_2Te_5$ and $Ag_{3.5}In_{3.8}Sb_{75.0}Te_{17.7}$ in the data deletion processes.

References
1. A. V. Kolobov, P. Fons, A. I. Frenkel, A. L. Ankudinov, J. Tominaga and T. Uruga; *Nature Materials*, **3**, 703 (2004)
2. S. Kohara, K. Kato, S. Kimura, Hitoshi Tanaka, T. Usuki, K. Suzuya, Hiroshi Tanaka, Y. Moritomo, T. Matsunaga, N. Yamada, Y. Tanaka, H. Suematsu and M. Takata; *Appl. Phys. Lett.*, **89**, 201910 (2006)
3. Y. Fukuyama, N. Yasuda, J. Kim, H. Murayama, Y. Tanaka, S. Kimura, K. Kato, S. Kohara, Y. Moritomo, T. Matsunaga, R. Kojima, N. Yamada, H. Tanaka, T. Ohshima and M. Takata; *Appl. Phys. Express*, **1**, 045001 (2008)

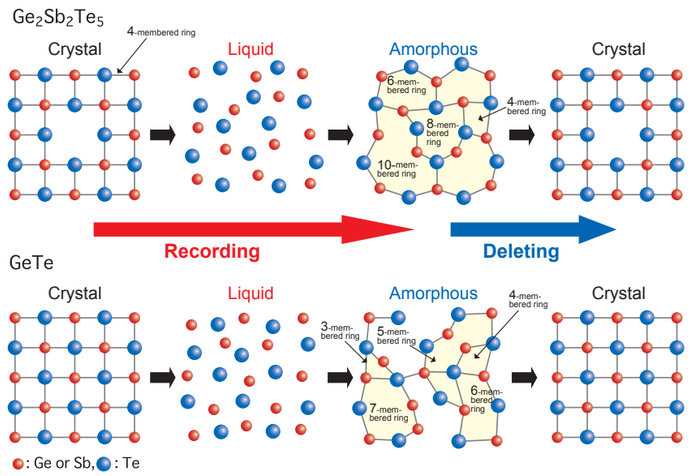

Fig. 2. Phase transition model of $Ge_2Sb_2Te_5$ and GeTe.

Drastically Changing the Material Properties through Nanoparticulation

The intrinsic properties of a material remain even if it is broken into tiny particles, especially for solid metals and metallic compounds. However, recent studies have revealed that some metals exhibit unexpected properties, which drastically differ from those in bulk, once they are broken at the nanometer level (nm = 10^{-9} m). This is analogous to a person showing one aspect of their personality when in a group, but showing other aspects when alone. Synchrotron radiation at SPring-8 contributed to the discovery of this new fact.

Surprise Finding—Gold Nanoparticles Have Magnetism!

Gold is an extremely stable metal and does not oxidize or rust. The melting point of gold, which is 1065 °C under normal conditions, decreases to ~700 °C when it is broken into particles measuring approximately a few nanometers. Although gold was once believed to be chemically inactive and unsuitable for catalysis, it has recently been reported that gold exhibits a high catalytic activity when it is in the form of few-nanometer sized clusters.

The phenomenon where the properties change when the material size becomes sufficiently small is called the size effect. To investigate the size effect in gold (diamagnetic in the normal condition), Dr. Yoshiyuki Yamamoto[1] (Assistant Professor, Japan Advanced Institute of Science and Technology) and colleagues have focused on the changes in the magnetic properties of gold nanoparticles. "It is difficult to maintain individual nanoparticles because nanosized particles tend to aggregate," explains Dr. Yamamoto. To overcome this difficulty, their research group developed a technique to protectively cover the surfaces of nanoparticles with various organic molecules, and successfully maintained individual nanoparticles under stable conditions. Utilizing this technique, they stabilized various sized gold nanoparticles (Fig. 1) and measured the magnetic properties using a high sensitivity magnetic field sensor, a superconducting quantum interference device (SQUID).

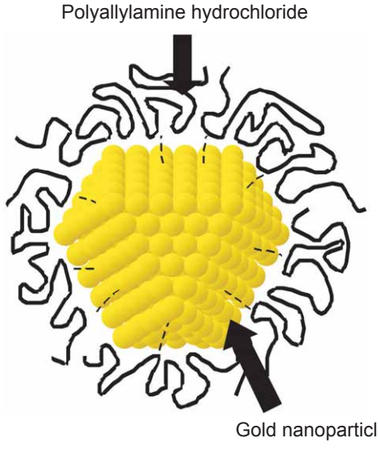

Fig. 1. Schematic view of polymer (polyallylamine hydrochloride) covered gold nanoparticles.

Their measurements yielded an unexpected result. Gold nanoparticles with diameters less than 3 nm appeared to become ferromagnetic at an extremely low temperature. However, because SQUID concurrently detects the magnetism from contaminants and the organic molecules covering the nanoparticles, it was difficult to verify that the gold nanoparticles are actually ferromagnetic. To overcome this problem, it was indispensable to develop techniques that enable just the magnetic properties of the gold nanoparticles to be measured.

To this end, Dr. Yamamoto and colleagues employed the Magnetic Materials Beamline (BL39XU) at SPring-8 and measured the magnetism of gold nanoparticles (diameter: 1.9 nm) covered by an organic polymer, polyallylamine hydrochloride, at 2.6 K and a 10 tesla external magnetic field using the X-ray magnetic circular dichroism (XMCD: see Topic 15 for more information) method. This verification measurement is only possible through the combined use of highly brilliant X-rays and the high-precision spectrometer available at SPring-8.

All elements preferentially absorb X-rays with an element-specific dependent energy, which is called the absorption edge. To determine whether gold nanoparticles have magnetism, detailed correlations between XMCD spectrometer data and SQUID data were examined (Fig. 2). The correlations confirmed that gold nanoparticles are actually magnetized. "Due to their size, the ratio of the number of gold atoms in the surface areas to the total number of gold atoms is significantly higher for nanoparticles than that for the bulk. We think this is why gold nanoparticles become magnetized," shares Dr. Yamamoto. The results of their research, which are expected to contribute to the promotion of magnetism research as well as the development of ultrahigh-density recoding media using ideal noble metal alloy magnetic nanoparticles, were published in *Physical Review Letters* (September 2004).

Discovering Nanoparticle Electrolytes Promotes the Development of an All-Solid-State Battery

Electrolytes (ionic conductors) determine the performance of instruments utilizing electrochemical reactions. Similar to the electrolytic solution (sulfuric acid solution) of lead acid batteries, liquid materials typically have high ionic conductivities. Thus, liquid electrolytes are commonly used in button and dry cell batteries. However, these types of batteries require secure metallic packaging, and there are the hazards of abnormal expansion and explosion due to heating or overcharging. From the perspective of stability (nonvolatility), safety (non-explosivity), and ease of manufacturing, including thin-film manufacturing, it is not surprising that the development of highly ionic conductive solid electrolytes is desired.

For this reason, silver iodide (AgI), a solid superionic conductor with a high ionic conductivity equivalent to a liquid, has been receiving much attention as a candidate for the electrolyte in all-solid-state batteries. However, the utility of AgI at ambient temperature is difficult because the superionic conductivity of AgI only appears at 147 °C or higher. Thus, many hurdles remain in the development of solid electrolytes. However, after much time and effort on this topic, Dr. Hiroshi Kitagawa[2] (Professor, Kyoto University, Japan) and colleagues hypothesized that, "Employing nanosized particles may work." Then they put this idea into practice.

First Dr. Kitagawa and colleagues developed a technique to synthesize AgI nanoparticles by mixing, filtering, and drying the solutions of silver nitrate ($AgNO_3$), sodium iodide (NaI), and silver ion conducting poly-N-vinyl-2-pyrrolidone (an organic polymer) under normal temperature and pressure. Next, they developed another technique to selectively produce nanoparticles with a uniform particle size ranging from 10 to 40 nm by optimizing the concentration of each solution and improving the mixing processes. Then in conjunction with Dr. Masaki Takata (Chief Scientist, RIKEN, Japan) and colleagues, they examined the relationship between AgI nanoparticle size and ionic conductivity using the Powder Diffraction Beamline (BL02B2) and a high-brilliance X-ray diffractometer at SPring-8.

They found that the phase transition temperature where superionic conductivity is manifested continues to decrease as a particle size decreases. Moreover, their experiment revealed that the phase transition temperature of ultra-small particles (less than 10 nm) is reduced to ~40 °C, which is ~100 °C less than that of normal AgI particles, while the superionic conductivity is maintained until the temperature decreases to this low phase transition temperature equivalent to room temperature. Additionally, Dr. Kitagawa and colleagues measured the temperature-dependent ionic conductivity of nanoparticles measuring 10 nm, and found that the ionic conductivity of such nanoparticles is more than 100,000 times higher than that of normal AgI particles even at 4 °C after transiting into the normal phase. Furthermore, these nanoparticles are stable under normal atmospheric conditions and maintain their high ionic conductivity even after repeating the heating-cooling cycles.

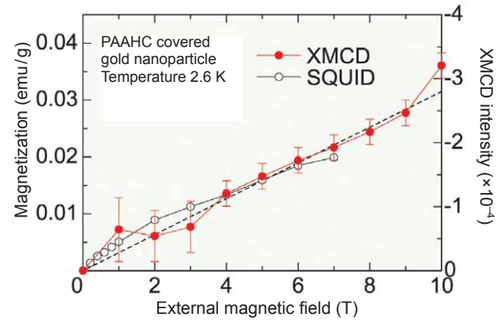

Fig. 2. XMCD intensity distribution and SQUID distribution of polyallylamine hydrochloride covered gold nanoparticles at 2.6 K.
XMCD intensity (red circles) and SQUID (white circles) are correlated, indicating gold nanoparticles are magnetized.

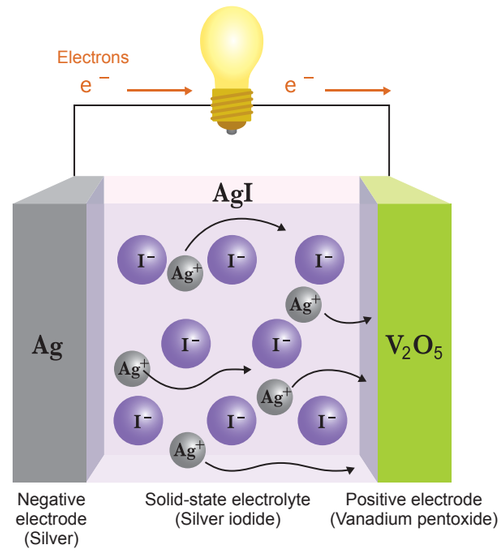

Fig. 3. Schematic view of a silver ion solid-state battery.
This ideal all-solid-state battery, in which all electrodes and electrolytes are composed of stable materials, does not have problems such as liquid leaks. It is resistant to electric leaks and deformation. Moreover, it is malleable and can be quickly charged/discharged because Ag^+ ions move fast in solid-state electrolytes.

Prior to their work, systematic studies on the relationship between particle size and the phase transition temperature had yet to be conducted, However, their research provided new techniques to explore superionic conductors. Dr. Kitagawa remarks, "Our research achievements will accelerate the development of all-solid-state batteries (Fig. 3). Sintering at high temperature is required to manufacture inorganic solid electrolytes. In contrast, superionic conductive nanoparticles can be manufactured through simple procedures: solution mixing, filtering, and drying under normal temperature and pressure, and thus, possess great industrial advantages." Their research achievements were published in the online edition of *Nature Materials* (May 17, 2009).

[1] Currently Associate Professor at Akita University, Japan.
[2] Also Visiting Professor at Kyushu University, Japan.

References

1. Y. Yamamoto, T. Miura, M. Suzuki, N. Kawamura, H. Miyagawa, T. Nakamura, K. Kobayashi, T. Teranishi and H. Hori; Phys. *Rev. Lett.*, **93**, 116801 (2004)
2. R. Makiura, T. Yonemura, T. Yamada, M. Yamauchi, R. Ikeda, H. Kitagawa, K. Kato and M. Takata; *Nature Materials*, **8**, 476 (2009)

Unexpectedly Changing the Physical Properties under Extreme Pressures and Super-Strong Magnetic Fields

Environments where conditions extremely differ from common environmental conditions are called "extreme environments," and include environments under ultrahigh temperature or ultrahigh pressures as well as those under super-strong magnetic fields. Because unique phenomena that do not occur under normal conditions exist in extreme environments, many physicists and chemists are attract to research of physical properties under extraordinary conditions. However, creating extreme environments in a laboratory and conducting highly precise experiments in such environments are very difficult. To overcome these obstacles, special devices capable of providing ultrahigh temperatures, ultrahigh pressures, and super-strong magnetic fields have been installed in the beamlines at SPring-8. These devices allow researchers to conduct advanced research on physical properties under extreme environments using highly brilliant synchrotron radiation.

Changing the Physical Properties of Liquids at High Pressure

Phosphorus, which is an important element in biological bodies, has various crystal structures. For example, the structural unit of white phosphorus is composed of regular tetrahedron-shaped molecules where each unit contains four phosphorus atoms, whereas the atoms in black phosphorus are arranged in layers. White phosphorus melts at 44 °C, while black phosphorus does not melt until heated over 600 °C at high pressure. Melted white phosphorus maintains the four-atom regular tetrahedrons. However, the structure of melted black phosphorus was unknown. Thus, Dr. Yoshinori Katayama[1] (Senior Scientist), Japan Atomic Energy Research Institute (JAERI)[2]) and colleagues conducted X-ray diffraction experiments using synchrotron radiation and a high-temperature high-pressure generator at SPring-8 to investigate the transformation of melted black phosphorus at ~1,000 °C by gradually increasing the applied pressure (Fig. 1).

They found that melted black phosphorus drastically transforms the phosphorus arrangement once the pressure exceeds ~1 GPa (GPa = 10^9 Pa = ~10,000 atm). Under low pressures, the regular tetrahedron-shaped molecules, which are composed of four phosphorus atoms, are randomly arranged, but this arrangement dissolves under high pressures to form a long stretch of interconnected phosphorus atoms, specifically a polymer. This reversible structural transition of melted black phosphorus is induced by pressurization or decompression, and occurs only within a limited pressure variation range of several hundred atmospheres. Moreover, this transition is complete within a few minutes in the fastest case, and the random arrangement and polymer conformation coexist during the transition. From these observations, they believed that this transition is likely due to an increase in a singular phenomenon called the "first-order phase transition of liquid."

A first-order phase transition is a sudden transition of a material phase accompanied by a drastic density change, which is similar to the phenomenon where graphite is transformed into diamond under high pressures. Several studies have suggested that phase transitions occur in solids as well as some types of liquid. However, a phase transition in liquid had yet to be reported, which inspired Dr. Yoshinori Katayama and colleagues to conduct an experiment at SPring-8 to demonstrate for the first time that a first-order phase transition occurs in neat liquid (melt) under the appropriate temperature and pressure conditions. Their results were published in *Nature* (January 2000).

Following this study, they then focused on the phase transitions of liquid phosphorus utilizing X-ray transmission imaging (similar to X-ray imaging of human body) and X-ray absorptiometry. In particular, under the conditions of 1,000 °C and 1 GPa, they video-taped the X-ray transmission images of the production and gradual growth of high-pressure liquid-phase spherical droplets. Additionally, they confirmed that the density of the high-pressure liquid phase in the final stage increases by 60% through X-ray absorption measurements. These experiments confirmed that liquid phosphorus exhibits a first-order phase transition, and the world's first example of a liquid-phase transition was published in *Science* (October 29, 2004). "This research opens a new approach to investigate the structures and phase transitions of liquids, which have not been as thoroughly explored as solids. Like a phase separation between water and oil, if other types of liquid exhibit a phase separation between two phases of the same liquid, then new research fields in fluid dynamics may lead to the development of extraction and transportation of materials," explains Dr. Katayama with hope.

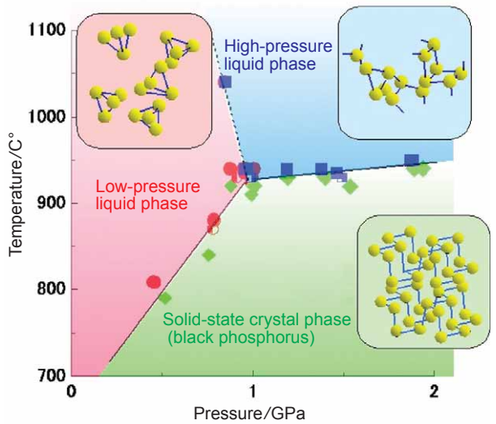

Fig. 1. Schematic plot of the temperature and pressure dependency of the phase transition of phosphorus.
Transition from the low-pressure liquid phase (low-density phase) to the high-pressure liquid phase (high-density phase) occurs with a phase boundary of 1 GPa (GPa = 10^9 Pa = ~10,000 atm) and a temperature of 900 °C or higher. Tetrahedron structures comprised of four phosphorus atoms in the low-pressure liquid phase are fragmented to form polymer structures in the high-pressure liquid phase. Bonded structures of phosphorus suddenly change at the phase boundary.

Observing Electrons in Special Magnetic Materials Using the World's Most Powerful Super-Strong Magnetic Field

Dr. Hiroyuki Nojiri (Professor, The Institute for Materials Research, Tohoku University, Japan), Dr. Yasuhiro Matsuda (Associate Professor, The Institute for Solid State Physics, The University of Tokyo, Japan), and colleagues revealed the properties of electrons in an europium magnetic material ($EuNi_2(Si_{0.82}Ge_{0.18})_2$) using an X-ray magnetic circular dichroism (XMCD) method, which can examine the magnetic properties of each individual element under a super-strong magnetic field. This super-strong field (40 tesla) is 1,000,000 times stronger than the Earth's magnetic field and is the world's strongest magnetic field.

Suppose that light (an electromagnetic wave) is traveling in space; when the tip of the resultant vector of the electric field (and also the magnetic field) vector components of light describes a circle in a plane perpendicular to the direction of traveling light, the light is called circular polarized light. Circular polarization can be divided into two categories: right (spin: +1) and left (spin: +1). XMCD is the absorption difference between right and left circularly polarized light when X-rays are irradiated onto a magnetized material. Because the magnitude of the absorption difference is proportional to that of material's magnetization, spectroscopy developed based on this phenomenon is used to probe magnetic materials.

All elements preferentially absorb X-rays with an element specific dependent energy, which is called the absorption edge. Thus, XMCD spectroscopic measurements can be performed by adjusting the energy of irradiated X-rays to the absorption edge of each target element. XMCD spectroscopy is suitable to examine the properties of elements, especially the electron states, which are origin of the magnetic properties. "XMCD spectroscopy has been only used to study ferromagnetic materials because compact super-strong pulsed magnetic field generators suitable for materials other than ferromagnetic materials were not available," comments Dr. Nojiri, who along with his colleagues were the first to observe electrons in europium magnetic materials under a substantially strong magnetic field (40 tesla) by combing their ultra-compact pulsed strong magnetic field generator (Fig. 2) and highly brilliant X-rays at SPring-8.

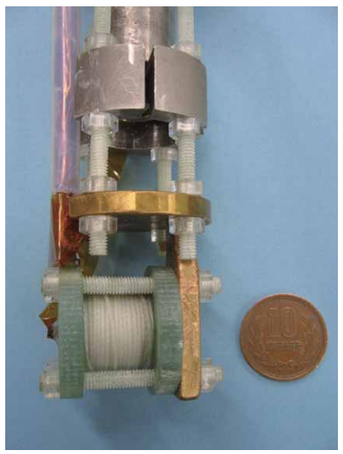

Fig. 2. Powerful superconducting mini-magnet.
This mini-magnet is composed of 0.7-mm diameter AgCu solenoid coils and reinforced outside by glass fibers. Flanges are made of fiber-reinforced plastics, which are attached onto the head of an insertion device of a refrigerator and cooled to the liquid helium temperature along with samples during the experiments. The 10 Japanese yen coin (diameter ~23.5 mm) is for size comparison.

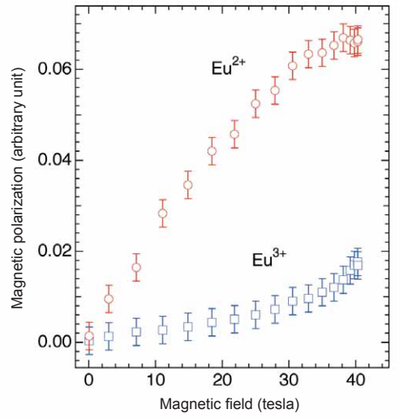

Fig. 3. Magnetic field dependence of the magnetic response of europium (Eu).
Magnetic field dependence of the magnetic response (magnetic polarization) of Eu for two different valence values (Eu^{2+} and Eu^{3+}). Magnetic responses of these two electron states completely differ. New techniques have enabled these two states to be separated, which was impossible with previous techniques.

Europium exhibits an unprecedented property; it suddenly exerts or loses its strong magnetism according to the quantum mechanical mixing state (both position and momentum are uncertain) of two atomic states with different valence values. Although observing the magnetic properties of this material by separating these two ultra-microscopic states was quite difficult, research conducted at SPring-8 has revealed that the magnetic responses of these two states under super-strong magnetic fields completely differ from each other (Fig. 3). Their results demonstrate that the XMCD spectroscopy developed by their research group is a powerful technique to unravel the unprecedented magnetic properties of various materials under super-strong magnetic fields. "I believe that this method can substantially contribute to the effective design and development of new magnetic substances for innovative magnetic memories and magnetic sensors," hopefully explains Dr. Nojiri. Their research achievements were published in the online edition of *Physical Review Letters* (July 28, 2009), and Dr. Matsuda received the 30th Honda Memorial Young Researcher Award (2009).

[1] Currently group leader, high-density material research group, Japan Atomic Energy Agency.
[2] Currently Japan Atomic Energy Agency (JAEA).

References

1. Y. Katayama, T. Mizutani, W. Utsumi, O. Shimomura, M. Yamakata and K. Funakoshi; *Nature*, **403**, 170 (2000)
2. Y. Katayama, Y. Inamura, T. Mizutani, M. Yamakata, W. Utsumi and O. Shimomura; *Science*, **306**, 848 (2004)
3. Y. H. Matsuda, T. Inami, K. Ohwada, Y. Murata, H. Nojiri, Y. Murakami, H. Ohta, W. Zhang and K. Yoshimura; *J. Phys. Soc. Jpn.*, **75**, 024710 (2006)
4. Y. H. Matsuda, Z. W. Ouyang, H. Nojiri, T. Inami, K. Ohwada, M. Suzuki, N. Kawamura, A. Mitsuda and H. Wada; *Phys. Rev. Lett.*, **103**, 046402 (2009)

Electronic Properties

Exploring Electron Movements Responsible for the Manifestation of Functions

SPring-8 Leads the World in Photoelectron Spectroscopy

All materials are composed of atoms, and most physical properties are manifested in accordance to the types of atoms and bonding states. Electrons play a fundamental role in determining the physical properties of a material. Specifically electrons control the electric properties (e.g., electric conductivity and insulation properties, color, reflectance/absorbance of light, thermal conductivity, and magnetic properties). Society depends on various products that utilize properties induced by electrons (Fig. 1). Moreover, environmentally-friendly, energy-saving products have recently been developed; hence, elucidating the electronic properties, which are the bases of these products, is indispensable to create innovative materials. So, various types of spectroscopy have been used to investigate the electronic properties.

Exposing a material to light causes the electrons in the material and light to interact, causing energy to be exchanged, which subsequently emits photoelectrons, Auger electrons, photoions, or new types of light. This circumstance allows the electronic states in a material to be examined by measuring the energies (wavelengths) of the incident light and emitted light/electrons/ions, and calculating the probability of occurrence of such events. This technique is called *spectroscopy*, and the obtained data are called *spectra* (Fig. 2).

Among the various types of spectroscopy, photoelectron spectroscopy is the most powerful technique to directly and precisely examine the electronic states in a material. Exposing a material to light allows photoelectric effects, in which electrons in a material receive the energy of the incident light and exit from the material, to be observed. These photoelectron energy measurements are the basis of spectroscopy. Because the energies of photoelectrons reflect the energy states of electrons in a material, researchers have strived to measure the energies of photoelectrons since the early 20th century. However, reliable data from photoelectron spectroscopy was not produced until about 1960 when Kai Siegbahn, who later shared the Nobel Prize in Physics in 1981, was the first to obtain reliable results.

Since the construction of synchrotron radiation factories began in the 1970s, photoelectron spectroscopy has become a common and powerful technique to directly measure electronic states. Moreover, the discovery of high-temperature superconductivity in 1986 greatly improved the resolution to distinguish electronic states, which has enabled more precise measurements, leading to a drastic enhancement in data accuracy. However, as mentioned in Topic 16, Developing High-Resolution Bulk-Sensitive Photoelectron Spectroscopy, conducted by Shigemasa Suga (Professor Emeritus, Osaka University, Japan) and colleagues, such high-resolution photoelectron spectroscopy has been performed mainly in the vacuum ultraviolet ray region, and the information obtained does not reflect the actual electronic states in solids. Fortunately this situation has been rectified with the high-resolution photoelectron spectroscopy performed in the high-energy regions ~1 keV at SPring-8's soft X-ray beamline; this spectroscopy has realized high-precision measurements of the actual electronic states within solids as well as in their surface areas. Since then, new techniques have been developed to measure not only the energy of photoelectrons, but also their momentum distributions, providing further information about the electronic states of materials. Through these endeavors SPring-8 has and continues to lead the world in this field.

Developing New Spectroscopic Techniques to Accelerate Research on Electronic Properties

High-resolution photoelectron spectroscopic experiments using hard X-rays with energy higher than that of soft X-rays, have been successfully conducted at SPring-8 due to the development of a technique called hard X-ray photoelectron spectroscopy (HAXPES). HAXPES can reveal information deep inside a solid. Moreover, HAXPES has expanded the usability of photoelectron spectroscopy using soft X-rays. Photoelectron spectroscopy using soft X-rays used to require ultra-high vacuum conditions and materials with clean surfaces to obtain precise information. However with the advent of HAXPES, researchers can now easily and quickly conduct preparation processes. Consequently, SPring-8 is a global leader in this field as HAXPES can support experiments on various samples, including industrial requests. Due to SPring-8's advances, researchers in the western world have recently begun to develop a similar experimental apparatus.

Besides photoelectron spectroscopy, other spectroscopic techniques, which are explained in the following sections, have contributed to the research on electronic properties. Absorption spectroscopy measures the amount of absorbed incident light by evaluating samples at various energy values of incident light. Absorption spectroscopy has been applied to a wide variety of research, including the development of various catalysts and battery related materials. Additionally, investigations on the magnetic properties using polarization, which is an advantageous feature of synchrotron radiation, have been vigorously conducted.

Although incident light is absorbed by materials, in some cases this light collides with the electrons in a material and is then emitted. Spectroscopic techniques utilizing this emitted light are indispensable in studies on the electronic states and include X-ray scattering spectroscopy, diffractometry, and fluorometry. By taking advantage of the highly brilliant synchrotron radiation at SPring-8, researchers have conducted unprecedented high-resolution experiments and innovative research projects. These achievements are expected to promote research on superconducting materials and spintronics materials, which are necessary to develop innovative devices.

In the field of spectroscopic research, microspectroscopy, which focuses light to the micrometer or nanometer size, has also advanced. Moreover, in the field of photoelectron spectroscopy, photoelectron microscopy, which magnifies emitted electrons using electron lenses, has achieved a 20-nm[1] spatial resolution, and is currently being well utilized to measure small quantities of samples to elucidate physical phenomena specific to microscopic regions (Fig. 3). Furthermore, research on the ultra high-speed changes in the electronic states at the nanosecond[2] or picosecond[3] level using synchrotron radiation like a strobe flash are advancing.

The spectroscopic techniques described here utilize phenomena induced by direct interactions of light and electrons in a material to obtain information about the electronic states. Additionally, other techniques that examine the electronic states around nuclei using resonant excitation phenomena between nuclei and γ-rays or X-rays are available (e.g., Mössbauer spectroscopy). These other techniques have drastically increased the number of nuclear species that can be spectroscopically measured by resonant excitations at SPring-8 where ultra high-energy X-rays are available. Numerous outstanding achievements have been accomplished through spectroscopic research conducted at SPring-8. However because it is not practical to describe every one, here we describe a select few.

[1] nm = 10^{-9} m
[2] nanosecond = 10^{-9} second
[3] picosecond = 10^{-12} second

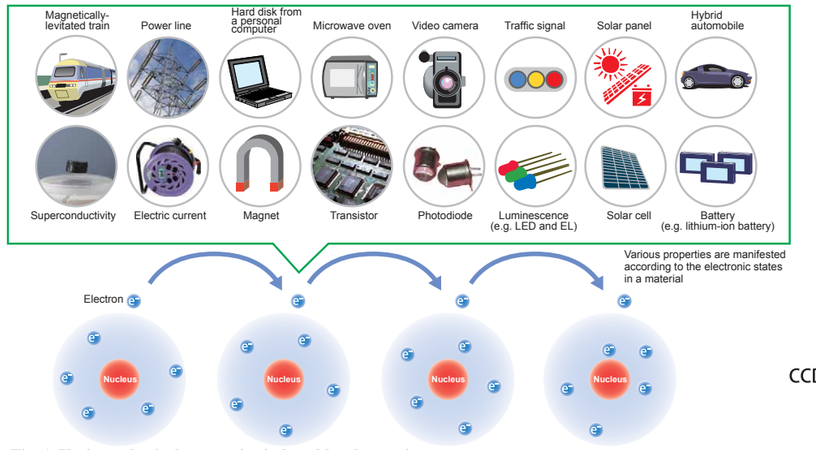

Fig. 1. Various physical properties induced by electronic states.

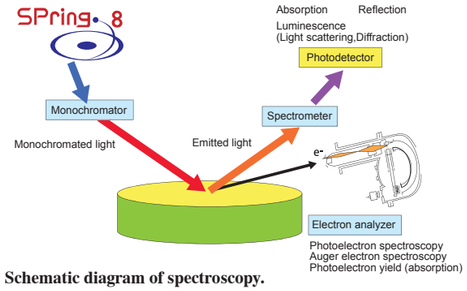

Fig. 2. Schematic diagram of spectroscopy.

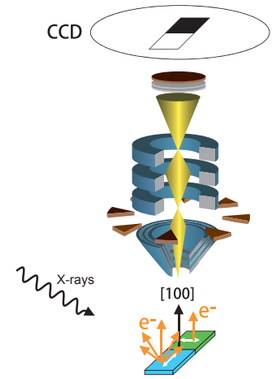

Fig. 3. Schematic diagram of micro-spectroscopy (photoelectron microscope) in microregions.

Unraveling Anomalous Physical Properties of Strongly-Correlated Electron Materials

Exposing a solid to light causes the electrons in the solid that receive the irradiated light energy to be emitted. This phenomenon is called the photoelectric effect, and the emitted electrons are called photoelectrons. Photoelectron spectroscopy refers to an energy measurement of the emitted photoelectrons to examine the states of electrons in a solid. Dr. Shigemasa Suga[1] (Professor, Osaka University, Japan), a leading authority on photoelectron spectroscopy in Japan, received the Helmholtz–Humboldt Research Award in 2008 for his outstanding long-term contributions in this field. This international prize is awarded to active researchers who have delivered notable academic accomplishments and are expected to continue to actively participate at the forefront of their research field. The research he conducted at SPring-8 played a crucial role in his award.

The Outstanding Achievements of Dr. Suga are Internationally Acknowledged

Dr. Shigemasa Suga, who received the Eugen and Ilse Seibold Prize (Deutsche Forschungsgemeinschaft, Germany) and the Shimadzu Prize (Shimadzu Foundation, Japan), is the first Japanese citizen to be awarded the Helmholtz–Humboldt Research Award. The Helmholtz–Humboldt Research Award is an international honor funded by the Helmholtz Association and Alexander von Humboldt Foundation (Germany).

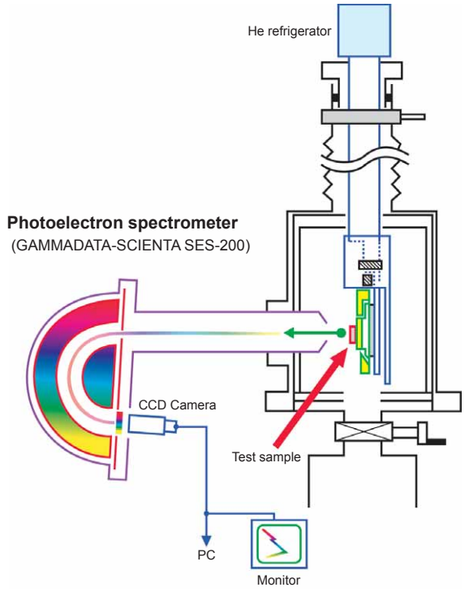

Fig. 1. High-resolution photoelectron spectroscopy detector installed in BL25SU beamline at SPring-8.
This detector is comprised of a measurement tank and a photoelectron spectrometer. Measurement tank holds the test sample while it is irradiated with synchrotron radiation (soft X-rays), and the spectrometer selectively measures the kinetic energy and intensity of the photoelectrons. Photoelectrons emitted from test samples pass through a long cylindrical-shaped electron lens (high-energy photoelectrons are decelerated) and enter a hemispherical fixture with a static electric field. When a low voltage is applied on the outside and high voltage is applied on the inside of this cup-shaped hemispherical fixture, a static electric field is produced in the hollow portion, bending the trajectory of the entering photoelectrons. By adjusting the voltage, only photoelectrons with specific energy can pass through a hollow portion and be detected (and counted) by a photoelectron detector (CCD camera) placed at the exit.

"The major research topic of the award is research on solid-state physics using bulk-sensitive photoelectron spectroscopy. Bulk refers to the inside of solid state materials," explains Dr. Suga. Using photoelectron spectroscopy, he was the first to successfully reveal the bulk electronic states of strongly-correlated electron materials. (These materials have strong interactions between electrons.) In 1976, Dr. Suga began researching photoelectron spectroscopy using synchrotron radiation when he was an Associate Professor at the Institute for Solid State Physics, the University of Tokyo, Japan. In 1989, he was appointed a Professor at Osaka University and served as a Visiting Professor at the High Energy Physics Laboratory (KEK)[2], Tsukuba, Japan. Throughout his career, Dr. Suga contributed to the development of synchrotron radiation facilities and was an advocate of synchrotron radiation research in Japan. He was actively involved with the entire construction process of SPring-8 from planning to launching the spectroscopic and experimental systems. His goal was that Japan becomes a global leader in bulk-sensitive photoelectron spectroscopy using soft X-rays as a light source. The term "soft" refers to X-rays with lower energies (< 2 keV: keV = 10^3 eV)[3] or longer wavelengths (> 0.6 nm: nm = 10^{-9} m) compared to common X-rays.

Since the mid-1990s, Dr. Suga along with young researchers and graduate students that he mentored at The University of Tokyo and Osaka University have fully dedicated themselves to developing bulk-sensitive photoelectron spectroscopy. In particular, SPring-8 took the initiative for soft X-ray spectroscopy by utilizing twin-helical undulators. Twin-helical undulators are devices that produce circular polarized synchrotron radiation by helically heaving electron beams with the use of the surrounding magnetic field. Since their inception, the Soft X-ray Spectroscopy of Solid Beamline (BL25SU) at SPring-8 and a high-resolution photoelectron spectroscopic detector (Fig. 1) installed in this beamline have been maintained as the world's best performing soft X-ray spectroscopy facility. As anticipated, these endeavors at SPring-8 have resulted in successfully developing bulk-sensitive photoelectron spectroscopy as a new field.

Successfully Measuring the Electronic States in a Solid

Although commonly used existing spectrometers can observe the surface of a solid using low-energy light, they cannot achieve a sufficient high-resolution measurement using high-energy light. Thus, little useful information has been obtained about the bulk electronic states (electrons inside a material). However at the end of the 20th century, Dr. Suga, Dr. Akira Sekiyama[4] (Assistant Professor, Osaka University), and colleagues were the first to reveal the real bulk electronic states of two types of solids ($CeRu_2Si_2$ and $CeRu_2$) using the ultra-high resolution soft X-ray monochromator and the high-resolution photoelectron spectrometer that they designed and developed (Fig. 2).

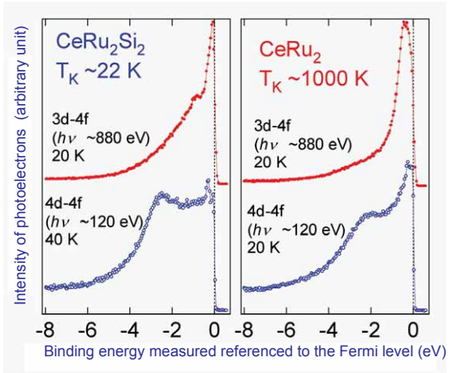

Fig. 2. High-resolution resonance photoelectron spectra of a heavy electron system, $CeRu_2Si_2$, and valence-fluctuating system, $CeRu_2$, of strongly-correlated electron systems.
Top (red circles): Resonance spectra from the first high-resolution measurements of Ce 3*d*–4*f*. These distributions strongly reflect the bulk (inside material) electronic states. Bottom (blue circles): Ce 4*d*–4*f* resonance spectra. These distributions have been confirmed to reflect the electronic states in the surface of a material.

The technique, which Dr. Suga and colleagues developed by bringing all relevant Japanese technologies together, has allowed real bulk electronic states to be observed, even near the 1 keV energy range with a resolution ten times higher than has been possible in the past (Fig. 3). This technique, which resolves almost all the weakness previously present in photoelectron spectroscopy, continues to contribute to research on the electronic states of strongly-correlated electron materials (such as new rare-earth compounds, superconductors, and even transition metal compounds). Their research achievement was published in *Nature* (January 27, 2000).

SPring-8 had been receiving international attention as a highly brilliant X-ray source and producing outstanding achievements. Additionally, SPring-8 possesses the world's best performing highly brilliant soft X-rays. Due to these reasons, the number of requests for collaborative research at SPring-8 from researchers around the world has been increasing.

In 2002, Dr. Suga and colleagues realized a revolutionary soft X-ray angle-resolved photoelectron spectroscopic measurement. This technique determines the momentum of photoelectrons based on their emission angle, allowing the band (existence range of electrons in a solid) structures of a material to be directly examined. Additionally, they are among the first to notice the importance of hard X-ray photoelectron spectroscopy (HAXPES), and have been leading the world in this field since initiating research using RIKEN SR Physics Beamline (BL19LXU) in 2004 at SPring-8.

Leading the World in the Development of Photoelectron Microscopes

Dr. Suga is committed to developing new measurement techniques and academic fields. In particular, a photoelectron emission microscope (PEEM), which is indispensable for research on microsized and nanosized magnetic materials, was developed through collaborative research between Dr. Suga and Dr. Jurgen Kirschner (Professor, Max-Planck-Institut für Mikrostrukturphysik, Germany). Their project, which was conducted between 1998 and 2000, demonstrated the superiority of the Soft X-ray Spectroscopy of Solid Beamline (BL25SU). BL25SU can produce perfect circular polarization of X-rays. Furthermore, Dr. Suga actively participated in the development of a spin-polarized scanning tunneling microscope (spin-STM), which should revolutionize research on nanosized magnetic materials. Moreover, he has been producing significant outcomes through collaborations with researchers at Osaka Kyoiku University, Max Planck Institute for Microstructure Physics, and Karlsruhe Institute of Technology (Germany). Through Dr. Suga's efforts, the combined utilities of synchrotron radiation PEEM at SPring-8 and laboratory spinSTM are expected to significantly contribute to the development of new basic scientific fields.

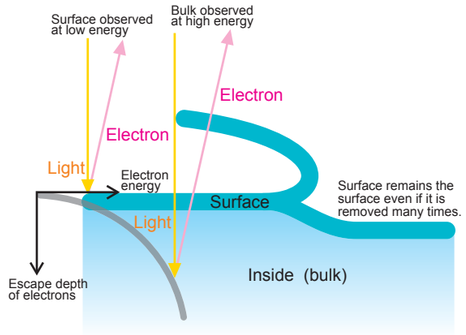

Fig. 3. Measurement principle of the bulk states within a material using soft X-ray synchrotron radiation.

The expectations for Dr. Suga as a leader who can extensively promote collaborative projects with Germany in research fields involving strongly-correlated electron materials and nanosized magnetic materials remain high. In addition, researchers in the field of synchrotron radiation from around the world have praised him for his dedication to encouraging young researchers to participate in these projects and mentoring world-class researchers. "I am very pleased that the cutting-edge research on photoelectron spectroscopy using synchrotron radiation at SPring-8 has been recognized. I earnestly hope that SPring-8 will continue to promote academic and cultural exchanges between young researchers around the globe and Japanese researchers as these exchanges will lead to a mutual understanding. Thereby, SPring-8 will lead the world in the advancement of science and peace," explains Dr. Suga with gratification and hope for the future. (In 2008, Dr. Suga received the Helmholtz–Humboldt Research Award, and to this date, remains the only person in Japan to whom this honor has been bestowed upon.) The award ceremony was held in Berlin, Germany, on June 24, 2008 (see picture on the page of the list of Major Awards/Prize Winners).

[1] Currently Professor Emeritus, Osaka University.
[2] Currently the High Energy Accelerator Research Organization (KEK).
[3] eV = electron volt.
[4] Currently Professor at Osaka University.

Reference

1. A. Sekiyama, T. Iwasaki, K. Matsuda, Y. Saitoh, Y. Onuki and S. Suga; *Nature*, **403**, 396 (2000)

Unraveling Mystery that Puzzled Dr. Mott, a Nobel Laureate

Insulators are materials that resist the flow of electric current. The most prevalent are band insulators, which cannot conduct electric current due to intrinsically lacking free-moving electrons. However, for unknown reasons some materials such as nickel oxide, which possess free electrons and should be conductors according to common knowledge in physics, exhibit the properties of insulators. Dr. Nevill F. Mott, who received the Nobel Prize in Physics in 1977, was fascinated by this mystery and tried to resolve it. This is why insulators such as nickel oxide are called Mott insulators. However, this mystery was only solved very recently by research conducted at SPing-8.

Why is Band Theory Not Applicable?

The behavior of the numerous electrons moving around in a solid characterizes various properties of the solid, including the electric properties. The energies of these electrons range from low to high. In a solid, electrons occupy distinct energy levels, forming a band structure. The aggregation of these electrons is called an "electron sea" or a "Fermi sea" (named after physicist Enrico Fermi), where all the bands below the uppermost level (Fermi energy) are filled with electrons.

In a Fermi sea, lower energy electrons stay near the bottom while higher energy electrons remain near the surface. Analogous to seawater where the normal sea moves more rapidly near the surface and more slowly near the bottom, a Fermi sea filled with electrons behaves similarly. Because the properties of each solid are thought to be characterized by a few electrons near the surface of the Fermi sea, a thorough understanding of the characteristics and states of such electrons is necessary to explore the properties of a solid.

Band theory, a basic theory of solid-state physics established around 1930, is used to describe and understand the states of various electrons in solid crystals. It describes the electronic states of materials with repeating regular structures of the same atomic arrangements based on quantum mechanics, and has contributed to the elucidation of physical phenomena of materials.

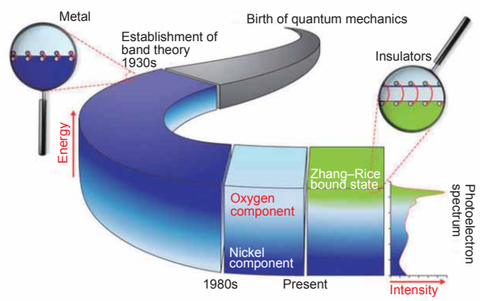

Fig. 1. History of the understanding of the electronic states in nickel oxide.
Many researchers have tried to decipher the mystery of nickel oxide, which is concurrently a metal and an insulator. Originally, nickel oxide was speculated to be an insulator because the electrons near the surface (dark blue) of the Fermi sea are highly condensed and cannot move freely. However in the 1980s, the understanding of the non-conductivity of nickel oxide drastically changed, and it was hypothesized the electrons near the surface are oxygen electrons (light blue). This theory had been commonly accepted until the Zhang–Rice bound state (green) was proposed to explain the mechanisms of copper-oxide high-temperature superconductors in 1988.

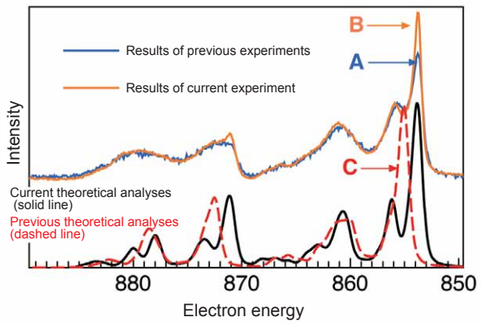

Fig. 2. Core-level hard X-ray photoelectron spectroscopy of nickel oxide.
Peak C, which is a single peak in the previous analyses (red dashed line), is divided into two peaks in this current analyses (black solid line). Current analyses agree with the experimental data. Height of Peak A (blue) from the previous analyses increases to Peak B (orange) in this study, indicating that current theoretical analyses can nearly reproduce the experimental data in terms of intensities.

However, a strange problem arose. According to band theory nickel oxide should be a metal, but it behaves as an insulator and blocks electric current. Dr. Neville F. Mott, a leading authority in physics, and his colleagues wrestled with this mystery. They hypothesized that electrons near the surface of the Fermi sea of nickel oxide are in an overly dense state and cannot move freely (Fig. 1: a dark blue parts). Their idea is analogous to a very crowded main street where people in crowd cannot move individually.

In the first half of the 1980s, the situation drastically changed, and a completely different explanation for this mystery was proposed. Research indicated that nickel oxide is an insulator because electrons near the surface of the Fermi sea are oxygen electrons (Fig. 1: light blue parts) while nickel electrons exist in a deeper location far from the surface. However, this hypothesis did not resolve all the issues.

"A problem with the theory proposed in the 1980s (Fig. 2: red dashed line) is that it cannot reproduce the experimental peak position of the energy spectrum of the photoelectrons emitted from nickel oxide obtained experimentally using core-level hard X-ray photoelectron spectroscopy (Fig. 2: blue solid line). Although two peaks are experimentally observed, the theory predicts a single peak (peak positions of A and C do not coincide, and there is only one peak at C in Fig. 2). Moreover, the valence band soft X-ray photoelectron spectroscopy shows that the theory from the 1980s (Fig. 3 red dashed line) does not well reproduce the experimentally obtained energy dependency of the photoelectron spectra (Fig. 3 orange line). Thus, the theory is incomplete," explains Dr. Shik Shin[1] (Team Leader, the Excitation Order Research Team, Quantum Order Research Group, RIKEN SPring-8 Center, Japan).

Hard X-rays at SPring-8 are Powerful Enough to Resolve the Mystery of Mott Insulators

Dr. Tetsuya Ishikawa (Director, RIKEN SPring-8 Center), Dr. Shin, Dr. Munetaka Taguchi (Research Scientist, RIKEN SPring-8 Center), and colleagues examined the properties of electrons near the surface of the Fermi sea of nickel oxide using core-level hard X-ray photoelectron spectroscopy and valence band soft X-ray photoelectron spectroscopy. Both techniques examine the properties of photoelectrons, which are electrons emitted from a material by X-ray irradiation. The former determines the properties of electrons near the surface of the Fermi sea by observing physical processes where electrons near the sea surface compensate for the "holes" created when individual electrons are extracted from the sea bottom upon irradiation with hard X-rays (high-energy X-rays with energy of 3–100 keV). In contrast, the latter examines the properties of electrons by directly extracting them from the sea surface using soft X-rays (X-rays with energy of 100–3,000 eV).

RIKEN Coherent X-ray Optics Beamline (BL29XU) enabled their research team to utilize core-level hard X-ray photoelectron spectroscopy. Hard X-rays allow researchers to examine the properties of electrons in a solid. Prior to the development of hard X-rays, existing core-level photoelectron spectroscopy could not probe the inside of solids because the low-energy X-rays could only penetrate near the surface of a solid. However, their research revealed nickel oxide possesses a unique electronic state, the Zhang–Rice bound state. The Zhang–Rice bound state is created through complicated interactions between nickel and oxygen in nickel oxide. This concept was theoretically driven by Dr. Fu–Chun Zhang[2] and Dr. Thomas M. Rice (both at the Swiss Federal Institute of Technology) in 1988 to explain the mechanisms of copper-oxide high-temperature superconductors.

Dr. Ishikawa and colleagues demonstrated that the energy components induced by electrons under such a unique electronic state increase significantly to raise the peak intensity (Fig. 2: Peak B). Additionally, they examined the energy-dependent electronic states near the Fermi sea and the energy peak properties using a valence-band soft X-ray photoelectron spectroscopic system at the RIKEN Coherent Soft X-ray Spectroscopy Beamline (BL17SU). They found that the patterns in the energy spectra of photoelectrons obtained from current theoretical predictions (Fig. 3: solid black lines), which consider the electron components induced from the Zhang–Rice bound state, agree well with those obtained from the experimental data (Fig. 3: solid orange lines).

Dr. Shin, Dr. Taguchi, and colleagues have performed theoretical analyses that consistently explain these two different experimental results. They revealed that electrons under the Zhang–Rice bound state (Fig. 1: green part) are responsible for the conduction mechanism of nickel oxide. Additionally, oxygen electrons, which were thought to be responsible for the conductivity, exist in an area deeper than the surface, while nickel electrons exist in an even deeper area. Furthermore, this unique Zhang–Rice bound state of electrons, which also plays an important role in copper-oxide high-temperature superconductors, has been suggested to be responsible for charge-transfer type insulators in general.

"The precise understanding of the electronic states of materials is of top priority in developing innovative devices. Thus, this discovery that the non-conductivity of nickel oxide is induced by complex interactions between nickel and oxygen may be an important guide for employing various transition metal oxides as raw, thermoelectric materials in next generation electronics," explains Dr. Shin. Their research achievements were published in *Physical Review Letters* (May 2008).

[1] Also Professor at the Institute for Solid State Physics, The University of Tokyo.
[2] Currently Professor at The University of Hong Kong, China.

Reference
1. M. Taguchi, M. Matsunami, Y. Ishida, R. Eguchi, A. Chainani, Y. Takata, M. Yabashi, K. Tamasaku, Y. Nishino, T. Ishikawa, Y. Senba, H. Ohashi, and S. Shin; *Phys. Rev. Lett.*, **100**, 206401 (2008)

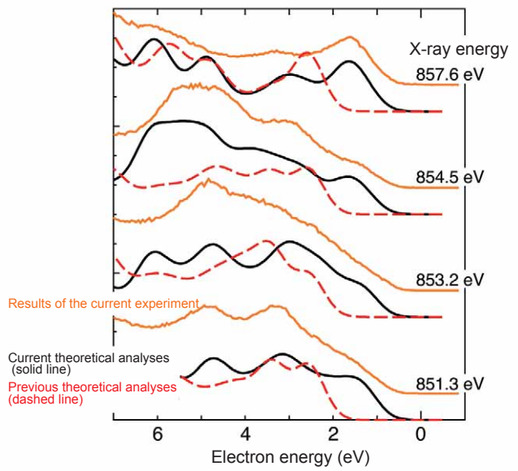

Fig. 3.Soft X-ray valence-band photoelectron spectroscopy of nickel oxide.
Electrons near the surface of the Fermi sea are directly observed using soft X-rays, which have energies less than hard X-rays. Soft X-rays with various energies were used to examine the energy dependency of photoelectron spectra. In contrast to previous theoretical analyses, current theoretical analyses, in which the components of the Zhang-Rice bound state are taken into account, nearly reproduce the energy-dependent experimental spectra in the low energy region (0–4 eV).

Strange States of the Outermost Electrons —Key to Developing New Technologies

Although electronic states determine the properties of a material, the actual states are unexpectedly difficult to reveal, especially the states of the outermost electrons (electrons in the outermost shell) of the constituent atoms in a material. However, these states are necessary to elucidate the properties of high-temperature superconductors and ferromagnetic materials as well as those of transition metal oxides exhibiting nonconductive properties. Unfortunately, relatively little information has been obtained about the electronic states due to limitations in the examination methods, but this has changed due to the work of Dr. Hidenori Takagi (Professor, The University of Tokyo, Japan), Dr. Takahisa Arima (Professor, Tohoku University, Japan), and colleagues.They used the highly brilliant synchrotron X-rays at SPring-8 to examine the states of the outermost electrons, and discovered materials capable of pioneering a field, spintronics.

Strong Correlation between the Direction of Electron Spin and Orbital Motion

An oversimplified explanation of the motion of electrons can be described as follows. Electrons spin around their own axis while rotating around nucleus, which is at the center of an atom. The former motion is called spin and the latter is called orbital motion. Individual electrons are like small magnets. The electron spin and orbital motion in an isolated atom interact. In contrast, the outermost electrons are affected by neighboring atoms in a solid where atoms are densely populated. Thus, opposite directions (clockwise (right-handed) and counter-clockwise (left-handed)) of electronic orbital motions around a nucleus occur with almost the same probability, and thereby cancel each other. This causes the overall electronic orbital motion to nearly disappear. In 1986, high-temperature superconductors were discovered. Since then oxides of 3*d* transition metals (titanium, manganese, iron, and copper) have been attracting attention as high-temperature superconductive materials. Because the outermost electrons terminate orbital motions, they assume a borderline state where some can but others cannot move to neighboring atoms. The functions of these outermost electrons are thought to be responsible for the superconductivities and ultra-giant magnetoresistance in the oxides of 3*d* transition elements. In the Periodic Table, 3*d* transition elements lie above 4*d* and 5*d* transition elements.

The ease of moving the outermost electrons to neighboring atoms has been speculated to increase as the atomic number increases (4*d*, 5*d*, etc.). Thus, oxides with larger atomic numbers would lose superconductivity and the ultra-giant magnetoresistance observed in 3*d* transition elements. However, recent studies have revealed new findings contrary to this hypothesis. For example, when iridium (Ir) in Sr_2IrO_4 (an insulator) is replaced with rhodium (Rh) or cobalt (Co), where Co, Rh, and Ir form a column in that order in the Periodic Table, both Sr_2RhO_4 and Sr_2CoO_4 become metals (conductors) although they have the same crystal structure as Sr_2IrO_4. It has been a mystery why Sr_2IrO_4 (iridium oxide), the oxide of a 5*d* transition element whose outermost electrons are supposed to move easily, is an insulator.

"We tried to explain this mystery based on the concept of resurgence of orbital rotation. The interactions between the direction of electron spin and that of orbital motion are stronger for heavier elements with larger atomic numbers. In iridium oxide (Sr_2IrO_4) and similar oxides, the effect of spin–orbit interactions is sufficient to surpass the effects from neighboring atoms. Thus, the possibility of recovering the electronic orbital motions is high. If electron transfer to neighboring atoms is suppressed due to this effect, then conductivity would be lost. This could explain why Sr_2IrO_4 is an insulator. However, it has been extremely difficult with existing techniques using magnetism to demonstrate whether the orbital motions of the outermost electrons are recovered because the magnetism of Sr_2IrO_4 is extremely weak," describes Dr. Takagi.

Fig. 1. Schematic diagram of resonant X-ray scattering.
Diffraction occurs due to the superposition of scattering X-rays from individual atoms. When the energy of the incident X-rays equals the excitation energy of an electron in an atom, the resonance between the incident and absorbed/emitted X-rays amplifies X-ray scattering. This results in an increased diffraction intensity. If there is a phase difference (time lag) between these two types of X-rays, then the resonance may be canceled due to interference.

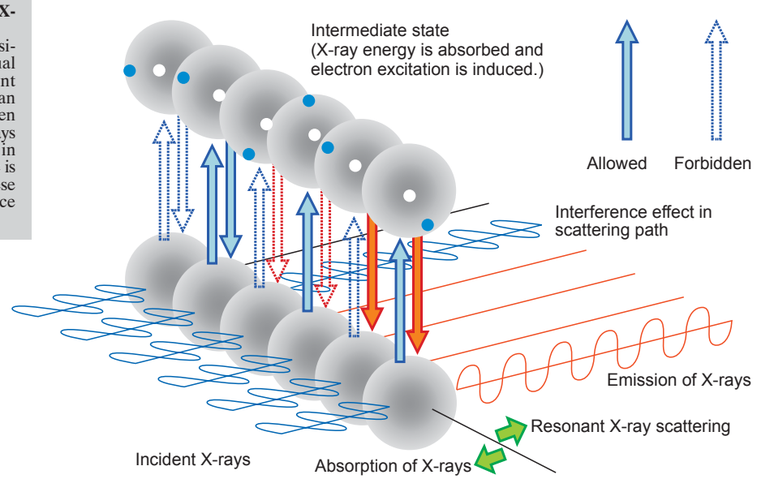

Spin and Orbital Motion of Outermost Electrons are Strangely Correlated

To examine the orbital motions of electrons that influence the conductivity and magnetism of Sr_2IrO_4, Dr. Takagi's research group utilized synchrotron radiation X-ray diffraction at SPring-8. First, they determined the spin arrangement (magnetic structures of electrons) of this nonconductive oxide. Although neutron beams are commonly used to determine spin arrangements, iridium atoms absorb neutrons, rendering this method ineffectively. Moreover, determining spin arrangements solely using X-ray diffraction is extremely difficult and has yet to be successful.

Thus, Dr. Takagi and colleagues conducted experiments using X-rays at SPring-8. They used specific wavelengths where the X-ray diffraction signals from the electron spins of the iridium atoms are amplified to successfully determine the spin arrangements. X-ray diffraction requires a smaller sample size compared to techniques using neutron beams. Hence, it is anticipated that SPring-8 will play a wider role in determining spin arrangements in the future.

Strong spin–orbit interactions occur in 5*d* transition elements. Thus, the electron arrangement of iridium with right-handed orbital motion and that with left-handed exhibit the same arrangement pattern as the spin arrangement. Therefore, their research group successfully demonstrated that when spin and orbital motion have the same period, X-ray waves diffracted by electron spin and those diffracted by electronic orbital motion interfere with each other depending on the wavelength of X-ray (Fig. 1). Thus, the intensity of the diffracted waves depends on whether the wavelengths for spin and orbital motion have the same period (Fig. 1). Experiments conducted using extremely strong synchrotron radiation X-rays with adjustable

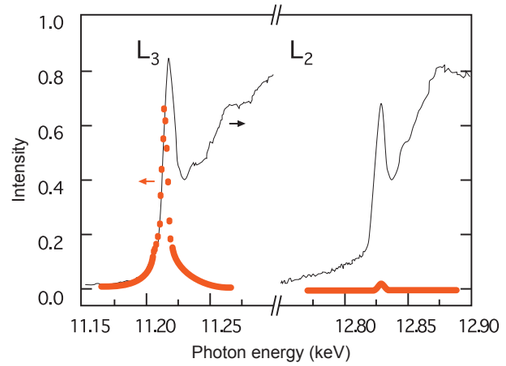

Fig. 2. Energy dependence of the magnetic X-ray diffraction intensity (red circles) and X-ray absorption intensity (black solid lines) of Sr_2IrO_4.
Rising edge of X-ray absorption (red circles) corresponds to the electron transition where the resonance in diffraction intensity (black solid lines) is maximized. Substantial increase occurs at the L_3 edge, while the increase at the L_2 edge is negligible. Relationship between energy and wavelength is roughly expressed as wavelength (nm = 10^{-9} m) × photon energy (keV = 10^3 eV) = 1.24 where the energy of the incident X-rays is expressed in terms of photon energy (keV) on the horizontal axis.

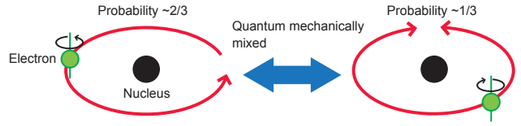

Fig. 3. Schematic diagram of the outermost electron state of iridium revealed by this research.
Probability of observing an electron orbiting in the opposite direction as the direction of its spin is about one-third. Orbital motion ceases when the electron orbits opposite to the spin direction. In the right figure, spin and orbital motion have opposite directions.

energy (wavelength) at SPring-8 revealed that a significantly enhanced resonance (amplification of X-ray scattering intensity) is observed at the longer wavelength (L_3 edge), but the resonance is negligible at the shorter wavelength (L_2 edge) (Fig. 2).

Their experimental results reflect the interference effects of electronic orbital motion waves in resonance. Further detailed theoretical analyses revealed the probability of observing an outermost iridium electron orbiting in the same direction as its spin is about two-thirds, whereas the probability of the opposite (and the orbital motion ceases) is about one-third (Fig. 3). This strange spin–orbit correlation, which is not observed in isolated atoms, is unique to the outermost electrons of Sr_2IrO_4. Thus, the transfer of electrons to neighboring atoms is suppressed, making Sr_2IrO_4 an insulator. In the past materials science research on physical properties mainly targeted oxides of elements with small atomic numbers, such as oxides of manganese, iron, and copper (3*d* transition metal oxides). Recently, research on the physical properties and functions of 5*d* transition metal oxides has been receiving increased attention. The properties and functions of 5*d* transition metal oxides have completely different orders of magnitude due to the much stronger electron spin–orbit interactions than those of 3*d* transition metal oxides.

"Directly observing spin–orbit interactions using resonance phenomena is very significant. Our success will lead to increased collaborations between theoretical research on the physical properties of materials and advanced measurement technologies," explains Dr. Takagi. If spintronic circuit elements, which control spin but not electric charge, are achieved, then the development of revolutionary energy-saving devices will become a reality. The development of electron spin control, which is still in the trial stage, requires a thorough understanding of spin–orbit interactions. The stronger the spin–orbit correlation, the easier it is to control the electronic/optical of spin information; therefore, electron spin control in 5*d* transition metal oxides may be realized if breakthrough control techniques are developed.

Their research achievement was published in *Science* (March 5, 2009), and in 2010 Dr. Takagi received the Prize for Science and Technology (Research Category), the Commendation for Science and Technology by the Minister of Education, Culture, Sports, Science and Technology of Japan, for his achievements and contributions.

Reference
1. B. J. Kim, H. Ohsumi, T. Komesu, S. Sakai, T. Morita, H. Takagi and T. Arima; *Science*, **323**, 1329 (2009)

Dreaming of Room Temperature Superconductors

Superconductivity is a phenomenon where the electrical resistance of a conductor vanishes, and is typically observed at extremely low temperatures. Successfully developing room temperature superconductors, a researcher's dream, would begin a new era in the energy revolution. For example, superconductive electric power transmission systems would enable electric power networks to be established with negligible loss in electric transmission, and they could store electric current itself in superconductive rings without external energy. Additionally, if superconductive circuit elements can be used in supercomputers, power consumption and heat generation would be drastically reduced, allowing further downsizing. Moreover, the construction of super fast, super energy-efficient magnetically-levitated trains would be possible. Although the mechanisms for superconductivity are not well understood, SPring-8 is playing a crucial role in solving these mysteries through the various types of superconductivity research conducted using synchrotron radiation.

Striving to Solve the Mysteries of Superconductivity using Inelastic X-Ray Scattering

Although electrons normally repel one another, superconductivity is a singular phenomenon where the electrical resistance vanishes due to electron pairing through an attractive force. Although electron pairing in high-temperature copper-oxide superconductor was discovered in 1986, its mechanisms were not elucidated. However, several hypotheses have been proposed. One is the BCS theory which postulates that lattice vibrations (vibrations of atoms situated at the vertices of a lattice) between atoms comprising a superconductor are the major cause of superconductivity. Another theory postulates that superconductivity is due to ordered spin or excitation motion (fluctuation) of electric charge. Yet others are a mixture of these two theories. To date, the highest critical temperature (T_c) below which superconductivity is present has been reported for a copper oxide (T_c of ~150 K (~ −123 °C)), but this value is still quite low. Therefore, determining the mechanisms of superconductivity and synthesizing materials with a high T_c based on these mechanisms are immediate measures to develop room temperature superconductors.

SPring-8's High-Resolution Inelastic Scattering Beamline (BL35XU), which boasts the world-best energy resolution at a few electron volts, has significantly contributed to unraveling the mechanisms of lattice vibrations and charge excitations of superconductors through inelastic X-ray scattering experiments. Inelastic X-ray scattering experiments measure tiny differences between the energies of the incident X-rays onto a material and the scattered X-rays. Thus, they require highly brilliant X-rays to examine the excitation states of atoms and electrons in materials.

Demonstrating the Correlation between Lattice Vibrations and Superconductivity

Dr. Alfred Q. R. Baron (Associate Chief Scientist, RIKEN, Japan), Dr. Hiroshi Uchiyama (Research Scientist, *ditto*), and colleagues examined the dispersion relations (relations among vibration direction, momentum, and energy) of the lattice vibrations in MgB_2 (a new high-temperature superconducting material discovered by Japanese researchers in 2001). They employed an inelastic X-ray scattering technique that they helped develop. Their research revealed that MgB_2 is an existing type of superconducting materials and its lattice vibrations are closely related to the onset of superconductivity. Additionally, they observed the softening (decrease) in the lattice vibrational energy of a copper-oxide high-temperature superconducting material, $HgBa_2CuO_{4+\square}$. These achievements were published in *Physical Review Letters* (2004).

Moreover, Dr. Jun-ichiro Mizuki (Deputy Director, the Quantum Beam Science Directorate, Japan Atomic Energy Agency (JAEA)), Drs. Moritz Hoesch, Tatsuo Fukuda, Kenji Ishii, Shuichi Wakimoto (collaborative researchers with Dr. Mizuki at JAEA), and colleagues at JAEA also studied superconductivity mechanisms at BL35XU. Through experiments on newly discovered iron–arsenic compound high-temperature superconducting materials ($LaFeAsO_{1-x}F_x$ and $PrFeAsO_{1-y}$), Dr. Fukuda and colleagues revealed that lattice vibrational energy induced by the motions of iron and arsenic atoms is lower than the theoretical prediction, questioning the validity of the common understanding. This finding was published in *the Journal of the Physical Society of Japan* (2008).

Dr. Mizuki and colleagues found that diamond, which is the same material used in jewelry, plays an important role in their research. Surprisingly, when a high concentration of boron is doped (injected) into diamond, which is a good insulator, it becomes superconductive. Since its discovery in 2004 by Russian researchers, boron-doped diamond has received much attention as a potential material to decipher the superconductivity mechanisms and to increase T_c. However, single crystal samples must be prepared to examine the lattice vibrations of boron-doped superconducting diamond using inelastic X-Ray scattering. Dr. Hiroshi Kawarada (Professor, Waseda University, Japan) and colleagues developed ideal single crystal samples (100-μm thick) of such diamond using a vapor phase method (a method to synthesize diamonds from hydrogen and methane), and Dr. Yoshihiko Takano (the National Institute for Materials Science, Japan) demonstrated that T_c of this diamond is 4.2 K.

The longitudinal optical lattice vibrational mode (LO mode) is a type of lattice vibration in which atoms repeatedly move closer and then farther from each other (Fig. 1). Dr. Mizuki and colleagues examined the LO modes of superconducting and non-superconducting diamonds. They found that the energy of the superconducting LO modes is significantly softened. Hence, this lattice vibration plays an important role in electron pairs responsible for superconductivity. These research achievements, which were realized through a series of experiments, were published in *Physical Review B* (2007).

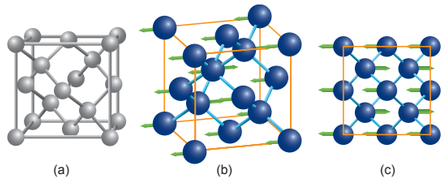

Fig. 1. Schematic diagrams of the crystal structures and longitudinal optical lattice vibration modes (LO modes) of diamonds.
(a) Crystal structure of a diamond. (b) 3D view of a LO mode. (c) Top view of a LO mode. Eight atoms at the vertices of a cube and six atoms at the center of each side of a cube vibrate in the opposite directions from other atoms. Softening of lattice vibrations is a phenomenon where this vibration energy is unusually weak.

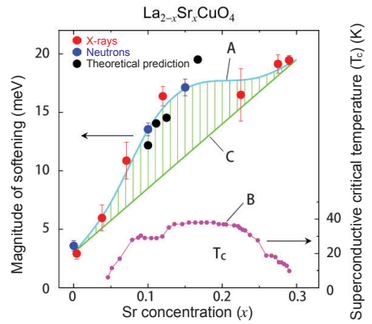

Fig. 2. Relationships among strontium (Sr) concentration, softening of lattice vibrations, and superconductivity critical temperature (T_c).
Relationships between the magnitude of the softening of lattice vibrations (decrease in vibration energy) and strontium concentration (A: blue), and between T_c and strontium concentration (B: purple). When plot A increases (decreases), plot B increases (decreases). Plot A deviates from the expected linear dependence on x when there is no enhancement (proportional plot C: green).

Additionally, research on the lattice vibrations of other high-temperature superconductors has also progressed. Figure 2 shows the relationship between T_c and the concentration (x) of strontium (Sr) in a superconducting lanthanum strontium copper oxide ($La_{2-x}Sr_xCuO_4$). The distribution reaches a maximum near x = 0.15 (B). $La_{2-x}Sr_xCuO_4$ is nonconductive when $x < 0.04$, but becomes superconductive when $0.04 \leqq x \leqq 0.3$ (T_c gradually increases as x increases passing the peak, and then gradually decreases), and lose superconductivity when $x > 0.3$. To promote further studies on $La_{2-x}Sr_xCuO_4$, Dr. Kazuyoshi Yamada (Professor, the Institute for Materials Research, Tohoku University, Japan) has fabricated a special rod-like single crystal of $La_{2-x}Sr_xCuO_4$ in which the strontium concentration gradually increases from one end at a constant rate.

As Dr. Mizuki has acknowledged, "This special crystal has enabled systematic measurements of the dependence of lattice vibrations on the strontium concentration while simultaneously reducing experimental errors." Research in this field has gained momentum since then. Experiments using this crystal have revealed that the softening of lattice vibrations do not match the expectation that the softening of lattice vibrations is proportional to the strontium concentration (C in Fig. 2). Additionally, Fig. 2 shows that the increase/decrease patterns in the relationships between strontium concentration and lattice vibration softening (A) and strontium concentration and T_c (B) are clearly correlated. This finding indicates that the longitudinal wave expansion and contraction of the lattice vibrations between copper and oxygen, which are the constituent elements of $La_{2-x}Sr_xCuO_4$, are strongly correlated with the mechanisms of superconductivity. Their research results were published in *Physical Review B* (2005).

Elucidating the Superconductivity Mechanisms through Studies on Electron Excitations

Dr. Ishii and colleagues have also conducted resonant inelastic X-ray scattering experiments at the JAEA Quantum Dynamics Beamline (BL11XU), and directly observed the electron excitation states of copper-oxide superconducting materials, $YBa_2Cu_3O_{7-\square}$ and $Nd_{2-x}Ce_xCuO_4$. They revealed that the strong coupling of electrons, which carry charge and induce unusual metallic states, are partly responsible for superconductivity. Additionally, they demonstrated that theoretical calculations obtained from the electron correlation theory proposed by the Tohoku University group reproduce the experimental data. Moreover, Dr. Wakimoto and colleagues are the first to observe the collective excitation of a group of electrons with strong couplings in copper-oxide high-temperature superconducting materials and related nickel oxides using resonant inelastic X-ray scattering (Fig. 3). These research achievements were published three times in *Physical Review Letters* (2005 and 2009). "Although a complete understanding of these unusual electron behaviors and paring mechanisms of electrons has yet to be achieved, I am hopeful that our research will pave the way toward the development of room temperature superconductors," expresses Dr. Mizuki with anticipation.

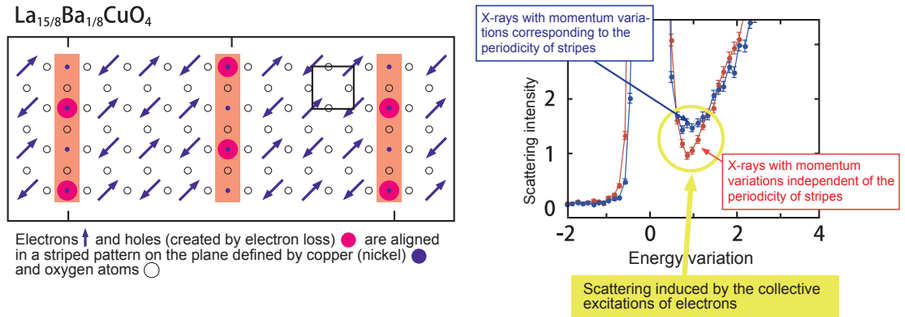

Fig. 3. Resonant inelastic X-ray scattering spectra.
Comparison of the resonant inelastic X-ray scattering spectrum measured by the momentum variations corresponding to the periodic structure of the aligned electrons in a striped pattern (blue) and that measured by the momentum variations independent of the periodic structure (red). Signals induced by the collective excitations of electrons are observed as an enhancement in the former data (yellow circle).

References
1. A. Q. R. Baron, H. Uchiyama, Y. Tanaka, S. Tsutsui, D. Ishikawa, S. Lee, R. Heid, K.-P. Bohnen, S. Tajima and T. Ishikawa; *Phys. Rev. Lett.*, **92**, 197004 (2004)
2. H. Uchiyama, A. Q. R. Baron, S. Tsutsui, Y. Tanaka, W.-Z. Hu, A. Yamamoto, S. Tajima and Y. Endoh; *Phys. Rev. Lett.*, **92**, 197005 (2004)
3. T. Fukuda, A. Q. R. Baron, S. Shamoto, M. Ishikado, H. Nakamura, M. Machida, H. Uchiyama, S. Tsutsui, A. Iyo, H. Kito, J. Mizuki, M. Arai, H. Eisaki and H. Hosono; *J. Phys. Soc. Jpn.*, **77**, 103715 (2008)
4. M. Hoesch, T. Fukuda, J. Mizuki, T. Takenouchi, H. Kawarada, J. P. Sutter, S. Tsutsui, A. Q. R. Baron, M. Nagao, and Y. Takano; *Phys. Rev. B*, **75**, 140508(R) (2007)
5. T. Fukuda1, J. Mizuki, K. Ikeuchi, K. Yamada, A. Q. R. Baron and S. Tsutsui; *Phys. Rev. B*, **71**, 060501(R) (2005)
6. K. Ishii1, K. Tsutsui, Y. Endoh, T. Tohyama, K. Kuzushita, T. Inami, K. Ohwada, S. Maekawa, T. Masui, S. Tajima, Y. Murakami and J. Mizuki; *Phys. Rev. Lett.*, **94**, 187002 (2005)
7. K. Ishii1, K. Tsutsui, Y. Endoh, T. Tohyama, S. Maekawa, M. Hoesch, K. Kuzushita, M. Tsubota, T. Inami, J. Mizuki, Y. Murakami and K. Yamada; *Phys. Rev. Lett.*, **94**, 207003 (2005)
8. S. Wakimoto, H. Kimura, K. Ishii, K. Ikeuchi, T. Adachi, M. Fujita, K. Kakurai, Y. Koike, J. Mizuki, Y. Noda, K. Yamada, A. H. Said and Yu. Shvyd'ko; *Phys. Rev. Lett.*, **102**, 157001 (2009)

Developing Amazing New Spectroscopic Technologies in the Quest to Determine the True Nature of Materials

The functions and combinations of the constituent elements determine the properties of a material; herein the functions and properties of each element are determined by the states of the constituent atoms and electrons. Mössbauer spectroscopy is an indispensable technique to fully understand the states of atoms and electrons, which are the fundamental components of a material. However, the application of Mössbauer spectroscopy in high-energy regions has been difficult due to limitations arising from the measurement mechanisms. To overcome this difficulty, Dr. Makoto Seto (Professor, Kyoto University, Japan) and colleagues developed new spectroscopic techniques applicable to high-energy regions by utilizing highly brilliant synchrotron radiation at SPring-8. Through their efforts, precise spectroscopic analyses for numerous elements, including almost all rare earth elements, are now possible.

Limitations of Mössbauer Spectroscopy in Examining Atoms and Electrons

Mössbauer spectroscopy is a technique to examine states, such as valences, electronic structures, and magnetic properties, of elements in a material. It utilizes a phenomenon where nuclei of elements are resonantly excited by absorbing the gamma (γ)-ray energy, which is irradiated with γ-rays with a specific energy. Thus, the radioactive isotopes of target elements are the main γ-ray sources. In particular, Mössbauer spectroscopy using γ-rays emitted from iron (Fe) has been extensively utilized not only in physics and chemistry, but also in biology and earth science. In 2004, samples collected by the Mars probe were analyzed using Mössbauer spectroscopy, revealing that water was once present on Mars. Despite these successes, with the exception of a few elements such as iron, preparing a radioisotope radiation source suitable to measure each element had been difficult. Moreover, analyzing elements that can only be measured using a very short-lived radioisotope had been nearly impossible.

"Although several ideas, which utilized high-intensity synchrotron radiation, had been proposed to overcome these difficulties, other issues remained. For example, new high-speed, high-precision detectors, which can tolerate high-intensity synchrotron radiation, needed to be developed for measurements for Mössbauer spectroscopy in high-energy regions (> 30 keV). Hence, many hurdles remained before realizing measurements of nuclei requiring high excitation energy," explains Dr. Seto.

Hyperfine interactions are interactions between electron systems and nucleus systems. These interactions are utilized to measure the structures and magnetic properties of electrons around the nuclei of a specific atom using the resonant excitation phenomena. This technique provides information about the structures and magnetic properties of such electrons without disturbing the electron systems by precisely measuring the transition of a nuclear energy level and removing degeneracy. The transition of a nuclear energy level (a quantum mechanical view of the discrete magnitude relation of energy) from one level to another is induced by the effects of the structures and magnetic properties of such electrons. In contrast, degeneracy (a quantum mechanical term describing two or more different physical states at the same energy level) is removed by splitting the degenerate energy levels.

Fig. 1. Measurement of Mössbauer absorption spectra using synchrotron radiation.
Synchrotron radiation X-rays are initially irradiated to a sample and the transmitted X-rays are sequentially irradiated to a reference sample. Fluorescent X-rays emitted from the reference sample are detected when nuclear resonant excitations occur. To measure absorption spectra, the scattering intensity of fluorescent X-rays is measured by varying the energy of the incident X-rays to a reference sample. To vary this energy, the Doppler effect, which is induced when the reference sample is moved by a velocity transducer, is utilized. When the energy of the fluorescent X-rays emitted from a sample (a dip in a top red plot) differs from that of the reference sample (top), synchrotron radiation X-rays with energy that induces nuclear resonant excitations in the reference sample (a bump in a top blue plot) will not be absorbed in the sample. This results in nuclear resonant excitations in the reference sample (the left-hand side red arrow in a right-most plot). However, when these two energies are equal (bottom), synchrotron radiation with energy to induce nuclear resonant excitations in a reference sample will be absorbed by the sample (a dip in a bottom red plot). Thus, nuclear resonant excitations will barely occur in the reference sample (a small bump in a bottom blue plot). Therefore, precise data of the scattering intensity reveals that absorption dips when the resonant excitation energies are equal (a dip indicated by a right-hand side arrow in a right-most plot). Conversely, if the locations of such absorption dips are identified, then the energy states of an unknown sample can be determined.

Developing Ultra-High Precision Spectrometry Required Perceptual Changes

Traditionally, Mössbauer spectroscopy using synchrotron radiation utilizes nuclear resonant forward scattering. This technique measures quantum beats, or more specifically the variations in the intensity of scattering γ-rays in the forward direction induced by mutual interference among many different energy levels of nuclei, when the nuclei are resonantly excited by pulsed synchrotron radiation. However, it is difficult to use high-energy synchrotron radiation in this technique. When high-energy γ-rays are emitted or absorbed, the nuclei recoil, reducing the energy of γ-rays, decreasing the likelihood of the Mössbauer effect. Thus, Dr. Seto and colleagues shifted their thinking, and realized Mössbauer spectroscopic measurements using high-energy synchrotron radiation.

They aimed to accomplish high-precision spectrometry by detecting the internal conversion electrons and fluorescent X-rays. When an excited state nucleus returns to a lower energy level, the internal conversion occurs where orbital electrons, instead of γ-rays, are emitted. The emitted electrons are called internal conversion electrons. Irradiating with X-rays whose energies exceed an element-specific value excites the inner-shell electrons (electron in the inner orbits) of the constituent atoms of a target material and the outer-shell electrons (electron in the outer orbits) transit into the holes created by the excitation. This element-specific energy is called the absorption edge energy. Because the energy levels of outer-shell electrons are higher than those of inner-shell electrons, X-rays with energy equal to this energy difference will be emitted upon this transition. These X-rays are called fluorescent X-rays.

Achieving Success in Mössbauer Spectroscopy using Highly Brilliant Synchrotron Radiation

Although spectral data can be obtained from internal conversion electrons and fluorescent X-rays, this is insufficient for Mössbauer spectroscopy using synchrotron radiation due to the low measurement precision and efficiency. To overcome these issues, Dr. Seto and colleagues developed a technique to obtain data about the properties of a sample by concurrently using a reference sample with known properties. Then they measured the differences in atomic energies between these two samples (Fig. 1 and explanation therein). This technique provides sufficient precision to measure nuclei with high-energy levels. Their research group conducted an experiment using a well-documented sample of Fe oxide, hematite (α-Fe_2O_3), at SPring-8's JAEA Quantum Dynamics Beamline (BL11XU) to determine if Mössbauer spectroscopy can be performed using this technique. Their demonstration experiment revealed that the resultant spectra agree with known spectra obtained using radioactive isotope sources (Fig. 2). Moreover, they conducted an additional experiment to measure the absorption spectra of an isotope of germanium (Ge), specifically the 68.752 keV third excited state of ^{73}Ge, which has high-energy, short-lived excitation levels, using the Nuclear Resonant Scattering Beamline (BL09XU). Then they successfully applied Mössbauer spectroscopy using synchrotron radiation to measure the absorption spectra of ^{73}Ge, which was difficult to obtain because suitable radioactive isotope sources were unavailable (Fig. 3). Their results clearly demonstrated that Mössbauer spectroscopic analyses are possible on numerous elements, including almost all rare earth elements.

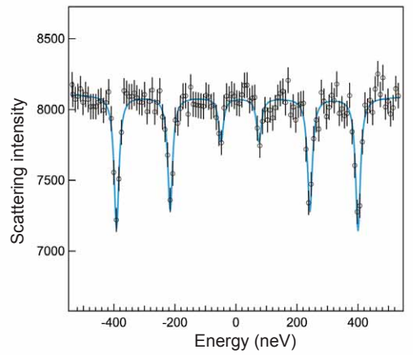

Fig. 2. Mössbauer absorbing spectrum of ^{57}Fe using synchrotron radiation.
Sample and references sample are iron oxide (α-Fe_2O_3) and palladium (Pd) metal containing 2% Fe atoms, respectively.

"Small sample measurements, imaging measurements, and measurements under complex extreme environmental conditions were very difficult until the development of Mössbauer spectroscopy using synchrotron radiation, but now they are easy. This new technique is also applicable to energy regions that are covered by existing techniques, which allows complicated spectral analyses to be conducted utilizing the vast amounts of existing data. Furthermore, spectrometry with a resolution at the nanoelectron volt level (neV = 10^{-9} eV) has become possible for nuclear excitations with very narrow energy widths (~1 neV) and quasi-elastic scattering (scattering energy is moving and scattering varies with time)," explains Dr. Seto.

Their research achievements were published in *Physical Review Letters* (May 29, 2009). Moreover, this method should promote research on the Earth's internal structure.

Reference
1. M. Seto, R. Masuda, S. Higashitaniguchi, S. Kitao, Y. Kobayashi, C. Inaba, T. Mitsui and Y. Yoda; *Phys. Rev. Lett.*, **102**, 217602 (2009)

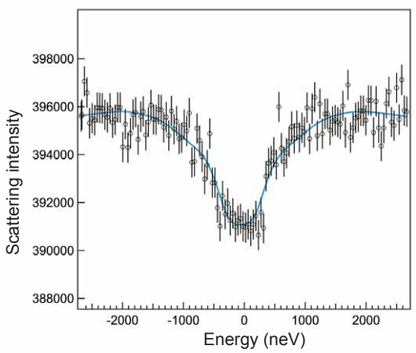

Fig. 3. Mössbauer absorbing spectrum of ^{73}Ge using synchrotron radiation.
Sample and reference sample are lithium germanate (Li_2GeO_3) and a germanium oxide (GeO_2), respectively.

High-Pressure Earth Science

Exploring Structures of Materials in Earth's Deep Interior

Observing Rocks under High-pressure, High-temperature Conditions with the "Eye of Light"

Our planet consists of a layered structure from the surface to the center (Fig. 1). The depths and thicknesses of these layers can be determined by analyzing seismic wave propagation utilizing their large density differences. However, this analysis requires information about the structures and properties of Earth's layers, and consequently, the rocks (minerals) that constitute the layers must be investigated. Currently the drilling depth is limited to only ~10 km, which is extremely small compared to Earth's radius of ~6,400 km. Therefore, high-pressure, high-temperature experiments that artificially reproduce the conditions of Earth's interior are very useful in these investigations.

In high-pressure, high-temperature experiments, experimental samples are encapsulated in high-pressure cells covered by heaters and a pressurizing medium. Thus, the actual processes in the cells cannot be directly observed using normal techniques. However, synchrotron radiation, "eye of light", can make such observations possible. Because synchrotron radiation provides powerful X-rays that can penetrate these materials, information about their crystal structures and volume changes such as density and compressibility can be obtained by analyzing the diffraction of X-rays from the samples. Moreover, the pressure values can be simultaneously determined using a reference material. Therefore, controlling the pressure and temperature in X-ray diffraction experiments allows the state changes in a sample to be observed at a desired depth. Such high-pressure, high-temperature X-ray diffraction experiments were initially conducted in the 1980s at the Photon Factory in Tsukuba, Japan, but are now performed around the globe.

In high-pressure experiments, the sample size typically decreases as the exerted pressure increases. For example, at a pressure of 25 GPa (GPa = 10^9 Pa = ~10,000 atm), which is equivalent to a mantle transition zone depth of 700 km, the sample size must be ~1 mm^3 or smaller. In contrast, at a pressure >100 GPa, which corresponds to the lowest region in the lower mantle, the maximum sample size is <50 μm^3. Additionally, the temperature increases with the depth inside the Earth, and it reaches 1,500 °C and 2,000 °C around in the mantle transition zone and lower mantle, respectively. Because maintaining such conditions for long periods of time is extremely tough, X-ray diffraction experiments are difficult to conduct under such conditions. However, the emergence of third generation of synchrotron radiation facilities, including SPring-8, which can provide highly brilliant and highly energetic X-rays, has completely changed the situation. Experiments on small sized samples can now be performed in a relatively short time.

World-First Discoveries at SPring-8

SPring-8 is a pioneer in providing high-pressure, high-temperature experimental conditions, which has allowed researchers to successfully observe the transition processes of olivine. Olivine is the principal mineral of the mantle and undergoes a transition from the spinel structure to the perovskite structure under conditions (24 GPa, 1,600 °C) corresponding to the mantle transition zone (660 km depth). This was the first significant achievement at SPring-8, and the result, which was published in *Science* (1997), attracted global attention. Since then, the development of high-pressure devices and high-temperature heating technologies using lasers to reproduce conditions equivalent to Earth's deep interior has been energetically pursued around the globe. SPring-8 has developed high-intensity beams to irradiate small samples (<50 μm^3) as well as realized higher intensity X-ray sources, which are at least ten times more powerful than previously existing ones by utilizing X-ray collector optics such as KB mirrors[1] and refractive lenses. These advances in high-pressure, high-temperature generating technologies along with improved synchrotron radiation technologies allow researchers to reproduce conditions that are equivalent to those of the lowest region of the lower mantle and even deeper core regions.

A collaborative research group from the Tokyo Institute of Technology, the Japan Agency for Marine–Earth Science and Technology, and the Japan Synchrotron Radiation Research Institute (JASRI) has successfully reproduced conditions equivalent to the D" (D double-prime) layer, which is situated between the lower mantle and the outer core, using a diamond anvil device and laser heater. This D" layer has very peculiar properties. The propagation velocities of seismic waves drastically change, depending on the propagation directions; thus, the D" layer remains a mystery. Their research group conducted X-ray diffraction experiments under conditions equivalent to the region near the D" layer (>125 GPa, >2,200 °C), and revealed that the $MgSiO_3$ perovskite phase is converted into a new high-pressure phase, post-perovskite phase. News about the discovery of a post-perovskite phase, which consistently explains the mysteries of the discontinuities and anisotropy of seismic wave velocities, made a striking impact on Earth scientists worldwide. Their remarkable accomplishment was immediately published in *Science* and *Nature* in 2004, and has been acknowledged as a significant breakthrough in science history. Additionally, their research group has further developed high-pressure, high-temperature technologies and successfully conducted experiments on quartz crystal under unprecedented conditions of 300 GPa and 2,000 °C. They demonstrated for the first time that a quartz crystal changes into a new dice-shaped pyrite-type mineral under pressure conditions exceeding 270 GPa. This pyrite-type mineral has received attention as a potential candidate for the principal mineral in the cores of Uranus and Neptune.

High-pressure, high-temperature experimental technologies and synchrotron radiation technologies have been used to investigate the crystal structures in X-ray diffraction experiments as well as in research on the physical properties such as viscosity, density, and elastic wave velocity. In addition to providing insight on Earth's origin, experimentally measuring the viscosity and density of magma, which stagnates at depths of several hundred kilometers, can provide information about its ascent, transportation velocities, and production mechanism. Additionally, comparing the experimentally measured elastic wave velocity to the actual seismic wave velocity can provide clues about the materials in Earth's interior. In recent years, the techniques to analyze seismic waves have remarkably progressed.

Image analysis, called seismic wave tomography, which utilizes large-scale computers to analyze data collected from seismometers placed worldwide, has become very popular. Seismic wave tomography has revealed the state of the subducted plates directly under the Japanese islands, which exist near the mantle transition zone. However, because the seismic wave velocity of the mantle transition zone and that of each plate material are unknown, seismic wave analyses could not identify specific rocks (minerals).

A research group at Ehime University, Japan and JASRI developed techniques to measure seismic wave velocities using elastic waves. They successfully carried out experiments in the mantle transition zone at a depth of 660 km. They measured the elastic wave velocities, and revealed that a major component of the mantle transition zone is olivine. Moreover, they discovered that a form of olivine, which is termed harzburgite, is a major material of the plate in the loweret region of the mantle transition zone at depth of 660 km. Their result that harzburgite stalls at depth of ~660 km due to its relatively low density is consistent with the result from seismic wave tomography. Their research results were published in *Nature* (February 2008).

Additionally, high-pressure earth science research that integrates high-pressure, high-temperature experimental technologies and synchrotron radiation technologies has been steadily advancing. Technology developed at SPring-8 will continue to lead the world in the high-pressure earth science research.

[1] Kirkpatrick and Baez mirrors can provide a highly efficient and energy-tunable focusing of X-rays.

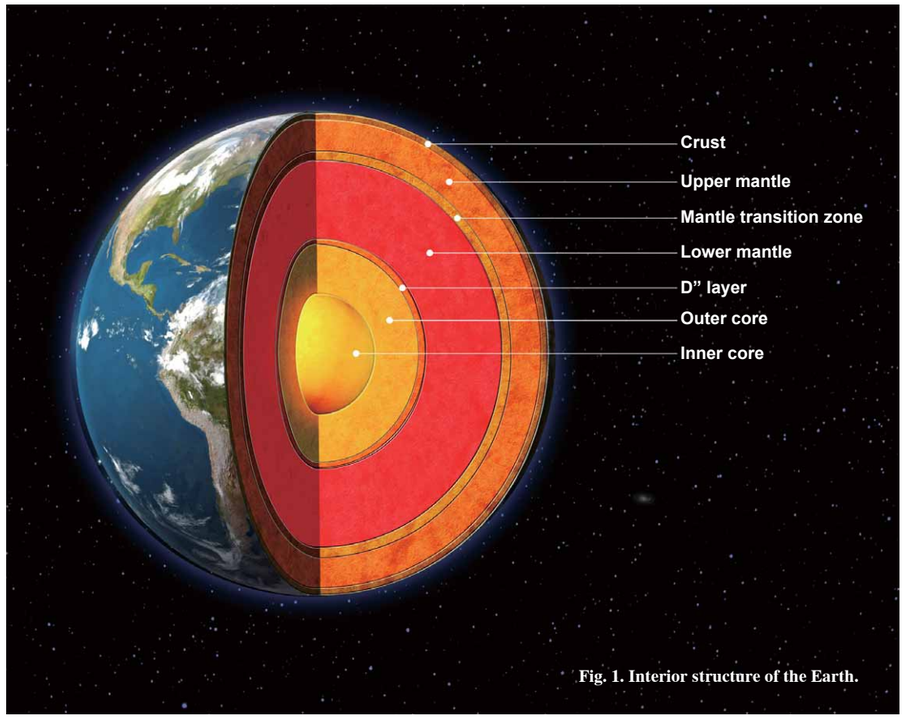

Fig. 1. Interior structure of the Earth.

Reproducing Earth's Deep Interior Conditions to Unravel its Structure

The structure of Earth's deep interior can only be explored by measuring seismic waves or conducting laboratory experiments that reproduce conditions similar to Earth's deep interior. However, a boundary layer region between the mantle and outer core, which exists 2,900 km underground, is at extraordinarily high pressure (>125 GPa: GPa = 10^9 Pa = ~10,000 atoms) and temperature (>2,200 °C) conditions, which are beyond imagination. Thus, reproducing such conditions has been extremely difficult. However, this all changed when these conditions were reproduced at the High Pressure Research Beamline (BL10XU) at SPring-8. Now researchers can determine whether an undiscovered mineral exists in Earth's deep interior. This remarkable discovery is invaluable in understanding the structure of Earth's deep interior, and has drawn worldwide attention as an achievement that can greatly advance mankind's understanding of volcanic activities.

Revealing the "Mystery of the D" Layer" using Ultra-High Pressure, Ultra-High Temperature Conditions

The Earth (~6,400 km in radius) is covered by a thin crust that is only several tens of kilometers thick. Underneath this crust is a mantle, which is 2,900 km thick and occupies about 83% of the Earth's volume. The mantle is a lithosphere with a layered structure comprised of the upper mantle, transition zone, lower mantle, and the D" (D double prime) layer (Fig. 1). Beneath the mantle is the outer core, which consists mostly of liquid iron, while the inner core at the center of the Earth is composed of solid iron.

Information about Earth's deep interior has been extracted from the analyses of data obtained from internal seismic waves. Additionally, research on the physicochemical properties of major minerals in the Earth has been conducted. However, because the minerals deep inside the Earth cannot be directly observed, the only feasible method is to conduct laboratory experiments that reproduce conditions equivalent to those found in Earth's deep interior. The major obstacle is the fact that Earth's deep interior is under ultra-high pressure, ultra-high temperature conditions. In particular, the D" layer, which is the lowest layer of the mantle, reaches more than 125 GPa and 2,200 °C, and artificially reproducing such ultra-high pressure, ultra-high temperature conditions is itself technically difficult.

The principal mineral of the D" layer had been tentatively assumed to be $MgSiO_3$ in the perovskite phase, which is a compound of magnesium and silicate, but this assumption has yet to be validated. In the D" layer, the observed velocities of seismic waves vary drastically, and the seismic polarization anisotropy where the velocity depends on the direction of vibration, is significant. Therefore, the distribution of the perovskite is likely non-uniform. Based on existing data, a large part of the lower mantle is occupied by minerals whose main component is $MgSiO_3$; however, the discontinuity and anisotropy of the velocities of the seismic waves passing through the D" layer cannot be explained if this is the case.

To unravel the mystery of the D" layer, Dr. Kei Hirose[1] (Associate Professor, Tokyo Institute of Technology, Japan) in collaboration with researchers at SPring-8 officially began to conduct research on the D" layer in 2000.

Discovering Minerals Hidden in Earth's Deep Interior

The biggest challenge in this research is reproducing the ultra-high pressure, ultra-high temperature conditions of the D" layer in a laboratory. "To achieve these conditions, we had to develop the necessary technologies one by one, which was really time-consuming," recalls Dr. Hirose. Dr. Hirose and colleagues initially prepared two brilliant-cut diamonds. These two diamonds were placed face-to-face at their tips, and $MgSiO_3$ was inserted between the tips (Fig. 2). Then $MgSiO_3$ was compressed by squeezing these diamonds while exposing this setup to laser irradiation. This experimental system is a laser-heated diamond anvil cell high-pressure generator, and allows researchers to reproduce extremely high-pressure, high-temperature conditions of more than 125 GPa and 2,200 °C, which are impossible with previous techniques.

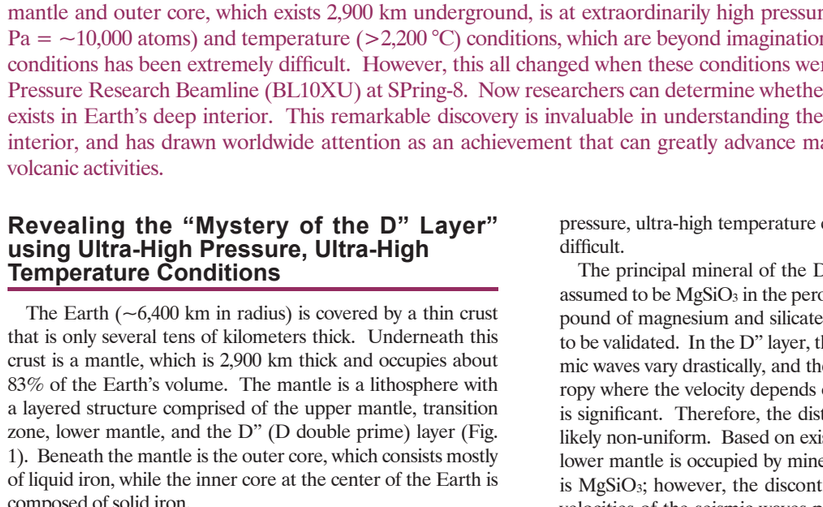

Fig. 1. Layered structure of Earth's interior.
The lower mantle and D" layer were once believed to be comprised of perovskite. However, the existence of post-perovskite in the D" layer found in this research has changed that perception.

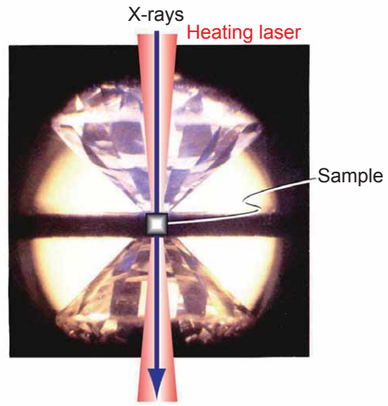

Fig. 2. Crystal structure analyses using X-rays under ultra-high pressure, ultra-high temperature conditions.
Crystal structure analyses using extremely luminous X-rays were conducted on $MgSiO_3$ samples, which were sandwiched and pressurized by diamonds and heated by laser.

Their research group installed this laser-heated diamond anvil cell high-pressure generator in BL10XU at Spring-8, and measured the intensity distributions of the scattering and diffraction of X-rays irradiated onto $MgSiO_3$ crystals as the pressure and temperature was increased. The BL10XU can produce 10^8 times more brilliant X-rays compared to conventional X-ray sources. Such extremely bright X-rays can be utilized to extract sufficient information about the structures and properties from a tiny sample crystal placed in a laser-heated diamond anvil cell.

The information extracted from the pressurized and heated crystal provides data about the phase transition properties, such as the structural changes of $MgSiO_3$ that occur deep within the Earth. In this way, the condition (>125 GPa and >2,200 °C) of the D" layer, which is a boundary between the core and mantle, was reproduced at the BL10XU. Their research revealed that the structure of $MgSiO_3$ under these extreme conditions completely differs from that of perovskite, and they called this new material $MgSiO_3$ "post-perovskite" (Fig. 3). In December 2002, they discovered a new material hidden in Earth's deep interior. Their achievement was published in *Science* (May 2004) and the crystal structure of $MgSiO_3$ post-perovskite appeared on its cover.

Consistently Explaining Both the Discontinuity and Anisotropy of Seismic Waves

The discovery of this new phase of $MgSiO_3$ led to many new questions. Thus, Dr. Hirose's group then focused on examining the elasticity tensor of the $MgSiO_3$ post-perovskite phase. An elasticity tensor is a set of proportional constants that represent the magnitude of stresses when a mineral is deformed. Additionally, the elasticity tensor is an index of the hardness of a mineral and determines the velocity of seismic waves. However, existing technologies cannot measure the tensor under such ultra-high pressure conditions. To overcome this difficulty, Dr. Toshiaki Iitaka (Scientist, the Computational Astrophysics Laboratory, RIKEN, Japan) and colleagues performed large-scale first-principle electron state calculations using supercomputers based on the experimental results obtained at SPring-8 to determine the elasticity tensors of perovskite and post-perovskite. They revealed that the discontinuity and anisotropy of the seismic waves at the boundary between the core and mantle can be consistently explained if the existence of post-perovskite is assumed. Their finding also demonstrated that post-perovskite exists in the lower part of the D" layer, and was published in *Nature* (July 22, 2004). Their accomplishment was featured in two prestigious academic journals, *Nature* (UK) and *Science* (US).

Upon discovering post-perovskite, the seismic wave structure model of the D" layer, a boundary layer of the mantle convection, has been refined. If the actual state of mantle convection, especially the generation mechanism of mantle upwelling (hot plume) from the bottom of the mantle, is revealed based on this refinement, then the mechanisms of large-scale volcanic activities due to heat transportation from Earth's deep interior toward the surface as well as Earth's environmental changes induced by such volcanic activities can be examined.

These research achievements in the D" layer and post-perovskite have significantly contributed to the development of earth science, and Dr. Hirose received the IBM Japan Science Prize in 2007 for his contributions.

[1] Currently Professor at the Department of Earth and Planetary Science, Graduate School of Engineering, Tokyo Institute of Technology, Japan.

References
1. M. Murakami, K. Hirose, K. Kawamura, N. Sata and Y. Ohishi; *Science*, **304**, 855 (2004)
2. T. Iitaka, K. Hirose, K. Kawamura and M. Murakami; *Nature*, **430**, 442 (2004)

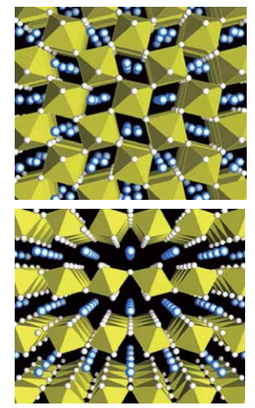

Fig. 3. Schematic representation of the unit cell structures of (a) $MgSiO_3$ perovskite and (b) $MgSiO_3$ post-perovskite.
Light blue balls represent Mg^{2+} ions. Each silicon atom is situated at the center of an octahedron and each oxygen atom is at a vertex.

Experimentally Measuring the Seismic Velocity in the Deep Mantle

Earth, whose radius is ~6,400 km, is covered by a thin crust. Beneath this crust is a 2,900 km thick lithosphere, called the mantle. The mantle has two seismic discontinuities at depths of 410 and 660 km where the seismic wave velocities and densities suddenly increase. The debate about the principal mineral of the mantle transition zone sandwiched by these two seismic discontinuities remains controversial. To resolve this dispute, high-pressure, high-temperature conditions equivalent to the transition zone must be reproduced. Then the velocities of these experimentally produced seismic waves (elastic waves) must be compared to actual seismic waves (elastic waves) measured on the ground. Recently researchers have successfully reproduced conditions equivalent to Earth's deep interior using a large-scale high-pressure generator at SPring-8, and they identified a principal mineral in the transition zone as well as obtained valuable clues about the lower transition zone.

Debate—Olivine or Carbuncle?

The mantle, which occupies 83% of the Earth's volume, is divided into the upper mantle, mantle transition zone, and lower mantle by two seismic discontinuities (Fig. 3). Although the principal minerals of the upper mantle are magnesium/iron silicate minerals, also called olivine, which is a sort of gem commonly known as peridot, there are various models for these minerals in the mantle transition zone. The two most prevalent models are: (1) olivine is the principal mineral of the mantle transition zone and (2) carbuncle is the principal mineral of the mantle transition zone. Carbuncle is a mineral composed of various elements, including calcium, magnesium, and iron, and is a sort of gem known as garnet. A special type of carbuncle created under high pressure is called majorite. The debate over these two models has raged for the last 20 years without reaching a consensus.

Seismic waves such as P-waves and S-waves, which can be observed on the ground, are clues about the conditions in Earth's interior. Depth-dependent propagation velocities of seismic waves have been determined with a high degree of accuracy. Therefore, by assuming candidate minerals in Earth's interior based on the data obtained from seismic waves and measuring seismic velocities (elastic wave velocities) of these candidates, the best candidate minerals can be determined. Because the mantle transition zone is at a pressure of 20 GPa (GPa = 10^9 Pa = ~10,000 atm), ground experiments are difficult. Thus, the best candidate, olivine or carbuncle, remained unclear until recently.

Revealing the Principal Mineral in the Mantle Transition Zone

In April 2005, Dr. Tetsuo Irifune (Professor, the Geodynamics Research Center, Ehime University, Japan), Dr. Yuji Higo[1] (Researcher, *ditto*), Dr. Toru Inoue (Associate Professor, *ditto*), Dr. Yoshio Kono (Researcher, *ditto*), Dr. Hiroaki Ofuji (Assistant Professor, *ditto*), Dr. Ken-ichi Funakoshi (Associate Senior Scientist, JASRI), and colleagues initiated research to end the debate.

It is important to experimentally reproduce the conditions equivalent to the mantle transition zone on the ground. Examples of high-pressure phases where the materials with identical compositions exhibit different properties under high-pressure conditions, such as carbon becomes diamond at ~5 GPa, are commonly reported. The high-pressure phase of olivine is ringwoodite, while that of carbuncle is majorite. Dr. Irifune and colleagues succeeded in *in situ* X-ray measurements of minerals at pressures exceeding 20 GPa using the High Temperature and High Pressure Research Beamline (BL04B1) at SPring-8. They published their initial research results in *Science* (1998).

To examine materials in the mantle, the seismic velocities should also be measured under high-pressure, high-temperature conditions. Although the State University of New York (SUNY), USA is a global leader in measurement techniques of such seismic velocities, their highest measurement pressure was limited to ~10 GPa. Thus, Dr. Irifune and colleagues combined their pressure generating techniques with SUNY's

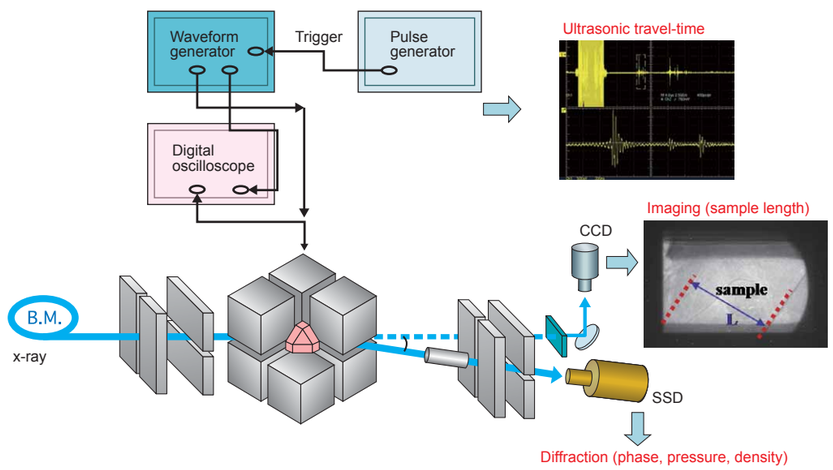

Fig. 1. Measurement systems at the High Temperature and High Pressure Research Beamline (BL04B1).
Propagation velocities of seismic waves (elastic waves) were measured using small samples that were pressurized and heated. Variations in sample lengths were also determined by simultaneously irradiating ultrasounds onto the samples.

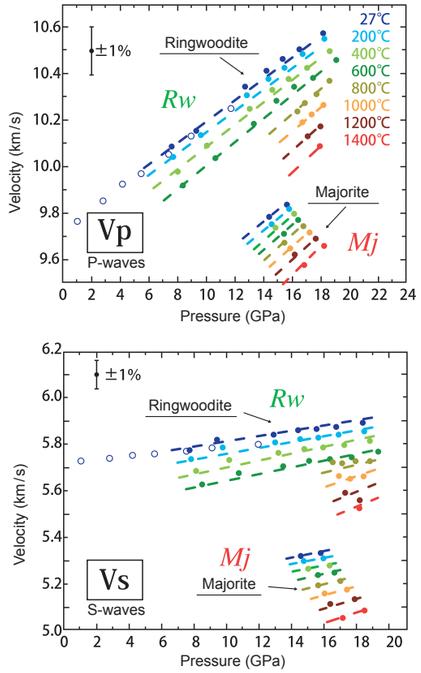

Fig. 2. Pressure and temperature dependent variations in the elastic wave velocities of ringwoodite olivine (Rw) and majorite carbuncle (Mj).
Elastic wave velocities of both minerals increase with pressure or temperature. However, majorite has smaller velocities than ringwoodite.

techniques and realized measurements under higher pressure conditions. Dr. Irifune explains the experimental procedure, "We irradiated ultrasounds possessing the same properties as a seismic wave onto ~2 mm sample, and measured the transit time of the ultrasounds through the sample. Additionally, we precisely measured the sample length upon irradiation with ultra-highly brilliant X-rays at SPring-8" (Fig. 1).

Their research group was the first to successfully determine the seismic wave velocities in ringwoodite and majorite under conditions at up to ~20 GPa and 1,400 °C, which are equivalent to those in the mantle transition zone (Fig. 2). Comparing their experimental results to seismologically obtained velocity data revealed that the principal mineral of the mantle transition zone is olivine. Thus, the carbuncle models were rejected.

However, one question, which even the olivine models could not explain, remained about the properties of seismic waves from the lower part of the mantle transition zone. Thus, their research group further examined the data obtained at SPring-8, and found that harzburgite, which is a form of olivine known as orthopyroxene peridotite, is the best mineral to explain the seismic velocities in the lower part of the transition zone immediately above the 660 km deep seismic discontinuities.

Are "Plate Graveyards" Possible?

Understanding that harzburgite is the principal mineral in the lower part of the mantle transition zone immediately above the 660 km seismic discontinuity has important implications that go beyond identifying the principal mineral. This knowledge suggests "plate graveyards" exists.

Harzburgite is the principal material of subducted plates, and stagnant slabs exist near subducted plates at a depth of ~660 km (e.g., directly under the Japanese islands). These stagnant slabs are thought to sink down into the lower mantle when they reach a certain size. By combining this understanding with the recent understanding that harzburgite is the principal mineral of the lower part of the transition zone, it is possible that stagnant slabs exist in the form of layers from a few tens of km to ~100 km depths across the entire globe. This is the area where subducted plates spread, and is called "plate graveyards" (Fig. 3).

Several models have been proposed to explain plate movements. Similar to flushing a toilet, in flushing models, plates sink down in the lower mantle and induce cataclysmic crustal movements when plates reach a depth of 660 km. In contrast, the giant hot plume models postulate a synchronized action where hot materials, which correspond to the mass of sinking cold plates, move up from the boundary between the mantle and core as the plates sinks. However, if plate graveyards broadly exist, many plates should remain in the ~600 km region. In other words, unlike the Japanese popular novel *Nippon Chinbotsu* (*Japan Sinks*), cataclysmic crustal movements due to the sudden sinking of plates would not occur. Their research achievements were published in *Nature* (February 2008), and received international attention.

Currently, their research group is developing new technologies to measure seismic velocities under conditions exceeding 25 GPa to explore materials in even deeper parts of the lower mantle as well as to measure the seismic velocities of oceanic crustal materials, which are other types of constituent materials of the plates. Moreover, they plan to conduct further research to confirm the existence of plate graveyards and to explore the possibility of flushing. Accumulation of data from these measurements will gradually, but steadily, elucidate the structures and dynamics of Earth's deep interior as well as Earth's evolution and creation processes.

[1] Currently Research Scientist at Japan Synchrotron Radiation Research Institute (JASRI).

References
1. T. Irifune, N. Nishiyama, K. Kuroda, T. Inoue, M. Isshiki, W. Utsumi, K. Funakoshi, S. Urakawa, T. Uchida, T. Katsura and O. Ohtaka; *Science*, **279**, 1698 (1998)
2. T. Irifune, Y. Higo, T. Inoue, Y. Kono, H. Ohfuji and K. Funakoshi; *Nature*, **451**, 814 (2008)

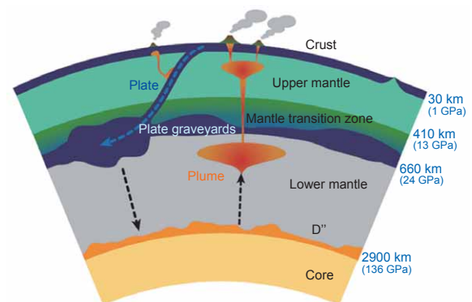

Fig. 3. Mantle structure and plate movements.
This research revealed that similar to the upper mantle, the mantle transition zone is mainly comprised of olivine. Additionally, it suggests the existence of "plate graveyards" under the mantle transition zone.

Discovering the Principal Minerals Hidden within the Cores of Ice Giants

Uranus and Neptune are called ice giants because their major constituent is ice. However, the cores of these ice giants are composed of rocks and metals, and their compositions were once believed to be similar to the solid part of the Earth. Unfortunately, only the average density of the entire planet can be observed, and the core's condition in an ice giant is unknown. However, the realization of ultra-high pressure conditions of 300 GPa (GPa = 10^9 Pa = ~10,000 atm) at the High Pressure Research Beamline (BL10XU) at SPring-8 has uncovered another candidate for the core of an ice giant, silicon dioxide (SiO_2). The ultra-high pressure conditions have revealed structural variations in SiO_2, leading to the discovery that a new mineral may exist deep within ice giants.

Examining Phase Transitions of Silica at a Pressure of 300 GPa

Terrestrial planets such as Mercury, Venus, and Mars have cores composed of metals such as iron and are surrounded by a mantle. The mantle, which is comprised of various minerals, is covered by a thin layer of rock, called the crust. In contrast, the mantle of ice giants such as Uranus and Neptune are composed of ice, whose main element is water. However, ice giants have cores composed of solid elements, which are similar to the mantle and crust of the terrestrial planets, but the core of an ice giant is believed to be much denser than the solid elements in terrestrial planets, including Earth.

The mantles and crusts of the terrestrial planets and the cores of Jovian planets (gas-giant planets) are composed of various minerals, whereas the principal mineral in the cores of ice giants is speculated to be silicon oxide (SiO_2). Silicon is the 7th most abundant element in the universe. Thus, SiO_2 is an important component of the solar system. SiO_2 is generally called silica and is in a crystalline form, termed quartz[1], under normal conditions.

However, placing silica under high-pressure, high-temperature conditions changes its structural state (phase) but not its composition (SiO_2). A structural change without altering the composition is called a phase transition. A good example of the phase transition is freezing water to make ice or pressuring graphite, which consists of carbon, at 5 GPa converts it to diamond.

The High Pressure Beamline (BL10XU) at SPring-8, which provides the world's highest pressure and temperature conditions, was further upgraded in Spring 2005. The maximum pressure was increased from 220 GPa at 2,200 °C to 300 GPa at 2,000 °C. Dr. Kei Hirose[2] (Associate Professor, Tokyo Institute of Technology (Tokyo Tech), Japan) and colleagues at the Japan Synchrotron Radiation Research Institute began experiments to study the phase transitions of silica under the high-pressure, high-temperature conditions available at the upgraded BL10XU.

Extracting Information from Small Sample Quantities using Highly Brilliant X-rays

Prior to their experiments at the upgraded BL10XU, a research group at Tokyo Tech and IFREE led by Dr. Hirose discovered in 2004 that $MgSiO_3$ post-perovskite is a principal mineral of the D" (D double-prime) layer, which is a boundary region (depth of 2,700–2,900 km) between the lower mantle and outer core (see Topic 21 for more details). This achievement was realized using the extraordinarily high pressure (125 GPa), high temperature (>2,200 °C) conditions only available at BL10XU beamline of SPring-8. "Elucidation of the phase transition of silicon, which is an abundant mineral in the universe and solar system, would be an invaluable clue in exploring the deep structures of planets other than the Earth, especially ice giants," Dr. Hirose explains the aim of their observation experiments on the phase transition of silica under the extraordinary high-pressure, high-temperature conditions.

To further pursue these studies, a laser-heated diamond anvil cell high-pressure generator was developed (Fig. 1). A crystalline silica sample was held in the gap between two diamonds placed face-to-face at their tips. Then this configuration was compressed by squeezing these diamonds while heating with

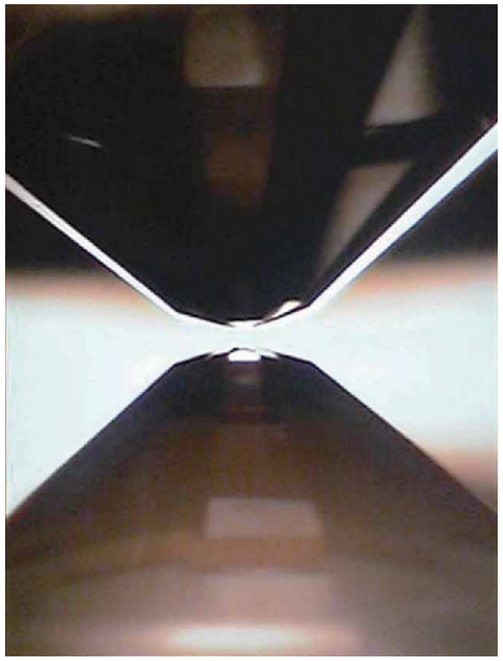

Fig. 1. Pressurization of a sample using a laser-heated diamond anvil cell high-pressure generator.
Crystalline silica sample is held in a gap between two brilliant-cut diamonds, which is subsequently compressed by squeezing these two diamonds and heating with an irradiating laser. Gap is only 5 μm.

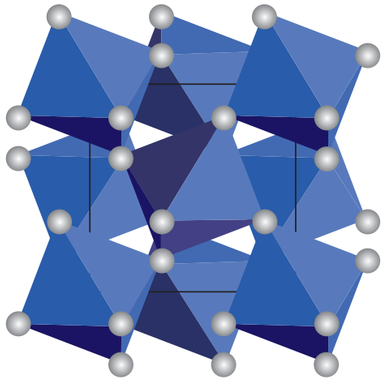

Fig. 2. Crystal structure of pyrite-type silicon dioxide (SiO_2).
White circles represent oxygen. Silicon atoms are situated at the centers of octahedrons indicated by the blue color.

laser irradiation. This system realized a pressure of 300 GPa and 2,000 °C. However, this powerful system has a drawback: the sample size is limited. To realize such extraordinary high-pressure conditions that exceed 200 GPa, the current limit of the gap between these two diamonds is 10 μm (μm = 10^{-6} m) and the sample must be less than half that of the gap. The scattering and diffraction intensities of X-rays irradiated onto such a small sample are very weak, which significantly limits the information that can be obtained. Fortunately, the capabilities of SPring-8 can overcome this drawback. "The highly brilliant X-rays obtained at BL10XU of SPring-8, which are 10^8 times brighter than those obtained from existing conventional X-ray sources, finally allowed us to obtain useful data," says Dr. Hirose.

Is Silica a Major Element in the Cores of Uranus and Neptune?

Dr. Hirose and colleagues measured the X-ray diffraction of pressurized silica. When the applied pressure exceeded 270 GPa, the hexagonal cylinder-shaped crystal structure changed into a dice-shaped structure. "We concluded this is a new pyrite-type mineral," explains Dr. Hirose. This new mineral is called a pyrite-type because it resembles a golden, dice-shaped pyrite crystal composed of iron disulfide (FeS_2). Thus, Dr. Hirose and colleagues successfully converted silica into an unknown form under the ultra-high pressure, ultra-high temperature conditions available at SPring-8.

More interestingly, this new mineral is much denser than other known silica minerals. In fact, the existence of pyrite-type silica was theoretically predicted in the 1980s by several research groups, including some Japanese groups, but it was not discovered until the ultra-high pressure conditions were realized at SPring-8. Pyrite-type silica, which is more than twice as dense as a quartz crystal at ordinary temperature and pressure, was predicted to be a metal, but is not. A pressure level of 270 GPa corresponds to the outer core of the Earth. Because iron is the major component of Earth's outer core, this new mineral does not naturally exist on Earth. Their research achievement was published in *Science* (August 2005), and received worldwide attention from planetary scientists.

"However, the cores of ice giants such as Uranus and Neptune may be composed of this pyrite-type silica," speculates Dr. Hirose. This research provides an important clue in solving the mystery of ice giants because actual measurements cannot be performed using existing technologies.

[1] Colorless and transparent quartz is typically called quartz crystal, which is valuable as a gem.
[2] Currently Professor at Tokyo Institute of Technology and is affiliated with the Institute for Research on Earth Evolution (IFREE), Japan Agency for Marine-Earth Science and Technology.

Reference
1. Y. Kuwayama, K. Hirose, N. Sata and Y. Ohishi; *Science*, **309**, 923 (2005)

Fig. 3. Quartz crystal and pyrite crystal.
Quartz crystals are hexagonal cylinder-shaped, whereas pyrite crystals are dice-shaped.

Microscopically Exploring the Basis of Human Survival

Making the Impossible Possible with Highly Brilliant, Highly Collimated, and Wavelength Tunable Synchrotron Radiation

In today's world almost everything consumes energy, and modern society is under immense pressure to actively reduce mankind's impact on the environment. Many challenges in materials science are directly linked to daily life, including the development of new energy storage systems that are alternatives to fossil fuels and the detoxification of toxic substances. However, these advances cannot be achieved in a day as scientific innovation is a process, which begins by understanding the phenomena that occur around us and building upon this knowledge.

Take dry cell batteries for example. To increase the capacity of manganese dry cells, alkaline dry cells, which are primary cells (single use), were developed. Over time, secondary cells (reusable by charging) became necessary, which led to the development of lithium-ion secondary cells. Today in the quest for the next generation of batteries, scientists strive to resolve current issues, including the development of shape-changeable dry cells using all solid batteries and polymers.

Behind every breakthrough are seeds to adequately meet society's needs. In materials research, one extraordinary seed is synchrotron radiation (or X-rays in the broad sense). This field investigates the structure of materials and their constituent elements to provide insight into the mechanisms of common everyday chemical reactions. Synchrotron radiation is a means to answer the questions such as: "What is this material?", "How is this material formed?", and "How can we examine this material?" Figure 1 shows several examples of the interactions between synchrotron radiation and materials.

The strength of synchrotron radiation is not that it creates new materials, but it is capable of probing the states of materials, and the gained knowledge can lead to innovations in materials science. Specifically, materials research uses synchrotron radiation experimental techniques in: 1) crystal structure analysis to elucidate the structures of materials, 2) X-ray absorption fine structure to clarify the chemical states and local structures of elements contained in materials, and 3) X-ray fluorescence analysis to examine the species and quantities of elements constituting materials. Although these techniques have been used with standard laboratory light sources for many years, combining them with synchrotron radiation has provided superior analyzing capabilities.

Synchrotron radiation at SPring-8 is highly brilliant, highly collimated, wavelength-tunable, and exhibits pulsing properties. These features lead to the following advantages, which cannot be realized in conventional laboratories. 1) Measurement time is significantly reduced (on the order of days to several minutes). 2) The appropriate wavelength (energy) can be selected. 3) Time-resolving measurements on the millisecond order are realized. 4) 2D analysis on the submicron order is possible.

Challenging the Limits of Nanobeam Technology

Focused nanobeams are expected to be a basic technology of synchrotron radiation, and should be indispensable in the study of nanoporous materials (Topic 24), battery materials (Topic 25), dioxin generation mechanisms (Topic 26), and decontamination mechanisms of heavy-metal contaminated soil (Topic 27). Previously most of these types of studies have been conducted using so-called "bulk" beams, but the obtained information is insufficient to provide details about the targets. Recent research has revealed that the reaction field, which determines the properties of materials, is in an extremely small region. Thus, to understand phenomena more accurately, the incorporation of nanobeam technology into these studies should be the key to success.

Thus, both synchrotron radiation and the development of light-focusing elements for X-rays have been advanced. Although there are several types of focusing elements, those best suited for the abovementioned experimental techniques in materials research have been developed based on total reflection mirrors and Fresnel diffraction. These elements themselves have been available since the 1950s, but applications to microbeams have only been available since the 1990s when second-generation synchrotron radiation facilities were realized. Second-generation synchrotron radiation sources such as those available at the Photon Factory at the High Energy Accelerator Research Organization in Tsukuba, Japan demonstrated that synchrotron radiation beams could be focused to 1 μm at 8.5 keV using a system that combines two total reflection mirrors, and could be further focused to 0.5 μm at 8.54 keV using diffraction-type mirrors called Fresnel zone plates. However, producing brilliant X-rays suitable for research requiring microbeams is difficult using second-generation synchrotron radiation facilities because the beam size (or spatial resolution) and brilliance of the focused X-rays conflict.

Fortunately, third-generation light sources such as those obtained at SPring-8 have resolved this issue. Third-generation light sources provide highly brilliant focused beams with a beam size on the nanometer order (nm = 10^{-9} m). Representative beam sizes are currently 30 nm at 15 keV using total reflection mirrors and 31 nm at 8 keV using Fresnel zone plates. Figure 2 summarizes the history behind the reduction of focused beam size. With the development of new light sources such as X-ray free electron laser (XFEL), it is expected that the limits of nanobeams will be challenged, which will consequently trigger new efforts in materials research.

In addition to attempts to develop focusing elements, some focusing technologies, which are in the high-energy X-ray regime, can only be pursued at SPring-8. For example, beam sizes of 0.4 μm at 80 keV have been realized using total reflection mirrors and 0.5 μm at 100 keV using Fresnel zone plates. Such microbeams utilized in the high-energy X-ray regime can effectively detect heavy metals (such as cadmium, uranium, antimony, and iodine), and due to recent attention, microbeams are receiving a growing interest from the viewpoint of materials research. For example, researchers have recently applied microbeams to analyze cadmium-accumulating plants using scanning microscopes as reported in Topic 27.

The new synchrotron light sources at SPring-8 have made extremely small beam sizes, which were a dream ten years ago, a reality. Based on the current pace of progress in research and technology, materials research using nanobeams should gain significant momentum in the not-so-distant future. For example, the chemical states within a few tens of nm of the surface layers of a single catalyst particle with a diameter of a few hundreds of nm and the distributions of metals in subcellular organelles (such as microsome and mitochondria) are both expected to be elucidated in the immediate future. Encouraged by the research projects introduced in this SPring-8 Scientific Achievements, materials research should advance into a new phase.

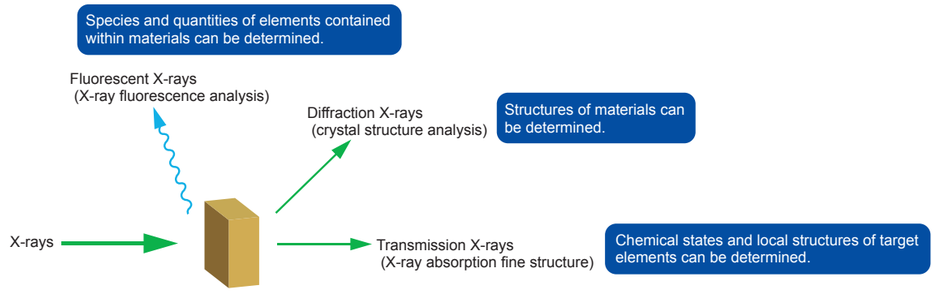

Fig. 1. Interactions between X-rays and materials.

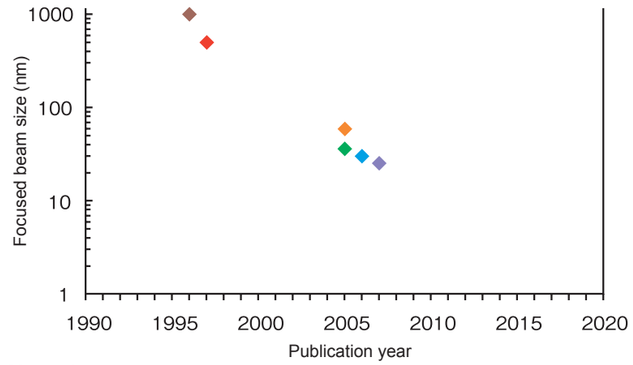

Fig. 2. History of focused beam size.

Unveiling the Secrets of Porous Coordination Polymers that Actively Adsorb Gases

Activated carbon, which has numerous small holes (nanopores) on its surface, is commonly used for deodorization and water purification due to its high capacity to absorb organic matter. Materials with such pores are collectively referred to as nanoporous materials. In particular, porous coordination polymers, which are synthesized from metal ions and organic molecules, have recently attracted increased attention. The advantages of porous coordination polymers are they can store various gases, including hydrogen, at a high density and various functions can be implemented. At SPring-8, researchers have been leading the world to elucidate the mechanisms by which the nanopores of porous coordination polymers adsorb gases. This topic presents examples of these remarkable accomplishments as well as research outcomes on hydrogen storage alloys.

Designing Nanoporous Materials with Desired Functions

In February 2002, a group led by Dr. Susumu Kitagawa (Professor, Kyoto University, Japan) initiated research on orderly adsorbing oxygen with nanoporous materials. This project was developed in collaboration with Dr. Masaki Takata[1] (Associate Professor, Nagoya University, Japan), Dr. Tatsuo Kobayashi (Professor, Osaka University, Japan), and Dr. Makoto Sakata[2] (Professor, Nagoya University). These nanoporous materials, which are porous coordination polymers composed of metal ions, such as copper and cobalt, and organic molecules, are capable of storing various gases at room temperature. Moreover, the area of several grams of nanoporous materials has a surface area equivalent to a basketball court or in some cases a soccer field. "We strived to demonstrate that nanoporous materials can be fully controlled to store gases," says Dr. Kitagawa.

They examined a copper coordination polymer (CPL-1) because the pores of CPL-1 are 0.4 × 0.6 nm (nm = 10^{-9} m) in size and adsorb oxygen. Synchrotron radiation diffraction experiments on CPL-1 powders cooled to −183 °C were conducted at the Power Diffraction Beamline (BL02B2). Analyses of the diffraction patterns, which indicate the adsorption of oxygen molecules, using the data processing algorithm developed by the Nagoya University group revealed that the oxygen molecules in solid-like aggregation states are perfectly aligned in the pores. Additionally, they found that oxygen molecules aligned in a double line parallel to the direction of the pores form a ladder structure with a minimum intermolecular distance of ~0.32 nm (Fig. 1). Their new findings were published in *Science* (December 2002).

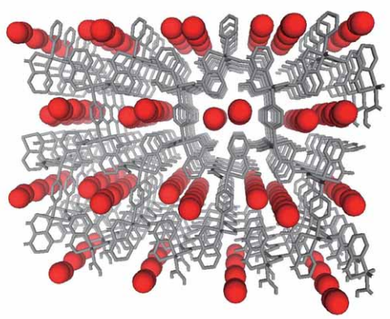

Fig. 1. Structure model of a copper coordination polymer, CPL-1.
Oxygen molecules (red) are regularly aligned in the pores formed in CPL-1.

Anticipating High Hydrogen Adsorption Capacity for Fuel Cells

If hydrogen is stored in porous coordination polymers, which are easily designed and synthesized, then porous polymers should be applicable to fuel cells. In April 2003, Dr. Kitagawa in collaboration with Dr. Yoshiki Kubota[3] (Associate Professor, Osaka Women's University, Japan), Dr. Masaki Takata[4] (Chief Scientist, the Japan Synchrotron Radiation Research Institute), and colleagues, conducted experiments to directly observe hydrogen molecules by adsorbing them into the pores of CPL-1, which was previously used in an oxygen adsorption experiment. Observing a hydrogen atom, which has only one electron, with X-rays is typically extremely difficult. "Understanding the behavior of hydrogen molecules is necessary to synthesize nanoporous materials," explains Dr. Kitagawa.

Although powder X-ray diffraction experiments were conducted at the Powder Diffraction Beamline (BL02B2), the amount of obtained data was very limited. To overcome this, Dr. Takata developed a new technique to effectively extract the electron density distributions from a small amount of data. The extracted distributions revealed that hydrogen molecules exist near oxygen atoms bound to copper atoms of porous coordination polymers (Fig. 2). Additionally, the pores have concavo–convex surfaces, and hydrogen molecules fit into the concave regions and move freely. These results suggest that porous coordination polymers may be an ideal molecular storage system if the pores and molecules have similar sizes. Their achievement was published in *Angewandte Chemie International Edition* (January 2005) and an image of their nanoporous material appeared on the front cover.

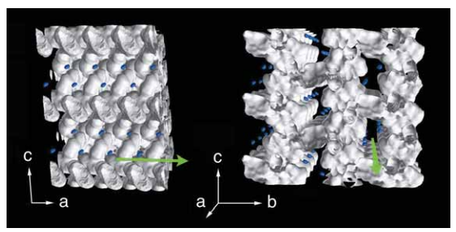

Fig. 2. Electron density distributions of porous coordination polymers where hydrogen molecules are adsorbed.
Blue dots denote hydrogen molecules. Hydrogen molecules are not situated at the center of the pore, but are closer to the pores' walls, and are regularly aligned regardless of the coordination polymer structure.
Yoshiki Kubota, Masaki Takata, Ryotaro Matsuda, Ryo Kitaura, Susumu Kitagawa, Kenichi Kato, Makoto Sakata, Tatsuo C. Kobayashi: Direct Observation of Hydrogen Molecules Adsorbed onto a Microporous Coordination Polymer; *Angewandte Chemie International Edition*; 2004, Vol. **44**, page 922. Copyright Wiley-VCH Verlag GmbH & Co. KGaA. Reproduced with permission.

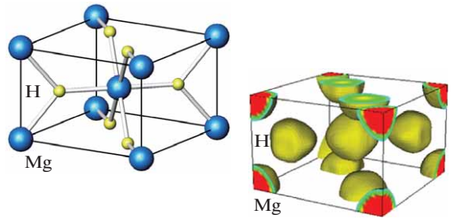

Fig. 3. Crystal structure of MgH_2 (left) and electron equidensity contour surface (right).
Crystal structure of MgH_2 (rutile-type structure) and surfaces of electron density at $\rho = 0.3e/(0.1\ nm)^3$ are depicted. An ionic bond is formed as magnesium and hydrogen become positive and negative ions, respectively.

On the other hand, the most promising material to store hydrogen is a hydrogen storage alloy. In May 2001, Dr. Tatsuo Noritake (Chief Researcher, Toyota Central R&D Labs, Japan), Dr. Makoto Sakata (Professor Emeritus, Nagoya University), and colleagues analyzed the electron density distributions of a hydrogen storage alloy called magnesium hydride (MgH_2). At that time, the amount of stored hydrogen in a hydrogen storage alloy was ~2% by weight, and consequently, the development of light alloys capable of storing more hydrogen was desired. Magnesium is light and has a hydrogen storage capacity of 7.6% by weight. However, MgH_2 must be heated to >300 °C to release hydrogen. Dr. Norikate recalls back on that time, "To overcome this issue, we had to go back to the basics and examine the distribution of electrons responsible for binding in MgH_2."

Their research group conducted experiments on MgH_2 powders by irradiating highly brilliant X-rays at BL02B2, and determined the electron density distributions of hydrogen (Fig. 3). They noted that the number of electrons was peculiar. The magnesium region of MgH_2 forms a sphere with a radius of 0.09 nm, which has 1.91 less electrons and becomes a positive ion, whereas the hydrogen region forms a sphere with a radius of 0.1 nm, which has 0.26 more electrons and become a negative ion. Thus, magnesium and hydrogen are ionically bonded. Moreover, the overall electron density in MgH_2 is very low and metallic bonds did not exist. MgH_2 exhibits a weak covalent bond with overlapping magnesium and hydrogen electrons. "When MgH_2 adsorbs hydrogen, the adsorbed hydrogen atoms become negative by attracting free electrons, and the magnesium atoms are ionically bonded with these hydrogen ions to become stable," explains Dr. Noritake. Their research achievement was published in *Applied Physics Letters* (September 2002).

Revealing the Adsorption States of Acetylene Gases

Dr. Kitagawa and colleagues conducted an experiment at BL02B where they revealed that acetylene gases interact with nanopores very strongly and are densely stored in the pores. Additionally, they determined that the adsorption processes contain several state changes. Their research results were published in *Nature* (July 2005).

"To utilize porous coordination polymers as adsorption materials for highly active gases, the states of the polymers after inserting gas molecules must be further elucidated," explains Dr. Kitagawa. Consequently, Dr. Kitagawa and colleagues conducted experiments to investigate the adsorption processes of acetylene gases by nanoporous materials at BL02B2. In their experiments, copper coordination polymer crystals were loaded into a glass capillary (a very thin glass tube), and acetylene gases were inserted. Powder diffraction data were collected with a large Debye–Scherrer camera with a camera radius of 287 mm. Controlling pressure and temperature allowed diffraction data to be simultaneously detected through the 2D detectors.

They found that acetylene molecules form hydrogen bonds with oxygen atoms in the pore wall in a saturated phase, causing acetylene molecules to absorb into the pore walls with a high density. In contrast, the structure changes in the polymer crystal from an intermediate phase to a saturated phase are small, and the bonds between the acetylene molecules and the pore wall in the intermediate phase are much weaker than those in the saturated phase (Fig. 4). Additionally, after adsorption, the crystal lattices expand to an intermediate phase, and the pores start to deform. Upon reaching the saturated phase, the pores contract. These observations revealed that the copper coordination polymer crystal flexibly changes its structure through the interactions of the acetylene molecules with the pore wall to adsorb acetylene. This achievement was published in *Angewandte Chemie International Edition* (July 2006).

Due to its great potential in many applications (e.g., the low-pressure stable storage of natural gases, adsorption of greenhouse gases, separation of toxic materials, and superconductive or magnetic materials), the development of nanoporous materials is thus highly anticipated.

[1] Currently Chief Scientist at RIKEN.
[2] Currently Professor Emeritus at Nagoya University, Japan.
[3] Currently Associate Professor at Osaka Prefecture University, Japan.
[4] Currently Chief Scientist at RIKEN.

References

1. R. Kitaura, S. Kitagawa, Y. Kubota, T. C. Kobayashi, K. Kindo, Y. Mita, A. Matsuo, M. Kobayashi, H. Chang, T. C. Ozawa, M. Suzuki, M. Sakata and M. Takata; *Science*, 298, 2358 (2002)
2. Y. Kubota, M. Takata, R. Matsuda, R. Kitaura, S. Kitagawa, K. Kato, M. Sakata and T. C. Kobayashi; *Angewandte Chemie International Edition*, **44**, 920 (2004)
3. T. Noritake, M. Aoki, S. Towata, Y. Seno, Y. Hirose, E. Nishibori, M. Takata, and M. Sakata; *Appl. Phys. Lett.*, **81**, 2008 (2002)
4. Y. Kubota, M. Takata, R. Matsuda, R. Kitaura, S. Kitagawa and T. C. Kobayashi; *Angewandte Chemie International Edition*, **45**, 4932 (2006)

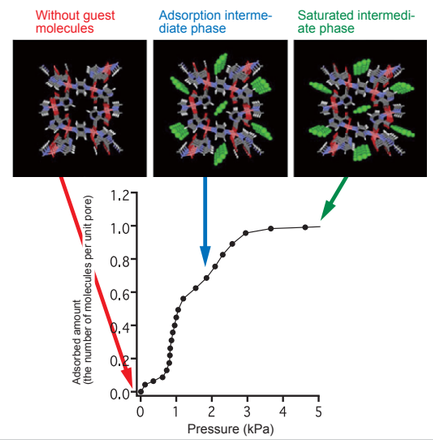

Fig. 4. Adsorption isotherm and crystal structures corresponding to three different adsorbed amounts.
Views from the nanochannel direction. Negligible chemical bonding is observed between acetylene molecules (green) and neighboring oxygen atoms in both sides of the former.

Developing Solar Batteries and Fuel Cells at the Nanolevel

Fossil fuels, including oil, are limited resources, and a lifestyle that fully depends on them cannot last forever. Moreover, there are concerns that the increases in emissions of air pollutants and carbon dioxide could worsen environmental problems. Thus, solar light, wind power, and tidal energy are gaining attention as alternative energy resources, and consequently, the developments of fuel cells have been energetically pursued around the world. The high analyzing power of SPring-8 has consistently produced numerous achievements in fundamental studies to develop various alternative energy resources. In this topic, research achievements realized at SPring-8 on the nanolevel toward new materials for solar batteries as well as elucidating the mechanisms of fuel cells at atomic and electronic levels are reported.

Designing Organic Semiconductors Exhibiting Liquid Crystal Properties

Although a solar battery is an ideal power generating system, its drawbacks include high manufacturing cost and low energy conversion efficiency. Organic semiconductors have been anticipated to overcome these difficulties. Unlike silicon semiconductors, which require expensive and complicated manufacturing processes, organic semiconductors are light and easily manufactured. Thus, there is hope the organic semiconductors will be more affordable. However, obtaining materials with a prominent charge transportation property is difficult.

Dr. Takuzo Aida (Professor, The University of Tokyo, Japan) and colleagues have focused their attention on a fused porphyrin copper complex as a promising candidate as an organic semiconductor. This organic molecule has properties similar to chlorophyll, i.e., it can generate electricity by absorbing a large quantity of light. Many of conductive polymers, which are candidates for organic semiconductors, have a structure where double and single bonds are alternatively arranged. This arrangement is called π-conjugation. Through this structure, the connection between electrons becomes smooth, producing conductivity. A large portion of a fused porphyrin copper complex is occupied by this π-conjugated structure, which is related to its prominent electron transport capability.

However, the hardness of organic semiconductor materials composed of solid crystals makes it difficult to manufacture large-area thin films. On the other hand, soft materials such as liquid crystals have superior manufacturability, but inferior electron transport capabilities. Thus, the development of organic semiconductors that combine high manufacturability and superior electron transport capabilities is demanded. "We were inspired by soap. Soap forms a highly ordered structure from spontaneously hydrophilic and hydrophobic portions," explains Dr. Aida. Dr. Aida and colleagues hypothesized that a fused porphyrin copper complex could maintain a liquid crystalline state though it is organic matter by implementing both hydrophilic and hydrophobic properties so that the complex is simultaneously water-soluble and water-insoluble.

In April 2006, their research group designed a new molecule with an amphipathic property by introducing hydrophilic side chains on one side of a fused porphyrin copper complex molecule and hydrophobic side chains on the other. This complex was initially heated to 120 °C and then cooled to room temperature. As a consequence, this new molecule spontaneously aggregates to form a column shape (cylindrical shape), and exhibits a liquid crystalline state. Compared to other liquid crystal materials, the electron transport speed of this molecule at room temperature is ten times faster.

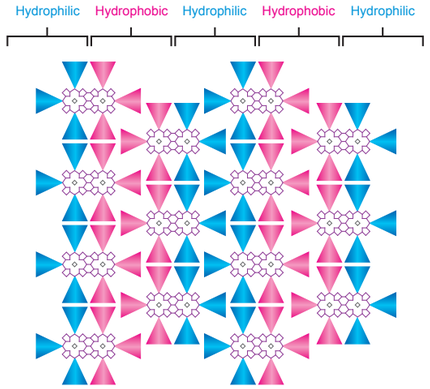

Fig. 1. Schematic representation of the 2D molecular arrangement of an amphipathic molecule.
Cross-view of columns (cylindrical structures) formed perpendicular to the plane. Adding hydrophilic side chains (blue triangles) and hydrophobic side chains (red triangles) implements an amphipathic property in fused porphyrins (purple), and yields a structure that exhibits a high electron transportation capability.

How does this molecule combine a prominent electron transport capability and liquid crystallinity? Dr. Aida speculated that the array structure of this molecule is critical. After he consulted with Dr. Masaki Takata (Chief Scientist, the RIKEN SPring-8 Center, Japan) and Dr. Sono Sasaki (Senior Scientist, the Japan Synchrotron Radiation Research Institute), his research team conducted an experiment using a 2D small angle scattering method at SPring-8. The 2D small angle scattering method irradiates X-rays onto a sample to visualize the nanolevel structures. Their experiment revealed that the hydrophilic and hydrophobic phases are separated by a 3–4 nm gap (nm = 10^{-9} m) (Fig. 1). Thus, integrating a fused porphyrin copper complex into a column shape through the amphipathic property can gain prominent electron transport capability.

This research result is the world's first remarkable accomplishment in this field, and was published in *the Journal of the American Chemical Society* (October 2008), which is the highest-ranked journal in chemistry.

Elucidating Mechanisms of Fuel Cells at the Atomic Level

Commercialization of vehicles powered by hydrogen fuel cells, which produce electricity from hydrogen and emit only water, has been eagerly anticipated. Although many issues must be resolved, including enhancing the cathode electromotive force and preventing catalyst degradation due to elution of platinum (Pt), the most serious hurdle to commercialization is the high cost due to the extensive use of Pt. (Pt is one of the most expensive elements naturally found on Earth.) To overcome this serious issue, Dr. Yasuhiro Iwasawa[1] (Professor, The University of Tokyo, Japan), Dr. Mizuki Tada[2] (Assistant Professor, *ditto*), and researchers from Toyota Motor Corporation, Toyota Central R&D Labs., High Energy Accelerator Research Organization, and Tottori University formed a research team in April 2005.

"A catalyst superior to platinum is currently unavailable for fuel cells. Even platinum, which is expensive and very durable, degrades with use. Thus, the catalyst itself needs to be further developed. Hence, we aimed to elucidate the electrochemical reactions on the surface of the catalyst at the atomic level during fuel cell operations," explains Dr. Tada.

The X-ray absorption fine structure (XAFS) technique analyzes the structures of this size of sample. Upon exposure to X-rays, atoms absorb X-rays and emit electrons (photoelectrons). The wave of the photoelectron emitted from an atom is scattered by neighboring atoms and the waves interfere, causing a specific oscillatory structure, called extended XAFS (EXAFS) oscillation, in the X-ray absorption spectrum. Analyses of such oscillations can provide information about the distance and the number of Pt–Pt and Pt–O bonds. However, each sample takes about ten minutes to measure because each energy point in the XAFS technique is individually measured, and these measurements should be repeated at various energies. Thus, real-time changes in the catalytic reactions could not be followed.

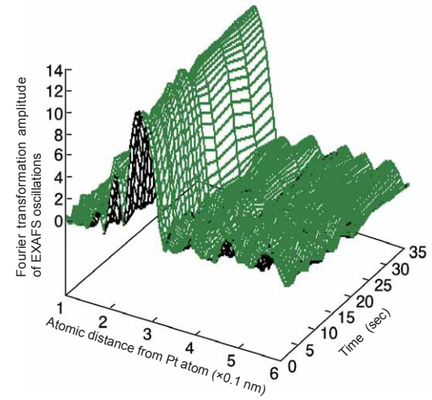

Fig. 2. Structural changes of platinum catalysts as a fuel cell operates.
Structural changes of platinum catalysts per second at one of the absorption edges. This data revealed the number of oxygen bonding to platinum increases with time. Measurements were performed using a time-gating quick X-ray absorption fine structure technique, which was developed in collaboration with SPring-8.

To overcome this difficulty, energy dispersive XAFS (DXAFS) and quick XAFS (QXAFS) techniques have been developed by several research groups. In the former, synchrotron radiation containing X-rays with various wavelengths is focused to irradiate onto a sample and spectrum data are captured in one shot. The latter is a technique that allows real-time measurements of a sample by quickly moving a spectroscope, which disperses X-rays of various wavelengths. Dr. Tada's research group developed a new measurement technique based on QXAFS.

Through their technique and full utilization of highly brilliant X-rays to detect small dynamic movements, they successfully observed the chronological changes in fuel cell catalysts with a 1-sec time resolution. They are the first to observe dynamic oxidation–reduction reactions of cathode platinum nanocatalysts under the actual working conditions of a fuel cell, revealing the reaction mechanisms induced by voltage changes during battery operations occur on the surfaces of cathode catalysts (Fig. 2). A particularly important finding is that when the battery cell voltage exceeds the open-circuit voltage, oxygen atoms begin to enter the platinum catalysts, causing catalyst dissolution (Fig. 3). This incursion of oxygen atoms is thought to be the major cause of deterioration of platinum cathode catalysts.

"By actually observing catalyst reactions using synchrotron radiation, the reaction mechanisms of fuel cells have been elucidated for the first time. This experiment has yielded clues to resolve the deterioration issue of cathode catalysts for the commercialization of fuel cells," explains Dr. Tada. Their research results were published in *Angewandte Chemie* (May 2007), and researchers around the globe are building upon their results to reduce platinum usage in fuel cells and to develop alternative materials.

[1] Currently Professor at the University of Electro-Communications, Japan.
[2] Currently Associate Professor at Institute for Molecular Science, National Institutes of Natural Sciences, Japan.

References

1. T. Sakurai, K. Shi, H. Sato, K. Tashiro, A. Osuka, A. Saeki, S. Seki, S. Tagawa, S. Sasaki, H. Masunaga, K. Osaka, M. Takata and T. Aida; *J. Am. Chem. Soc.*, **130**, 13812 (2008)
2. M. Tada, S. Murata , T. Asakoka , K. Hiroshima , K. Okumura, H. Tanida, T. Uruga, H. Nakanishi, S. Matsumoto, Y. Inada, M. Nomura and Y. Iwasawa; *Angewandte Chemie*, **119**, 4388 (2007)

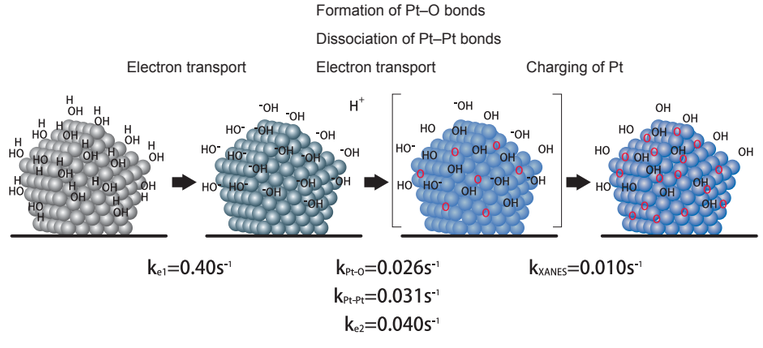

Fig. 3. Mechanisms for the dissolution and deterioration of platinum catalysts.
When the battery cell voltage exceeds the open-circuit voltage, oxygen atoms begin to enter the platinum catalysts, triggering platinum dissolution, which leads to catalyst dissolution.

Revealing Why Dioxins Are Produced Even in Perfect Combustion

Dioxins, many of which are highly toxic, are produced in various processes, including combustion processes in metal refining and chlorine bleaching of paper. The major source of dioxins is speculated to be the imperfect combustion during combustion processes in refuse incinerators. Recently, refuse incinerators have adopted high-temperature combustion (> 800 °C) with the goal of reducing the amount of dioxin produced through perfect combustion, followed by rapid cooling of the exhaust gas, and dioxin absorption via activated carbon. Despite these efforts, dioxins are still being produced. However, research conducted at SPring-8 has elucidated the production mechanisms of dioxins, and this cutting-edge research has provided insight to eliminate dioxin production.

Role of Copper Compounds in Dioxin Production

Polychlorinated dibenzo-p-dioxins (PCDDs) and polychlorinated dibenzofurans (PCDFs) are called dioxins. However, there are 75 types of PCDDs and 135 types of PCDFs. Dioxins are a collective name for 210 chemical compounds with a common structure where one to nine chlorine atoms are connected to two benzene rings that sandwich oxygen atoms. The skeletal structure, binding site, and number of chlorine atoms all determine the toxicity of a particular dioxin.

Various measures have been sought to reduce the production of dioxins. Recently, perfect combustion and temperature control in refuse incinerators have been implemented to reduce dioxin production. Unfortunately, dioxins are resynthesized during the cooling processes of exhaust gas in refuse incinerators. Exhaust gas contains smoke dust or fly ashes. In the cooling process of fly ashes, the resynthesis of dioxins is initiated, and it is maximized at 300–400 °C and terminated below 200 °C. The reaction involves a catalyst. Numerous experiments have demonstrated that copper, which is found in copper wires, substrates, and paints in refuse, forms copper compounds, and these copper compounds play a catalytic role in the resynthesis of dioxins. However, the reaction mechanisms of the catalytic actions have yet to be elucidated.

"We aimed to thoroughly explore how copper compounds contribute to dioxin production," explains Dr. Masaki Takaoka (Associate Professor, Kyoto University, Japan), who majored in urban environmental engineering. He has been conducting research to prevent the resynthesis of dioxins during the cooling processes of refuse incinerators and consequently, to reduce the amount of dioxin produced. To prevent dioxin resynthesis, the detailed mechanisms of the resynthesis must be elucidated. In other words, the following must be determined: 1) the role of copper compounds in the resynthesis of dioxins during the cooling processes of fly ashes, and 2) the types of copper compounds and the mechanisms promoting the resynthesis.

XAFS—Most Promising Technique to Decipher the Secret of Dioxin Resynthesis

To elucidate the dioxin resynthesis mechanisms, researchers have great expectations for the XAFS Beamline (BL01B1) at SPring-8. XAFS is an abbreviation for X-ray absorption fine structure. At BL01B1, the absorbed X-ray dose by a sample is measured by continuously varying the energy of the incident X-rays that are irradiated onto a sample. In this energy scan measurement, the absorbed X-ray dose sharply increases at a specific energy called the absorption edge. The absorption edge varies by element, and fine variations in the distribution of absorbed X-ray dose are observed near the absorption edge. This distribution is called the absorption spectrum, which reflects the atomic structure of a material.

XAFS analyses occur in two separate energy regions: 1) near the peak of the absorption edge and 2) at some distance above the absorption edge. The fine structure in the former is called the X-ray absorption near edge structure (XANES), while that in the latter is called the extended X-ray absorption fine structure (EXAFS). Because XANES largely depends on the electron states of the atoms of a specific element in a sample, the following information can be obtained: the valence values, elemental species, and content rates of X-ray absorbing atoms. On the other hand, the interference between the waves of photoelectrons emitted from X-ray absorbing atoms and those scattered by neighboring atoms induces EXAFS; thus, the distance of the X-ray absorbing atoms from the neighboring atoms and the number of the latter (coordination number) can be obtained.

In October 2000, Dr. Takaoka and colleagues conducted experiments at SPring-8 to examine the copper contained in fly ashes extracted from incinerators. Fly ash samples were prepared by reproducing the temperature and gas conditions equivalent to those in actual incinerators in their university's laboratory, and they analyzed their samples at SPring-8.

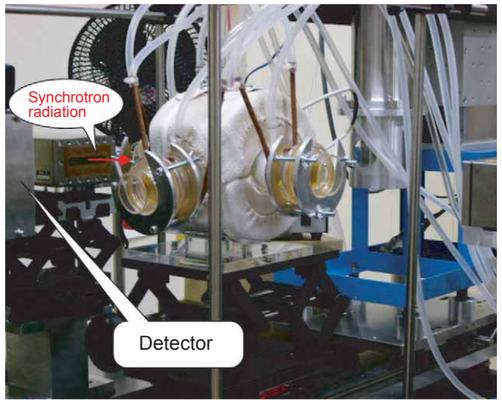

Fig. 1. Experimental apparatus at SPring-8's beamline.
Fly ashes were encapsulated in a white container and irradiated by synchrotron radiation. Measurements were performed by setting the inside temperature of the container to that of an incinerator.

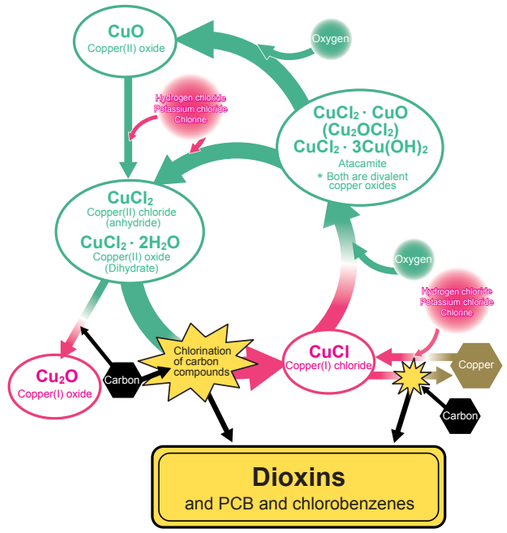

Fig. 2. Changes in the chemical forms of copper during dioxin synthesis.
During the reduction process of copper(II) chloride ($CuCl_2$) by carbon, chlorine leaves $CuCl_2$ to make copper(I) chloride (CuCl). In this case, chlorine is added to carbon, and partly makes dioxins. However, chlorine leaves CuCl, and in some cases couples with carbon. Additionally, CuCl reacts with oxygen in the atmosphere to produce divalent copper compounds (and copper(II) oxide (CuO) is produced in some cases). These divalent copper compounds react with chlorides or chlorine in the surrounding environment to produce $CuCl_2$. This cycle is repeated to produce dioxins.

However, the results were unsatisfactory. To overcome this problem, they conducted further experiments in October 2003. They encapsulated fly ash in a glass container, and the temperature and gas conditions were maintained so that they were equivalent to actual incinerators to directly observe the real-time reactions of the ashes (Fig. 1).

Chlorine Removed from Copper Compounds Becomes a Raw Material of Dioxins

Dr. Takaoka's group conducted the following experiments. 1) First, X-rays were irradiated onto samples at various temperatures, 2) then the obtained spectra were compared to those of a standard reference material, and 3) finally the content of various copper compounds were estimated at each temperature. These experiments revealed that the major component of the copper compounds contained in incineration ashes is atacamite, which is a compound of copper(II) chloride ($CuCl_2$) and copper(II) hydroxide ($Cu(OH)_2$).

Heating atacamite initiates the reduction of copper at ~200 °C, which is also the temperature where the synthesis of dioxin begins. Upon further heating, copper exists mainly as copper(I) chloride (CuCl) at 300 °C, but at 400 °C, $CuCl_2$ decreases and copper(II) oxide (CuO) is produced. The complex oxidation–reduction reactions depend on temperature.

On the other hand, an oxidative chlorination reaction, termed oxychlorination, was observed in the reduction process of copper. This is a reaction where carbon compounds contained in fly ashes are chlorinated. Past studies have suggested that organochloride compounds, which have a slightly simpler structure than dioxins, are also produced. Dr. Takaoka and colleagues' results support this assertion.

Consequently, they found that chlorine coupled to copper can be decoupled, and used as a raw material for dioxins (Fig. 2). In fact, the dioxin content increased more than 500-fold from 84 ng (ng = 10^{-9} g) per 1 g of fly ash at room temperature to 4,900 ng at 400 °C. These experiments were repeated using various mock fly ashes. Not all cases produced CuCl (Fig. 3: mock fly ash B). "This finding indicates that adjusting the conditions can terminate the copper catalytic cycle and control the chemical reactions. Thus, preventing CuCl formation reactions may suppress dioxin production," notes Dr. Takaoka. Their achievement was published in *Environmental Science & Technology* (August 2005), which is a well-established journal in environmental science and engineering. Additionally, their findings were spotlighted at an X-ray analysis discussion meeting held at Kyoto University in October 2005.

Their research group is conducting further experiments using mock fly ashes to accumulate data about the relationship between dioxin production and the chemical changes of chlorine, copper, and other metals as well as researching the effects of chemical suppressors. These suppressors are highly effective in the laboratory; thus, after overcoming some technical issues, suppressors may be applicable in an optimized process for the entire exhaust gas processing system.

Reference
1. M. Takaoka, A. Shiono, K. Nishimura, T. Yamamoto, T. Uruga, N. Takeda, T. Tanaka, K. Oshita, T. Matsumoto and H. Harada; *Environ. Sci. Technol.*, **39**, 5878 (2005)

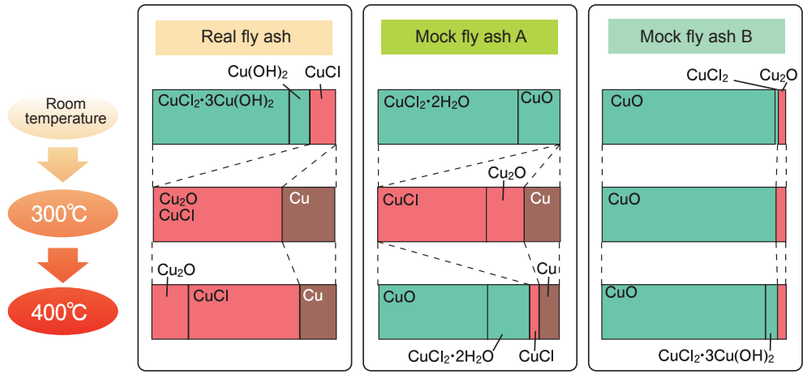

Fig. 3. Environment in which dioxins are resynthesized during refuse combustion.
Compositional changes of copper compounds contained in combustion fly ashes from room temperature to 300–400 °C. ■ indicates univalent copper compound, while ■ indicate divalent copper compounds. For mock fly ash B, few univalent copper compounds are observed.

Exploring the Secrets of Plants that Decontaminate Heavy Metal Contaminated Soils

Some plants absorb heavy metals from the environment, and accumulate them at high concentrations during the growth process. Reports have documented plants with heavy metal concentrations 300 times higher than that of the surrounding soil. Not surprisingly, the idea of removing heavy metals in contaminated soil and restoring the environment using plants, which is called phytoremediation, has recently received much attention. However, to apply this special phenomenon to practical environmental decontamination technology, the behavior of heavy metals in the plant bodies must be understood. Thus, the distributions and chemical forms of heavy metal elements must be elucidated at the cellular level. Fortunately, the high-energy X-ray microbeam at SPring-8 has made this possible. This topic reports cutting-edge research achievements at SPring-8.

Observing the Elemental Content in Live Plants

Soils contaminated with arsenic, lead, cadmium, chromium, or radioactive elements are problematic in various parts of the world. Phytoremediation is a pollutant reduction treatment in which harmful heavy metal elements are removed from the soil by reaping plants that absorb these elements. Compared to existing decontamination technologies, phytoremediation uses less energy, is more economical, and environmentally friendly. Thus, the potential demand for phytoremediation is huge.

However, plants with a hyperaccumulation ability for heavy metals are very limited. For example, the first land plant hyperaccumulator, Pteris vittata (Pteridaceae), was only identified in 2001 as an arsenic hyperaccumulator plant. Since then the hyperaccumulation ability for zinc and cadmium has been found in Arabidopsis halleri (Brassicaceae) in Japan. Thus, the application of heavy metal hyperaccumulator plants to phytoremediation is just beginning. Before hyperaccumulator plants can be identified and applied for soil decontamination, many questions must be answered. These include determining where and how these plants accumulate heavy metals, and why hyperaccumulators can absorb higher concentrations of heavy metals.

In April 2003, Dr. Izumi Nakai (Professor, Tokyo University of Science, Japan), Dr. Akiko Hokura[1] (Assistant Professor, *ditto*), and colleagues initiated research to answer these questions using X-ray imaging. They studied the heavy metal hyperaccumulation ability of various plants, and decided to focus on Pteris vittata in Japan after meeting Dr. Nobuyuki Kitajima (Fujita Corporation, Japan), who had conducted a soil decontamination project using Pteris vittata. To elucidate the mechanisms of its arsenic hyperaccumulation ability, analysis with the resolution of 1 μm (μm = 10^{-6} m) was required. "SPring-8's Trace Element Analysis Beamline (BL37XU), which provides a combination of X-ray microbeams and X-ray fluorescence analysis, was the only facility that could perform element analysis and chemical form analysis at the cellular level," explains Dr. Nakai.

Elucidating the Transition of Arsenic to Leaves

When X-rays are irradiated onto a sample, an inner-shell electron of the constituent atom in a sample is excited or emitted out, and an outer-shell electron moves down to the resultant hole[1]. Then a fluorescent X-ray whose energy is determined by the difference between the energy levels of these two electrons is subsequently emitted. Because each element has a specific fluorescent X-ray energy, the constituent elements can be identified from the obtained spectrum (wavelength-dependent intensity distribution). Additionally, the element concentration can be obtained from the fluorescent X-ray intensity. This analysis technique is called X-ray fluorescence (XRF). However, the spatial resolution is limited to 10 μm in conventional XRF using non-directional X-rays and not synchrotron radiation, making it difficult to obtain the complex behavior of elements in plant tissues. To overcome this difficulty, an X-ray microbeam was prepared by exploiting the highly brilliant and directional synchrotron radiation to measure the 2D distributions of contained elements. This is called synchrotron radiation microbeam X-ray fluorescence (SR-μ-XRF).

SR-μ-XRF can measure live plants and fresh tissues, but investigating the elemental distribution at the tissue/cellular level requires sample manipulations. These manipulations prevent shrinkage and tissue deformation due to drying as well as the migration and outflow of contained elements during the measurements. Along with the aid of botanical experts, Dr. Nakai and colleagues have been accumulating the know-how about plant cultivation and sample preparation. For example, to maintain the structure of a sample at the cellular level, it must be quickly frozen to prevent ice crystals from forming in the cells and to maintain the sample shape. Through this frozen technique, XRF imaging of samples in a near-living state has become possible, allowing the anatomical positional relationship between the element distributions and the tissue structure to be measured.

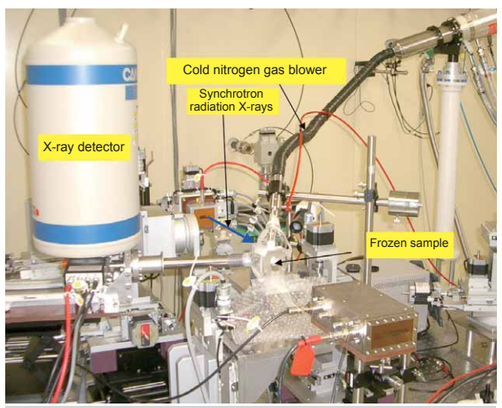

Fig. 1. Experimental apparatus of XRF measurement.
BL37XU allows researchers to analyze frozen sections of Pteris vittata in a near-living state.

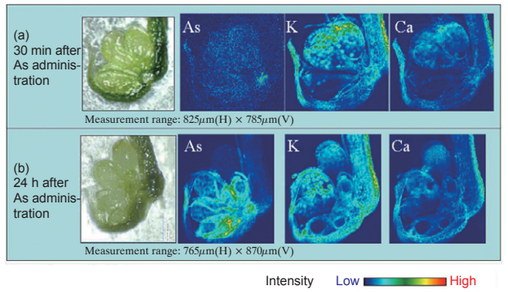

Fig. 2. XRF 2D imaging of arsenic, potassium, and calcium in the marginal regions of Pteris vittata's leaves (pinnae).
(a) Distribution of elements 30 min after arsenic administration. Arsenic reaches the base of the sporangium of Pteris vittata's pinna in 30 min. (b) Distribution of elements 24 h after arsenic administration. Arsenic concentrates in the base of the sporangium, but the entrance into a spore is suppressed.

In addition to freezing the sample, sample thickness is very important. If the thickness of a section is ~150 μm, several cells will overlap, preventing the elemental distributions within a single cell to be determined. Fortunately, their research group has successfully prepared 10–20-μm thick frozen sections.

After these careful preparations, they were ready to measure Pteris vittata at SPring-8 (Fig. 1). Pteris vittata was grown under optimal conditions with the help of Dr. Kitajima and Dr. Tomoko Abe (RIKEN, Japan). After immersing Pteris vittata in an arsenic solution for a given length of time (30 min or 24 h), frozen sections were resected from the leaves. Scanning the samples at 3-μm intervals every 0.3 sec was realized using the X-ray microbeam with a beam cross-section of 2 × 2 μm^2. In this manner, the changes in the arsenic distribution were visualized with time (Fig. 2).

Surprisingly, arsenic reaches the marginal regions where it is stored 30 min after administration, which is amazingly fast. Additionally, they found that arsenic initially accumulates in the conductive tissues, and is then preferentially distributed to paraphyses and false indusium.

Precisely Analyzing Cadmium Contained within Rice

In addition to studying arsenic-accumulating plants, Dr. Nakai's research group has studied various cadmium-accumulating plants, such as Arabidopsis halleri and Athyrium yokoscense. Because cadmium has a larger atomic number than arsenic, high-energy synchrotron radiation at SPring-8 is indispensable to excite inner-shell electrons of cadmium. Dr. Yasuko Terada (Senior Scientist, the Japan Synchrotron Radiation Research Institute) and colleagues were the first to conduct SR-XRF analyses using high-energy X-rays with a 1-μm beam size at BL37XU. Currently BL37XU at SPring-8 is the only experimental facility in the world where cadmium is examined at the cellular level.

In Arabidopsis halleri's leaves, cadmium along with zinc and manganese accumulate in the trichome, which is a capillary outgrowth that consists of tiny cells with ~20-μm diameter. SR-XRF using the X-ray microbeam revealed that cadmium accumulates in the joint of trichome. Additionally, X-ray absorption fine structure (XAFS) analysis revealed that cadmium is bonded to oxygen or nitrogen.

In Japan, the cadmium content in brown rice is regulated by law, but the actual analyses of a very small quantity of cadmium in plants are cumbersome and difficult. However, high-energy SR-XRF can easily measure the cadmium distribution in brown rice. Their research group also examined the 2D distribution of cadmium within rice, and found that cadmium is uniformly distributed over the edible parts of white rice (endosperm) obtained from rice plants grown with an additional 1 ppm of cadmium. Their work indicates that polishing rice does not remove cadmium (Fig. 3).

As just described, their research group was the first to reveal where arsenic and cadmium reside in plants as well as their chemical forms at the cellular level. "High-energy SR-XRF is quite powerful in analyzing heavy metal elements in plants. We will continue to elucidate the accumulation mechanisms of heavy metals in heavy metal hyperaccumulator plants using synchrotron radiation," comments Dr. Nakai as he talks about the future.

[1] Currently Associate Professor at Tokyo Denki University, Japan.
[2] This process is called a *transition*.

Reference
1. R. Onuma, A. Hokura, N. Kitajima, I. Nakai, Y. Terada, T. Abe, H. Saito and S. Yoshida; *Proc. 8th Int. Conf. X-ray Microscopy*, IPAP Conf. Series, **7**, 326 (2006)

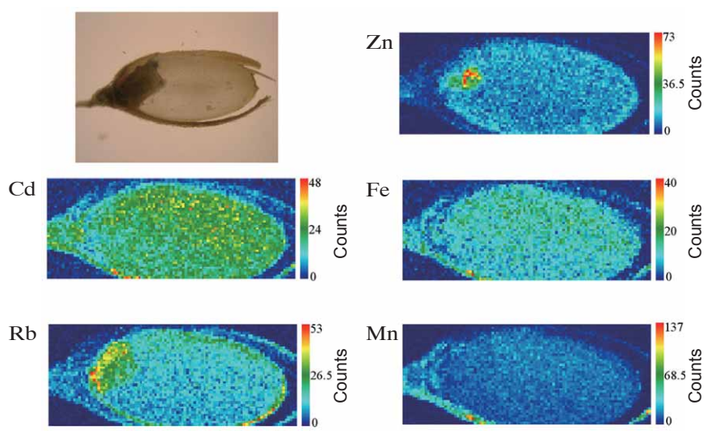

Fig. 3. Distributions of elements in brown rice grown by adding 1 ppm of cadmium.
Zinc, an essential element, concentrates in the germ, while cadmium is uniformly distributed over the endosperm, which is consumed as white rice.

Nuclear Physics

Unraveling the Extreme Fundamentals of Materials Using High-Energy Photon Beams

Exploring Quarks using Laser Electron Photon Beams with the World's Shortest Wavelength

At SPring-8, scientists are conducting research on quark nuclear physics. A quark is an elementary particle, which constitutes hadrons such as proton and neutron. Although quarks are always confined in hadrons, the confinement mechanisms, confinement states, and mass acquiring mechanisms of hadrons whose masses are heavier than the sum of the constituent quarks have yet to be elucidated. Quark nuclear physics research aims to reveal these mysteries. The potency of laser electron photon beams, which are produced by revolutionary methods, has been confirmed. Laser electron photons, also called laser inverse Compton photons, are highly energetic photon beams obtained from the recoil of laser light by electron beams.

A research group, Laser Electron Photon at SPring-8 (LEPS), which is led by researchers at the Research Center for Nuclear Physics, Osaka University, is conducting nuclear experiments at SPring-8. Their research uses laser electron photon beams (maximum energy: 2.4 GeV)[1] produced by head-on collisions of ultraviolet laser light (3.5 eV, 350 nm)[2] and electron beams in a storage ring (8 GeV).

Because photon energy and wavelength are inversely related, amplifying the photon energy seven million-fold from 3.5 eV to 2.4 GeV shortens the photon wavelength seven million-fold from 350 nm to 0.5 fm.[3] To generate laser electron photon beams, the following are indispensable: high-intensity high-energy electron beams with stable orbits, a high-intensity laser, and the technology to ensure precise collisions. Laser electron photon beams obtained at LEPS have the world's highest energy (shortest wavelength).

Although a 0.5-fm wavelength is very short, it is still about the same size as a nucleon such as a proton and neutron. Therefore, it is impossible to directly observe (in its normal meaning) nucleons or quarks in nucleons with a 2.4-GeV laser electron photon. It should be noted that the particle nature of light (a packet of pure energy or a photon), which exhibits wave–particle duality, is more important than the wave nature of light when examining the quark world.

At the LEPS facility, more than 10^6 photons are produced per second, and these photons are irradiated onto targets such as hydrogen and nuclei. A photon, which is a packet of energy, changes its form into various types of charged particle–antiparticle pairs in nuclei to induce photonuclear reactions. There are six types of quarks: up, down, strange, charm, bottom, and top quarks. Protons and neutrons, which constitute a nucleus, consist of up quarks and down quarks. A 2.4-GeV photon can produce strange quark–antistrange quark pairs where a strange quark is much heavier than the up and down quarks found in protons and neutrons.

Composite particles composed of multiple quarks, including strange quarks, are termed hyperons. Hyperons have extremely short lifetimes ($< 10^{-20}$ sec) and decay immediately; therefore, it is difficult to detect hyperons themselves. However, investigating the production and decay of such short-lived hyperons may elucidate the quark confinement mechanism.

Shattering Common Notions and Making the Impossible Possible

With the expectation that the quark confinement mechanism can be solved, a five-quark particle, which consists of an antistrange quark and four normal quarks, was first discovered at LEPS.

The photon beams produced by bremsstrahlung using existing electron beams cannot achieve high-spin polarization. However, a laser electron photon has the following three advantages. (1) Spin-polarized high-energy photon beams can be easily produced using linearly or circularly polarized laser light. (2) Photon beams contain a very small amount of low-energy components ($< \sim$100 MeV)[4], which are noise sources in nuclear and elementary particle experiments. (3) Because photon beams are highly directional, compact detector systems can be used.

In the hadron world, interactions between hadrons are mediated by the exchange of particles; herein many particles can be involved, which complicates the analysis of the experimental data. However, some information about exchanged particles can be determined by examining the angular correlations between the direction of photon polarization and the angular distribution of the mesons emitted in the hadron production. Because single quarks cannot be extracted from hadrons, the capability of examining the hadron production processes by detecting such observables (angular correlations) would be a great advantage in the study of hadron structures. Thus, characteristics that make analyses difficult are converted into powerful clues for the analyses. In this way, the studies conducted at LEPS have redefined the common understanding of quarks.

The intensity of laser electron photon beams is proportional to that of the incident laser. Over the last ten years, the intensity of laser electron photon beams at LEPS has been increased several-fold through the top-up operation where the losses in the electron beams in a storage ring are compensated as necessary, improvement of the laser oscillators themselves, and utilization of parallel injections where two lasers are simultaneously injected. Our future goal is to realize higher energy laser electron photon beams by developing a new laser with an even shorter wavelength. These technologies will be powerful weapons to decipher the mysteries of quarks.

[1] 1 GeV = 10^9 eV
[2] 1 nm = 10^{-9} m
[3] 1 fm = 10^{-15} m
[4] 1 MeV = 10^6 eV

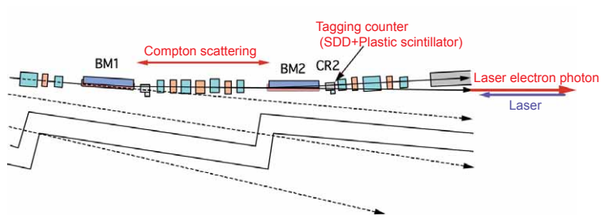

Fig. 1. Schematic diagram of the region where the electron beams in a storage ring and laser collide.

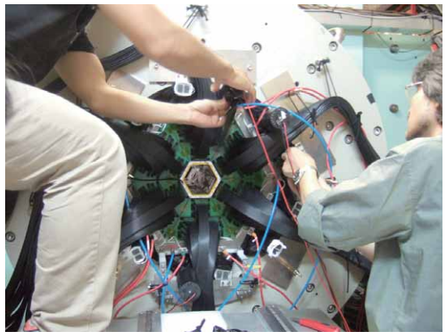

Fig. 2. Charged particle detector and its adjustment.

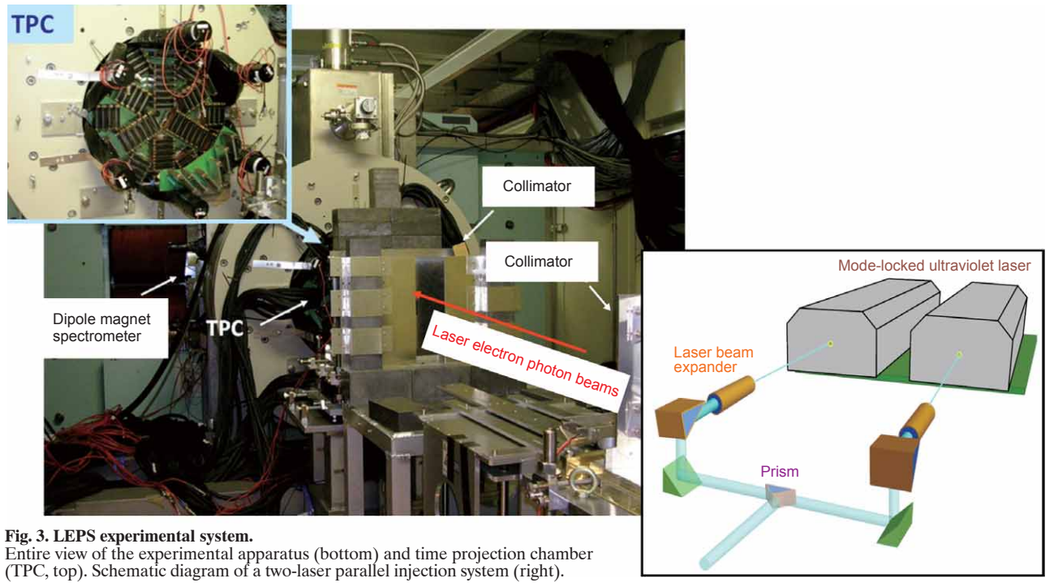

Fig. 3. LEPS experimental system.
Entire view of the experimental apparatus (bottom) and time projection chamber (TPC, top). Schematic diagram of a two-laser parallel injection system (right).

Realizing a 30-Year-Old Dream in Nuclear Physics—The Five-Quark Particle

A quark is the most fundamental elementary particle, and cannot be divided any further. Each proton and neutron consists of three quarks. Although particles consisting of four or more quarks are theoretically possible, evidence for such particles had not been obtained at the turn of the 21st century. Believe it or not, quarks are extraordinarily small (they are on the order of 10^{-18} m), and a single quark cannot be observed by itself. Thus, quarks are extremely difficult to investigate. However, in 2003, a new particle consisting of five quarks was discovered using high-energy photon beams at SPring-8. Thus, the decades-long dream of physicists was finally realized. The persistence and determination of the scientists who worked on this project along with the power of the extremely brilliant photon beams at SPring-8 contributed to this achievement.

Prediction of Russian Physicists

There are six types of quarks: up (u), down (d), strange (s), charm (c), bottom (b), and top (t). However, the only stable quarks on Earth are the u- and d-quarks. Furthermore, the only observable form is a composite particle or a hadron, which consists of multiple quarks. The force binding quarks is called a color charge, and is much stronger than electromagnetic force. Quark binding forces include "red", "blue", and "green", which are named after the three primary colors of light. Each of the three-colored quarks has an anti-quark of its complementary color.

Quark–hadron theories state, "only white hadrons exist in the natural world," and only two types of hadrons have been observed: baryons and mesons. Baryons consist of three quarks (red, blue, and green), whereas mesons consist of a quark and an anti-quark with a color and its complement, respectively. Due to the mixture of the three primary colors, baryons are white, whereas mesons are white due to the mix of a color and its complement. For example, a proton, which is a type of baryon, consists of two u-quarks and one d-quark, while a neutron, another type of baryon, consists of one u-quark and two d-quarks. According to quantum chromodynamics (QCD), a basic theory of quark–hadron, particles consisting of four quarks (two mesons) or five quarks (a meson and a baryon) are theoretically possible, but particles with four or five quarks had yet to be experimentally observed after 30 years of exploration. Thus, the Laser Electron Photon at SPring-8 (LEPS), a group led by Dr. Takashi Nakano (Professor, the Research Center for Nuclear Physics, Osaka University, Japan), and colleagues from the Japan Atomic Energy Research Institute,[1] Japan Synchrotron Radiation Research Institute, and 19 universities and research centers around the globe, took the initiative to pursue this "unachievable dream".

Their project began in February 2000 when Dr. Nakano, who attended an international conference in Adelaide, Australia, had lunch with Dr. Dmitri Diakonov, Russian physicist. Dr. Diakonov predicted that a five-quark particle, called Θ^+, which consists of two u-quarks, two d-quarks, and one anti s-quark ($uudd\bar{s}$), has a mass of 1530 MeV/c^2 (1 eV/c^2 = 1.783×10^{-36} kg) and a decay width (fluctuations in mass) less than 15 MeV/c^2. A particle with a smaller decay width has a lower decay probability per unit time. Because Dr. Diakonov knew that the construction of SPring-8 was nearly complete, during lunch he suggested to Dr. Nakano, "You should look for a Θ^+ particle using the laser electron beams at SPring-8."

In December 2000, Dr. Nakano and colleagues began their experiments at the Laser Electron Photon facility of SPring-8 with the objective of producing ϕ-mesons by colliding high-energy photons with protons in hydrogen atoms. Through collisions and instantaneous decays into different particles, various types of mesons, including ϕ, π, K, ρ, and B, have been

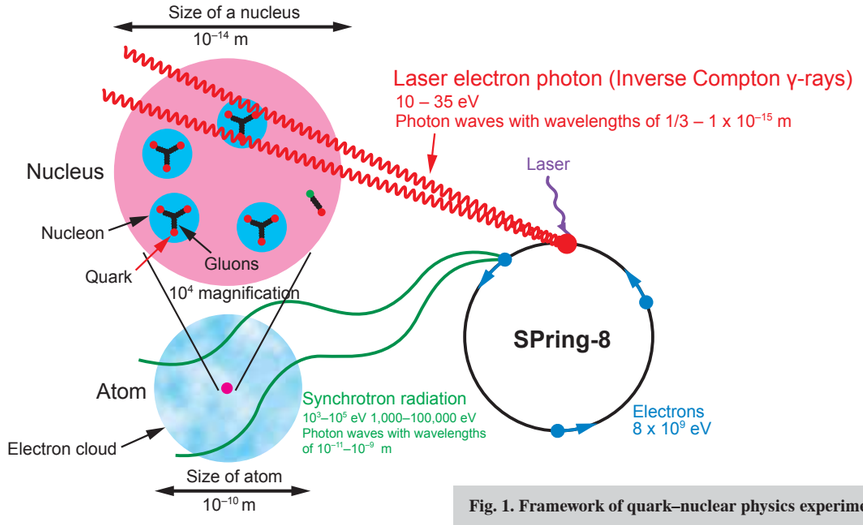

Fig. 1. Framework of quark–nuclear physics experiments.

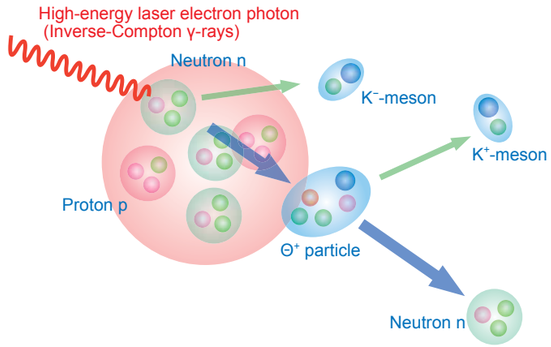

Fig. 2. Schematic diagram of the production reaction of Θ^+ particles at LEPS.

identified. Because a ϕ-meson decays into a K^+K^--meson pair in 10^{-22} sec where K-mesons are relatively long-lived (10^{-8} sec), a ϕ-meson can be identified by detecting the creation of a pair of K^+K^--mesons.

Finally Discovering a Five-Quark Particle

Their experiment was conducted in two parts. First, high-energy laser electron photons (inverse Compton γ-rays) were obtained from the head-on collision of laser light with 8 GeV high-energy electron beams. Then protons in hydrogen atoms were irradiated with these high-energy photons (Fig. 1).

"However, our experiment had another objective. We installed plastic scintillators behind the hydrogen target hoping that data relating to five-quark particles might be obtained if the carbon atoms in the scintillators were targeted by γ-rays," describes Dr. Nakano. Scintillators, which emit light upon the irradiation of particles such as radiation, were used as part of the measurement system to detect particle energy. When γ-rays collide with neutrons (n) in carbon atoms contained in the plastic scintillators, the following reaction occurs

$\gamma n \rightarrow K^-\Theta^+ \rightarrow K^-K^+n$

They designed their detectors to be extremely sensitive to K^+K^- meson pairs. Therefore, Dr. Nakano expected that if a five-quark Θ^+ particle is produced according to this reaction, then it would be identified by detecting its decay product, a K^+K^- meson pair (Fig. 2). Their data analyses provided evidence that Θ^+ particles are produced by the mass distribution of the K^+n system. "We observed a sharp peak at 1540 MeV/c^2," says Dr. Nakano. Furthermore, the peak width is narrower than 25 MeV/c^2, consistent with Dr. Diakonov's prediction.

Searching for Firm Evidence of Five-Quark Particles

Immediately after the discovery of a Θ^+ particle was published in *Physical Review Letters* in July 2003, validation studies for this particle were conducted around the world. Researchers at the Institute for Theoretical and Experimental Physics in Russia and at the Jefferson Lab in the US reanalyzed data they collected during experiments conducted in 1986 and 1999, respectively. Additionally, researchers at the Electron Stretcher and Accelerator in Germany reexamined the data from their past experiments. All three groups confirmed the same mass value as the LEPS's result. Because it is unlikely for four independent experiments to observe a mass peak at the same value, the existence of a Θ^+ particle was thought to be confirmed. However, many research groups reported that the Θ^+ particle had not been identified. "The extremely small production rate of a Θ^+ particle makes it difficult to identify," notes Dr. Nakano, who along with colleagues have resumed experiments with the goal of detecting a Θ^+ particle. This time they used a more precise setup containing deuterium atoms, which contain neutrons, as a γ-ray target at SPring-8. Their results were published in *Physical Review C* in February 2009 (Fig. 3). Dr. Nakano received the Nishina Memorial Prize in 2003 for discovering five-quark particles.

Furthermore, construction of a new facility equipped with a laser electron light beamline that will provide the world's highest beam intensity and energy along with high-resolution spectrometers begun at SPring-8 in 2010. This facility will support further experiments on five-quark particles.

[1] Currently the Japan Atomic Energy Agency.

References
1. T. Nakano, D. S. Ahn, J. K. Ahn, H. Akimune, Y. Asano, W. C. Chang, S. Daté, H. Ejiri, H. Fujimura, M. Fujiwara, K. Hicks, T. Hotta, K. Imai, T. Ishikawa, T. Iwata, H. Kawai, Z. Y. Kim, K. Kino, H. Kohri, N. Kumagai, S. Makino, T. Matsumura, N. Matsuoka, T. Mibe, K. Miwa, M. Miyabe, Y. Miyachi, M. Morita, N. Muramatsu, M. Niiyama, M. Nomachi, Y. Ohashi, T. Ooba, H. Ohkuma, D. S. Oshuev, C. Rangacharyulu, A. Sakaguchi, T. Sasaki, P. M. Shagin, Y. Shiino, H. Shimizu, Y. Sugaya, M. Sumihama, H. Toyokawa, A. Wakai, C. W. Wang, S. C. Wang, K. Yonehara, T. Yorita, M. Yoshimura, M. Yosoi and R. G. T. Zegers; *Phys. Rev. Lett.*, **91**, 012002 (2003)
2. T. Nakano, N. Muramatsu, D. S. Ahn, J. K. Ahn, H. Akimune, Y. Asano, W. C. Chang, S. Daté, H. Ejiri, H. Fujimura, M. Fujiwara, S. Fukui, H. Hasegawa, K. Hicks, K. Horie, T. Hotta, K. Imai, T. Ishikawa, T. Iwata, Y. Kato, H. Kawai, Z. Y. Kim, K. Kino, H. Kohri, N. Kumagai, S. Makino, T. Matsuda, N. Matsuoka, T. Matsumura, T. Mibe, M. Miyabe, Y. Miyachi, M. Niiyama, M. Nomachi, Y. Ohashi, H. Ohkuma, T. Ooba, D. S. Oshuev, C. Rangacharyulu, A. Sakaguchi, P. M. Shagin, Y. Shiino, A. Shimizu, H. Shimizu, Y. Sugaya, M. Sumihama, Y. Toi, H. Toyokawa, A. Wakai, C. W. Wang, S. C. Wang, K. Yonehara, T. Yorita, M. Yoshimura, M. Yosoi and R. G. T. Zegers; *Phys. Rev. C*, **79**, 025210 (2009)

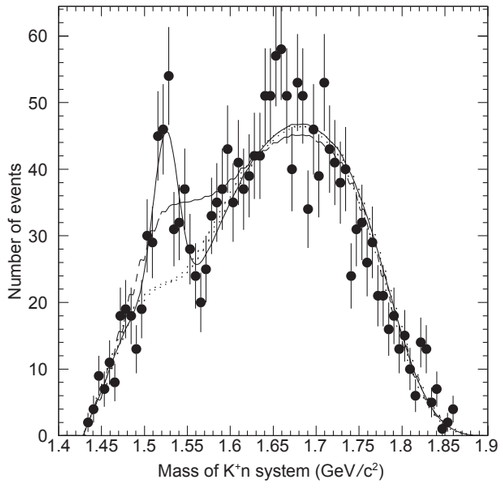

Fig. 3. Mass distribution of the K^+n system obtained in a more precise experiment by targeting deuteron.
Peak corresponding to the production of a Θ^+ particle is observed near a mass of 1530 MeV/c^2.

List of Major Awards/Prize Winners

Many researchers have been recognized for their research conducted at SPring-8. Here is a list of major awards received.

The Asahi Prize

2009 Clarification of the Mechanical Operation of the Calcium Pump
Chikashi Toyoshima (Professor, The University of Tokyo)

The Nishina Memorial Prize

2003 Discovery of a New Particle by using LASER Compton Gamma Rays
Takashi Nakano (Professor, Osaka University)

The IBM Japan Science Prize

2007 Invention of Diffracted X-ray Tracking and its Application to Interdisciplinary Fields
Yuji Sasaki (Senior Scientist, JASRI)

Discovery of Post-Perovskite Phase and Research on the Earth's Core–Mantle Boundary
Kei Hirose (Professor, Tokyo Institute of Technology)

The Shimadzu Prize

2006 Development and Application of High Precision and Resolution Spectroscopy using Synchrotron Radiation
Shigemasa Suga (Professor, Osaka University)

Director-General of the National Police Agency Award

2009 Application of X-ray fluorescence analysis using High-Energy Synchrotron Radiation to Forensic Science
Yoshinori Nishiwaki (Crime Laboratory, Hyogo Prefectural Police Headquarters)

Eugen und Ilse Seibold-Preis (The Eugen and Ilse Seibold Prize)

2003 Japan–Germany Collaborative Research on the Nanotechnologies of Semiconductors, Magnetic Materials, Superconductors, and Nanomagnetic Materials, and Achievements in Photoelectron Spectroscopy Research using SPring-8
Shigemasa Suga (Professor, Osaka University)

The Humboldt Research Award

2007 Research on Earth's Interior Science and Structural Materials, and Synthesis of Ultrahard Nano-Polycrystalline Diamond (HIME-DIA)
Tetsuo Irifune (Professor, Ehime University)

2008 Research on Synthesis and Functionalization of Microporous Coordination Polymers
Susumu Kitagawa (Professor, Kyoto University)

The Helmholtz Humboldt Research Award

2008 Solid State Physics Research using Bulk-Sensitive Photoelectron Spectroscopy
Shigemasa Suga (Professor, Osaka University)

The Commendation for Science and Technology by the Minister of Education, Culture, Sports, Science and Technology

Prizes for Science and Technology (Research Category)

2005 Research on High Resolution Photoelectron Spectrometer using Wide Energy Range Electrons
Shigemasa Suga (Professor, Osaka University), Shin Imada (Associate Professor, Osaka University), Akira Sekiyama (Assistant Professor, Osaka University)

Research on Short-Period In-Vacuum Undulators
Hideo Kitamura (Chief Scientist, RIKEN)

2006 Research on the X-ray Crystal Structure Analysis of Cytochrome Oxidase
Shinya Yoshikawa (Professor, The University of Hyogo), Kazumasa Muramoto (Associate Professor, The University of Hyogo), Kyoko Ito (Assistant Professor, The University of Hyogo)

2008 Research on the Visualization of Electron and Nuclear Density Distributions based on Information Theory
Makoto Sakata (Professor Emeritus, Nagoya University)

Development of High Brilliance Infrared Synchrotron Radiation and its Application to Materials Science
Takao Nanba (Professor, Kobe University), Shin-ichi Kimura (Associate Professor, Institute for Molecular Science)

Research on Atomic Stereo-Photography using Circularly-Polarized Synchrotron Radiation
Hiroshi Daimon (Professor, Nara Institute of Science and Technology), Fumihiko Matsui (Assistant Professor, Nara Institute of Science and Technology), Tomohiro Matsushita (Senior Scientist, JASRI), Fang Zhun Guo (JASRI)

2009 Research on Materials Structure using Neutron and Synchrotron Radiation X-ray Scattering
Yasuhiko Fujii (Director, Japan Atomic Energy Agency)

Research on High Strength Steal Pipe Welding Metallurgy using Heterogeneous Nucleation
Yu-ichi Komizo (Professor, Osaka University)

Prizes for Science and Technology (Development Category)

2006 Development of Ultrasensitive Analysis Techniques in Forensic Science
Shin-ichi Suzuki (Chief, National Research Institute of Police Science), Yasuhiro Suzuki (Director, Forensic Science Laboratory, Shiga Prefectural Police), Masaaki Kasamatsu (National Research Institute of Police Science)

2007 Development of Large-Scale Synchrotron Radiation X-ray Optical System
Tetsuya Ishikawa (Director, RIKEN SPring-8 Center)

2007 Development of Inspection/Maintenance/Repair Technologies of Nuclear Reactor using Lasers
Yuji Sano (Toshiba), Naruhiko Mukai (Toshiba), Makoto Ochiai (Toshiba), Yoshinobu Makino (Toshiba), Masaki Yoda (Toshiba)

The Young Scientists' Prize

2009 Research on Operation Mechanisms of Secondary Transporter Proteins on Biological Membranes
Atsuko Yamashita (RIKEN)

The Nishikawa Prize, The Crystallographic Society of Japan

2005 Promotion of Diffraction Physics and Synchrotron Radiation Science
Seishi Kikuta (Professor Emeritus, The University of Tokyo)

SPring-8's Users have been awarded the following awards/prizes

The Physical Society of Japan Award for Academic Papers on Physics, The Chemical Society of Japan Award, The Award of the Society of Polymer Science, The Japan Institute of Metals Prize, The Japanese Society for Synchrotron Radiation Research Prize, The Japanese Society of High Pressure Science and Technology Prize, The Crystallographic Society of Japan Prize, The Particle Accelerator Society of Japan Encouragement Prize, The Japanese Society for Plant Systematics Prize, The Ceramic Society of Japan Award for Contributions to Promotion of Society Activities, The International Association for the Advancement of High Pressure Science and Technology Jamieson Award, The Hyogo SPring-8 Award, etc.

Detailed information about awards/prizes is available at SPring-8's website (in Japanese)
http://www.spring8.or.jp/

Award Presentation Ceremony, Asahi Prize


Award Presentation Ceremony, Helmholtz Humboldt Research Award

Factory to produce “dream light”

One of our goals is for people to have a better understanding of SPring-8. To make our vision a reality, we created this brochure entitled, *Challenging the Mysteries of Science with Dream Light*. This is our first publication of collective scientific achievements since SPring-8 was opened to users in October 1997.

I am often asked to describe SPring-8 in one word. However, it is nearly impossible to pick just one word. If you look at the beamline map on the next page, you will intuitively understand why this is so difficult. Unlike other factories that mass produce the same product, SPring-8 has 57 unique beamlines. Before I answer the question, “What is SPring-8?” ponder the following. Suppose that you visited all 57 beamlines and asked each researcher, “What are you doing at SPring-8?” Although each researcher would easily answer, the individual responses would vary considerably. One researcher may answer, “I am investigating the structures of proteins that govern biological phenomena,” while another may reply, “I am analyzing the interior structure of the Earth.” The range of responses is due to the fact that a wide variety of experiments are conducted at SPring-8 from probing the fine structure of semiconductors to examining automobile catalysts and everything in between.

Now that you grasp some of the diversity at SPring-8, you can understand how difficult it is to describe SPring-8 in a single word. In my opinion, the single word that best describes SPring-8 is a giant “microscope” because our facilities are used to “see” materials. Like an enormous microscope, SPring-8 utilizes light (or electromagnetic waves) in the broad sense to “visualize” materials. This light, which is emitted from accelerators, is called synchrotron radiation. Synchrotron radiation includes various types of light ranging from infrared light to X-rays. (Visible light of synchrotron radiation is not utilized because lasers are a high quality visible light source.) SPring-8 is the one of the world’s most powerful synchrotron radiation sources, and consequently, it produces superior, bright, and highly directional synchrotron radiation to “see” materials.

Hence, we have referred to synchrotron radiation as “dream light.” Researchers fully grasp the advantageous of this “dream light”. For example, the general laboratory X-ray sources commonly used at universities and research centers are not powerful enough to probe molecular structures, but they can be clearly seen with synchrotron radiation X-rays at SPring-8. I hope you understand why this brochure is titled *Challenging the Mysteries of Science with Dream Light*. SPring-8 is a factory to produce “dream light.” To date, our “dream light” has elucidated many mysteries of nature.

This brochure is a collection of select major achievements. Because advances and achievements encompass a broad range of fields, we have categorized them into seven fields. In addition to these seven fields, numerous achievements have been attained in industrial applications, and about 20% of SPring-8’s users are affiliated with industry (and these advances are published in a separate brochure entitled, *Successful Results of Industrial Applications at SPring-8*, which is available on the SPring-8 website).

Figuratively speaking, I like to compare SPring-8 to Mt. Yatsugatake (an eight peak mountain). Although Mt. Yatsugatake is not as distinctive as Mt. Fuji, it is attractive. Similarly, the eight peaks of *Mt. SPring-8* are the seven fields and the industrial application. Because *Mt. SPring-8* has numerous peaks, even weathered professionals have a hard time conquering all eight peaks. Thus, I recommend that you climb one peak at a time, beginning with the one that interests you most. I hope this brochure will be a good companion for your adventure.

Sakata Makoto
Editor in Chief, Editorial Board for SPring-8 Scientific Achievements

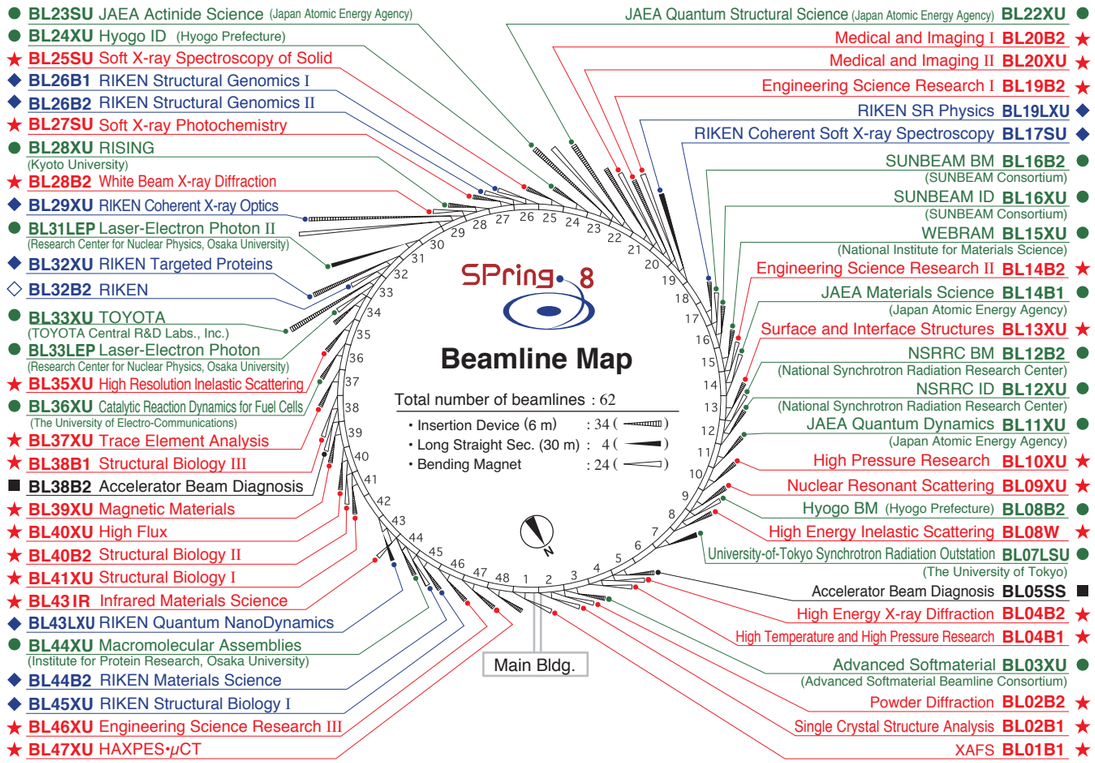

BL: Beamline
B1, B2: Bending Magnets
XU: X-ray Undulator
SU: Soft X-ray Undulator
W: Wiggler
IR: Infrared Radiation
LEP: Laser-Electron Photon
LXU: Long-length X-ray Undulator
LSU: Long-length Soft X-ray Undulator
SS: Straight Section

★ : Public Beamlines
● : Contract Beamlines
◆ : RIKEN Beamlines
■ : Accelerator Diagnostics Beamlines
☆ ○ ◇ □ : Planned or Under Construction

WEBRAM: Wide Energy Range Beamline for Research in Advanced Materials
NSRRC: National Synchrotron Radiation Research Center, Taiwan
RISING: Research & Development Initiative for Scientific Innovation of New Generation Batteries

Status	Beamlines				Total
	Public Beamlines	Contract Beamlines	RIKEN Beamlines	Accelerator Diagnostics Beamlines	
Operational	26	19	9	2	56
Planned or Under Construction	0	0	1	0	1
Total	26	19	10	2	57

October 03, 2013

SPring-8 Scientific Achievements: Challenging the Mysteries of Science with Dream Light

Editorial Office

Research Coordination Division, Japan Synchrotron Radiation Research Institute

Public Relations Office, Japan Synchrotron Radiation Research Institute

Production

Shigechika Honda, Yasunari Eshi, Tetsuro Ueda, Shy Company, Zenis

Photo

Satoru Yoshioka

Publisher

RIKEN

Registered Institution for Facilities Use Promotion
Japan Synchrotron Radiation Research Institute (JASRI)

2014.1

RIKEN
1-1-1 Kouto, Sayo-cho, Sayo-gun, Hyogo 679-5148, Japan

General Affairs Section
Phone: +81-791-58-0808, Fax: +81-791-58-0800
http://www.harima.riken.jp

Registered Institution for Facilities Use Promotion
Japan Synchrotron Radiation Research Institute (JASRI)
1-1-1 Kouto, Sayo-cho, Sayo-gun, Hyogo 679-5198, Japan

Public Relations Office
Phone: +81-791-58-2785, Fax: +81-791-58-2786
http://www.spring8.or.jp